RICE UNIVERSITY

CHARACTERIZATION OF METABOLITES AND GENES IN THE FERMENTATION PATHWAY OF *CLOSTRIDIUM ACETOBUTYLICUM* ATCC 824

BY

ZHUANG LUO BOYNTON

A THESIS SUBMITTED
IN PARTIAL FULFILLMENT OF THE
REQUIREMENTS FOR THE DEGREE

DOCTOR OF PHILOSOPHY

APPROVED, THESIS COMMITTEE:

F. B. Rudolph, Professor, Thesis Director
Biochemistry and Cell Biology

J. W. Campbell, Professor
Biochemistry and Cell Biology

G. N. Bennett, Professor
Biochemistry and Cell Biology

G. Palmer, Professor
Biochemistry and Cell Biology

Ka-Yiu San, Associate Professor
Chemical Engineering

Houston, Texas
May, 1996

Abstract

Characterization of Metabolites and Genes in the Fermentation Pathways of *Clostridium acetobutylicum* ATCC 824

By

Zhuang Luo Boynton

In *Clostridium acetobutylicum*, central-fermentation-pathway enzymes involved in butyryl-CoA synthesis play key roles in acid and solvent production, whereas the acetate production is an important element during acidogenesis and generates ATP. Genes encoding enzymes involved in acetate- and butyryl-CoA-synthesis were cloned, sequenced and expressed. CoA and its derivatives, which are intermediate metabolites for these pathways, were isolated and analyzed to identify regulatory factors for the enzymes involved in such fermentation.

Five genes: *crt*, *bcd*, *etfB*, *etfA* and *hbd*, which encode the central clostridial pathway enzymes crotonase, butyryl-CoA dehydrogenase (BCD), putative electron-transfer flavoprotein (ETF) β- and α-subunits, and β-hydroxybutyryl-CoA dehydrogenase, respectively, were cloned and shown to be clustered in the chromosome. These genes are co-transcribed and form an operon, suggesting that BCD in clostridia might interact with ETFs in its redox function.

Cloning and sequencing studies reveal that *pta* and *ack*, encoding acetate-production-pathway enzymes phosphotransacetylase (PTA) and acetate kinase (AK), respectively, are adjacent in the chromosome.

Primer extension analysis suggests an operon arrangement for these tandem genes. Overexpression of *ack* and *pta* in *C. acetobutylicum* shows that the final ratios of acetate to other major products were higher and also results in a greater proportion of two- versus four-carbon-derived products. Formation of a mutant strain by inactivation of the chromosomal *pta* gene decreased acetate formation. The PTA and AK activities of such a mutant were correspondingly reduced.

Intracellular levels of CoA and its derivatives involved in the metabolic pathways were analyzed using reverse-phase high performance liquid chromatography. During the the acidogenic-to-solventogenic shift, butyryl-CoA concentration increased rapidly, whereas those for free CoA and acetyl-CoA decreased. These observations were accompanied by a rapid increase of solvent-pathway enzyme activity and a decrease of acid-pathway enzyme activity. Levels of acetoacetyl-CoA, β-hydroxy-butyryl-CoA and crotonyl-CoA in crude cell extracts were below detectability. The possible roles of CoA and its derivatives in regulating specific enzyme activity were evaluated.

Acknowledgements

I would like to express my deepest gratitude to my advisor, Dr. Frederick Rudolph, and to my co-advisor, Dr. George Bennett, for their insightful guidance and remarkable patience throughout my graduate school years.

I would also like to thank Dr. Campbell, Dr. Palmer, and Dr. San for their valuable suggestions as members of my thesis committee.

I am thankful to the people in both Dr. Rudolph's and Dr. Bennett's labs for their help and friendship, especially Drs. Bruce Cooper, Kathleen Stim-Herdon, John Wong, Edward Green, Xiao-lu Shi and Mike Peredeltchouk, and to Stephanie Wardwell, Edward Belouski, Vera Sideraki, Jenneatte Martinez, Sandra Clark and David Watson, for teaching me so many lab techniques and giving me so much helpful advice. Many others in the department have graciously helped me but they are too numerous to mention here.

Thanks should also be given to my husband John, for his constant encouragement and patience in advising me regarding, and his skillful editing of my difficult writing on numerous occasions and finally to my two daughters, Li and Lin, for their pure love and trust.

Table of Contents

List of Figures

List of Tables

List of Abbreviations:

AAD	Acetaldehyde/alcohol dehydrogenase
AADC	Acetoacetate decarboxylase
ACD	Acyl-CoA dehydrogenase
ADH	Alcohol dehydrogenase
AK	Acetate kinase
ATCC	American Type Culture Collection
ATP	Adenosine triphosphate
BAD	Butyraldehyde dehydrogenase
BCD	Butyryl-CoA dehydrogenase
BDH	Butanol dehydrogenase
BHBD	β-hydroxybutyryl-CoA dehydrogenase
BK	Butyrate kinase
BSA	Bovine serum albumin
CGM	Clostridium growth medium
CoA	Coenzyme A
CoA Tr	Acetyl-Coenzyme A:acetate/butyrate:Coenzyme A transferase
CoQ	Coenzyme Q
DEAE	Diethylaminoethyl
DTT	Dithiothreitol
ECH	Enoyl-CoA hydratase
Em	erythromycin
ETF	electron-transfer flavoprotein
FAD	Flavin adenine dinucleotide (oxidized form)
GC	Gas chromatography

HAD	Hydroxyacyl-CoA dehydrogenase
HPLC	High preformance liquid chromatography
kb	Kilo base pair
kDa	kilodalton
Ki	Inhibition constant
Km	Michaelis constant
LB	Luria broth
MACD	Medium-chain specific acyl-CoA dehydrogenase
Mr	Protein molecular mass
NAD	Nicotinamide adenine dinucleotide (oxidized form)

This thesis is dedicated with sincere gratitude to my paternal grandmother and my parents, who have sacrified so much of themselves for their children.

Chapter 1. Introduction

The bacterium *Clostridium acetobutylicum*, the investigative history of acetone-butanol fermentation for this organism, a summary of related biochemical, physiological and molecular studies, and the beneficial genetic manipulation of *C. acetobutylicum* are introduced. The chapter concludes with a clear statement of experimental goals for this study using this bacterium.

1.1 Background

1.1.1. Saccharolytic clostridia

Several species of the bacterial genus *Clostridium* are known to ferment carbohydrates to produce a variety of extracellular products that include alcohols, acids and hydrogen and therefore are collectively referred to as the saccharolytic clostridia (Doelle, 1975). Such species are strictly anaerobic, fermentative microorganisms, and have the ability to form endospores, which give these bacteria unusual resistance to heat and other adverse conditions (Brock, 1979). Some saccharolytic clostridia, such as *C. pasteurianum*, produce acetic and butyric acids, hydrogen and carbon dioxide as major products and are commonly called the butyric acid-producing clostridia. Others, which are the most well known, such as *C. beijerinckii* (*C. butylicum*), *C. aurantibutyricum* and *C. acetobutylicum*, produce industrial solvents, including ethanol and butanol, in addition to the products mentioned above, and are generally classified as solvent-producing clostridia.

C. acetobutylicum produces the highest yields of acetone and butanol from a variety of starchy substrates and is the most common species employed for the studies of acetone/butanol-producing fermentation. A variety of strains have been reported. The type strain American Type Culture Collection (ATCC) 824 is used throughout this study. Other strains that have been intensively studied include P262, Deutsche Sammlung von Mikroorganismen (DSM) 792 and National Collection of Industrial and Marine Bacteria (NCIMB) 8052. Another widely reported species, *C. beijerinckii*, produces isopropanol instead of acetone. *C. aurantibutyricum*, on the other hand, produces both acetone and isopropanol in addition to butanol (Doelle, 1975; George and Chen, 1983; Gottschalk, 1979).

Recent studies have shown that the commonly used *C. acetobutylicum* contains a heterologous collection of different species (Woods, 1995). Two groups of solvent-producing clostridia, one is amylolytic and the other is saccharolytic, are quite different in phylogenetics. *C. acetobutylicum* ATCC 824 and DSM 1731 are typical strains of amylolytic group, whereas *C. acetobutylicum* P262, NCIMB 8052 and N1-4 belong to the saccharolytic solvent-producing clostridia. In order to design strategies to improve the strains which is suitable for industrial application, it is of great importance to understand the different *Clostridium* strains. For example, the strain P262 is by far the best naturally derived strain for solvent production, however, it is impossible to transform this strain using any of the current techniques (Woods, 1995). The rationale for choosing strain ATCC 824 throughout this study are: (1) this strain has been the most widely studied among strains of *C. acetobutylicum*, (2) mutants of this

strain exist which are useful for applied and fundamental studies, (3) the cloning resources are available with this strain, (4) electroporation can be used in transformation and therefore, in genetic manipulation of the strain.

1.1.2. Industrial fermentation producing acetone and butanol

Acetone/butanol clostridial fermentation producing acetone and butanol was one of the chief sources for these solvents from about 1914 until just after World War II, and the history of this process has been thoroughly reviewed (Jones and Woods, 1986). There are many advantages in using *C. acetobutylicum* for fermentation process. For example, anaerobic fermentation is relatively inexpensive to maintain compared to those which are aerobic, where efficient oxygen mixing is required. In addition, clostridia accumulates a high surplus of reduction energy during its growth that can be utilized to produce chemicals in significantly higher yields.

Recently, however, the more economical use of petrochemicals in producing solvents has virtually eliminated commercially based fermentation. There are several important reasons to account for this discontinued use: (1) significantly higher raw material costs, (2) very low overall reactor productivity because solvents are not produced until the end of a long batch process, (3) high product separation cost because of solvent toxicity to microorganisms, (4) relatively low final yields (approx. 0.3 g solvents/g sugar substrate), and (5) limited product selectivity.

Many improvements have been made since World War II, through significantly improved chemical processing technology, to make the fermentation more economically attractive. Such improvements include changing from batch to continuous mode of operation to increase reactor productivity, and a more efficient use of substrates through biomass recycling. Now, with recent advances in genetic engineering, interest has focused again on the possibility that solvent-producing clostridial metabolism can be commercially viable. The genetic improvements have been largely focused on (1) modification or isolation of strains with increased solvent, especially butanol tolerance therefore reduced separation cost, (2) modification of the metabolic pathways, by enhancing the enzyme activity of desired pathway and eliminating those in the less desired pathway; therefore product selectivity, yield and productivity will be improved.

Even with significant improvements as discussed above, the acetone/butanol fermentation may still not be able to compete economically with the petro-chemical industry for sometime due to the relative abundance of petroleum. Nevertheless, this fermantation exhibited many features that may be common to several other fermentations of more immediate utilization and may thus serve as a valid model system for understanding the regulation and genetic character of complex primary metabolism. This is particularly true that the biochemistry, physiology and molecular biology of *C. acetobutylicum* have been studied extensively and much is known about the organism and the biochemical pathways for product formation.

1.2. Literature overview

1.2.1. Biochemistry and physiology of acid and solvent production

The biochemical pathways of the acetone-butanol fermentation have been relatively well understood, even though there are some specific areas are still need to be defined (Doelle, 1975; Gottschalk, 1979; Jones and Woods, 1986). These pathways are shown in Fig. 1.1. In batch cultures, the typical acetone-butanol fermentation proceeds in two distinct phases. In the acidogenic phase, the organism grows exponentially and produces acetate and butyrate. The cells are highly motile and exhibit a rod-shaped morphology. The external pH of the medium decreases because of acid accumulation. In the solventogenic phase, the organism grows slowly and the culture produces acetone, butanol and ethanol, with the pH increasing slightly because of acid reassimilation. The cells are nonmotile, encapsulated and exhibit a cigar-shaped morphology. The transition from the acidogenic to the solventogenic phase is regulated by complex physiological and genetic mechanisms which are still under extensive investigations.

Three key intermediates located at the branched points in the central fermentation pathways, acetyl-CoA, acetoacetyl-CoA and butyryl-CoA, lead to the production of both acids and solvents. Acetyl-CoA is produced from glycolysis product, pyruvate, in the presence of coenzyme A (CoA) and pyruvate-ferredoxin oxidoreductase. Acetoacetyl-CoA is formed from acetyl-CoA in a pathway catalyzed by thiolase, this CoA derivative is then converted to butyryl-CoA in a reaction catalysed by β-

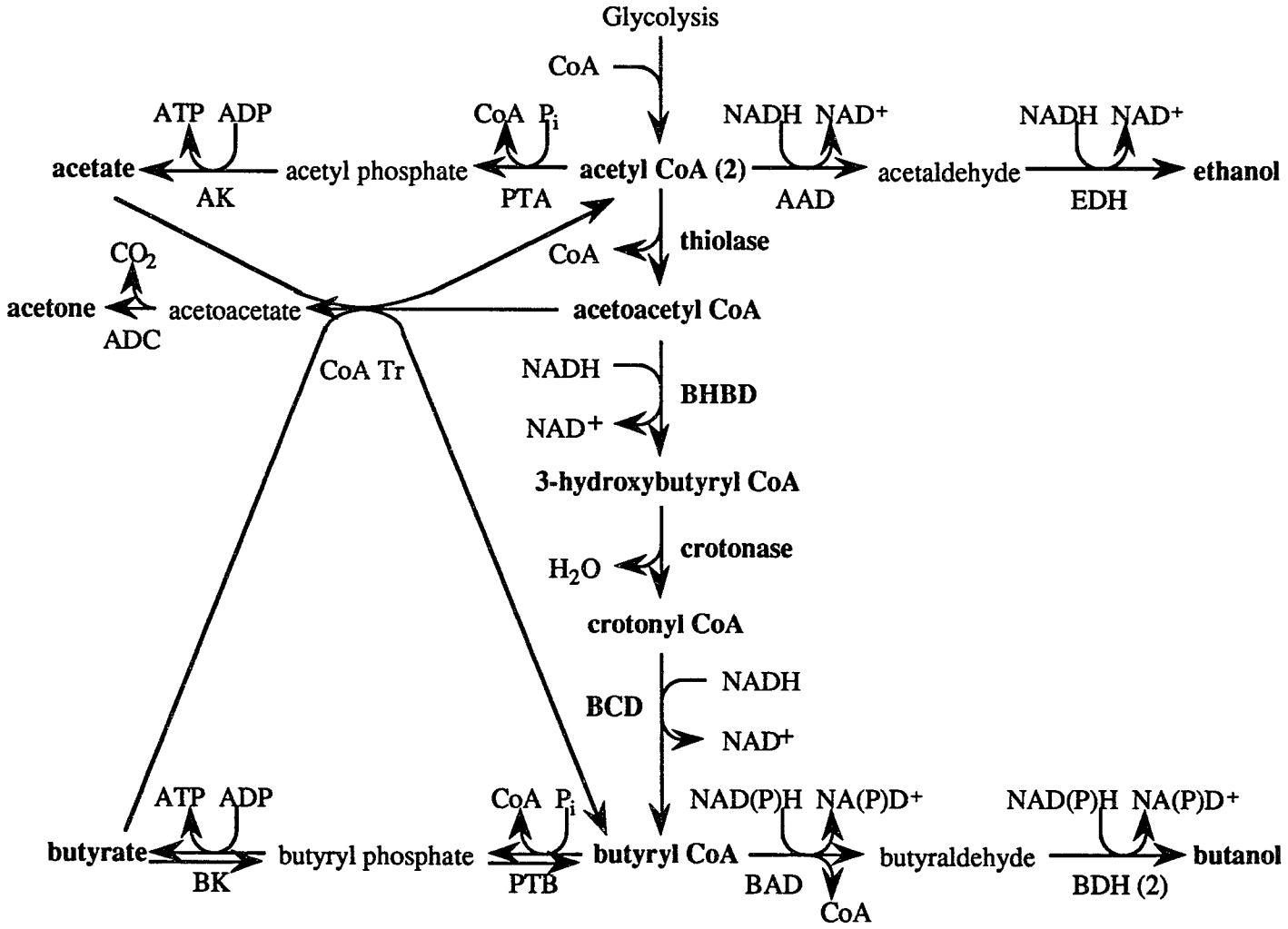

Fig. 1.1. Metabolic pathways of *Clostridium acetobutylicum*

hydroxybutyryl-CoA dehydrogenase (BHBD), crotonase and butyryl-CoA dehydrogenase (BCD).

During acidogenesis, acetate and butyrate are produced from acetyl-CoA and butyryl-CoA by two similar pathways involved functionally distinct ezymes. First, acetyl- and butyryl-phosphate are produced from their corresponding CoA-derivatives in reactions catalysed by phosphotransacetylase (PTA) and phosphotransbutyrylase (PTB). The acyl-phosphates are then converted to acetate and butyrate by acetate kinase (AK) and butyrate kinase (BK) with the generation of ATP. During solventogenesis, acetyl-CoA and butyryl-CoA function as key intermediates for ethanol and butanol production, also through two similar pathways involved functionarily distinct ezymes. First, acetylaldehyde and butyraldehyde are produced from the corresponding CoA derivatives in reactions catalysed by acetylaldehyde and butyraldehyde dehydrogenase (AAD and BAD, respectively). Acetylaldehyde and butyraldehyde are then converted to ethanol and butanol in reactions catalyzed by alcohol and butanol dehydrogenase (ADH and BDH, respectively).

One of the major solvent products, acetone, is produced through reassimilation of acetate and butyrate to their corresponding CoA derivatives. This reassimilation is directly coupled to the irreversible production of acetoacetate from acetoacetyl-CoA catalysed by acetoacetyl-CoA:acetate/butyrate:CoA transferase (CoA Tr). During the conversion of acetyl-CoA to acetoacetyl-CoA, CoA Tr has been shown to be able to use acetate or butyrate as the CoA receptor (Andersch et al., 1983). The

irreversible reaction catalyzed by acetoacetate decarboxylase is suggested to shift the equilibrium of the CoA Tr reaction toward the formation of acetoacetate, acetone is eventually produced from these two reactions.

At the end of the fermentation, the cells undergo sporulation in the presence of excess glucose and the fermentation stops. The formation of endospores allows the cells to withstand long term storage. However, in some conditions such as repeated transfer to fresh media, cells become degenerate and lose the solventogenic capacity (Jones and Woods, 1986). The inducing condition for degeneracy is not known.

1.2.2. Molecular studies of acid and solvent production

The acid (acetate and butyrate) and solvent (acetone, ethanol and butanol) production pathways, as well as the central fermentation pathway leads to acid and solvent production have been extensively studied at the molecular level over the past ten years. Many of these enzymes have been purified and the encoding genes cloned. A summary of the well-studied genes and enzymes involved in these pathways in *C. acetobutylicum* ATCC 824 was shown in Table 1.1.

The enzymes involved in ethanol and butanol production, AAD, ADH and BAD, have not been purified from *C. acetobutylicum*. Evidence suggested that there are two types of each of these dehydrogenases, one is NADH dependent and the other is NADPH dependent (Dürre et al., 1987, Peterson et al., 1991). However, it is still not clear the number of genes encoding these enzymes.

Table 1.1. Genes and enzymes involved in acid and solvent production from acetyl-CoA in *C. acetobutylicum*.

Pathway	Enzyme	MW (Kda)	Purification	Gene	Cloning	Sequencing
Acetate	PTA	No report		*pta*	This study	This study
	AK	No report		*ack*	This study	This study
Butyrate	PTB	31 (8 X*)	Wiesenborn et al., 1989b	*ptb*	Walter et al., 1993	Cary et al., 1988
	BK	39 (2 X)	Hartmanis, 1987	*buk*	Walter et al., 1993	Cary et al., 1988
Acetone	CoA Tr	23 (2 X) (a)	Wiesenborn et al., 1989a	*ctfA*	Cary et al., 1990	Petersen et al., 1993
		24 (2 X) (b)	Wiesenborn et al., 1989a	*ctfB*	Cary et al., 1990	Petersen et al., 1993
	AADC	28 (8 X)	Peterson et al., 1990	*adc*	Peterson et al., 1990	Petersen et al., 1993
Ethanol	AAD	No report		*aad*	Cary et al., 1990	Nair et al., 1994
	ADH	No report		*aad*	Cary et al., 1990	Nair et al., 1994
Butanol	BAD	No report		*aad*	Cary et al., 1990	Nair et al., 1994
	BDH	42 (2 X) (I)	Welch, 1989	*bdhB*	Peterson et al., 1991	Walter et al., 1992
	(NAD-dep.)	42 (2 X) (II)	Welch et al., 1989	*bdhA*	Peterson et al., 1991	Walter et al., 1992
Central	Thiolase	44 (4 X)	Wiesenborn et al., 1988	*thl*	Peterson et al., 1990	Stim-Herndon et al., 1995
	BHBD	No report		*hbd*	This study	This study
	Crotonase	43 (4 X)	Waterson et al., 1972	*crt*	This study	This study
	BCD	No report		*bcd*	This study	This study

* Number of the subunit.

A specific gene encoding BAD has not yet been cloned. However, an NADPH-dependent alcohol dehydrogenase encoding gene, *adh1*, has been cloned in *C. acetobutylicum* P262 (Youngleson et al., 1989). The expressed gene has activity for both butanol and ethanol. A multifunctional aldehyde/alcohol dehydrogenase (AAD) was also suggested in playing a role in butanol formation (Nair et al., 1994). Expression of the *aad* gene in the *aad* mutant strain *C. acetobutylicum* M5, restored the butanol production (Nair and Papoutsakis, 1994). In addition, inactivation of the *aad* gene resulted in an almost complete elimination of butanol production (Green and Bennett, 1996). The involvement of AAD in butanol production was also demonstrated by mRNA analysis (Sauer and Dürre, 1995). The gene encoding AAD, *adhE* (an *aad* homolog of different clostridial strains), has been cloned and sequenced from *C. acetobutylicum* DSM 792 (Fischer et al., 1993). The *adhE* is adjancent to the genes encoding the two subunits for CoA Tr (*ctfB* and *ctfA*) and these clustered genes form a *sol* operon. In addition, the *sol* operon is located directly upstream of *adc*, encoding AADC, with a convergent direction of transcription.

Two butanol dehydrogenase isozymes (I and II) have been purified (Welch et al., 1989) and the encoding genes, *bdhB* and *bdhA* (Peterson et al., 1991, Walter et al., 1992) respectively, have been cloned. The *bdhA* and *bdhB* genes are linked in adjacent monocistronic operons, each of which is controlled by a single promoter. Butanol dehydrogenase I is twice as active toward butyraldehyde than acetaldehyde, whereas butanol dehydrogenase II is 46-times more active toward acetaldehyde than butyraldehyde (Welch et al., 1989).

The genes and enzymes involved in the acetone formation have been well studied and described (Peterson, 1991, Peterson et al., 1993, Fischer et al., 1993, Gerischer and Dürre, 1990 and 1992). The genes and enzymes involved in the central and acid-fermentation pathways are going to be detailed in later chapters of this study.

1.3. Genetic manipulation

Genetic manipulation of bacteria depends on the development of gene transfer techniques. The genetic study of clostridial pathway genes has been largely restricted to cloning into *E. coli*, primarily because it is difficult to transfer DNA back into *C. acetobutylicum*. However, several plasmid origins of replication have recently been found to be functional in *C. acetobutylicum*, such as the *B. subtilis* plasmid pIM13 and the *C. butylicum* cryptic plasmid pCBU2 (Williams et al., 1990; Lee et al., 1992a and 1992b; Mermelstein and Papoutsakis, 1993). From these plasmids, several shuttle vectors were constructed that contain functional origins of replication for both *E. coli* and *C. acetobutylicum*. These accomplishments make it possible to reintroduce genes into *C. acetobutylicum*. In addition, recent development of gene-inactivation systems via integrational plasmids (Wilkinson and Young, 1994, Green and Bennett, 1996) had made it possible to inactivate the specific gene in the wild-type strain, permitting the study of the physiological roles of its encoded enzyme, and eventually resulting in genetic engineering schemes.

1.4. Research goals

Recent advances in recombinant DNA methods allow for the possibility of restructuring metabolic networks so that specific pathways in C. *acetobutylicum* can be either added to, enhanced, or eliminated (Mermelstein et al., 1994, Green and Bennett, 1996). The commercial potential of the clostridial fermentation for solvent production has therefore grown because of the development of such metabolic engineering. However, successful genetic manipulation still requires a better understanding of gene regulation. The cloning and overexpression of genes encoding enzymes in the fermentation pathways, for example, will provide materials for gene inactivation or overexpression, enzyme analysis and progressive metabolic studies. Such studies not only make possible the generation of efficient strains for industrial applications, but also provide a better understanding of the functions of metabolic enzymes and the factors controlling their expression. The objectives of this project, therefore, are the cloning and characterization of the genes encoding enzymes involved in the acetate production as well as those of the central fermentation pathway. In conjuction with the above, the levels of intermediates involved in these pathways, specifically free CoA and its derivatives, are measured to determine the influencing roles of these metabolites in regulating these reactions.

Chapter 2. Materials and Methods for Gene Manipulation

To follow is a listing of all the bacteria, plasmids and bacteriophage used in this study. The techniques used in DNA manipulation, including purification, ligation, concentration, methylation and transformation are described in detail. This chapter also presents the enzymatic and RNA studies related to the gene cloning performed and ends with a brief description of the computer programs used in analyzing the DNA data.

2.1. Bacterial strains, plasmids and bacteriophage

The bacterial strains used in this study are listed in Table 2.1. The plasmids and phage employed for this study are described in Table 2.2. The restriction maps of the *C. acetobutylicum*/*E. coli* shuttle vectors and their corresponding methylating plasmids used in this study are shown in Figs. 2.1 and 2.2, respectively.

2.2. Maintenance and growth conditions of bacteria and phage.

C. acetobutylicum ATCC 824, the wild type strain, was stored as endospores in a corn mash medium (CMM, McLaughlin et al., 1985) at 4°C. Wild-type and mutant vegetative cells were grown inside an anaerobic chamber in a clostridium growth medium (CGM), as described previously (Ross et al., 1985). Colonies were grown on reinforced clostridial medium plates (RCM, DIFCO) at 37°C and maintained at room temperature inside the chamber. The inoculation of cultures between different media was performed as described (Wong, 1995). Media were supplemented with 100 ug/ml erythromycin (Em) when required.

Table 2.1. Bacterial strains employed in this study.

Strains	Function	Characteristics	Source or reference
C. acetobutylicum			
ATCC 824	DNA/RNA isolations		ATCC
824::pta$^-$	*pta*-knockout integrant	AK$^-$, PTA$^-$	This study
M5	Non-solventogenic mutant	solventogenic enzymes deficient	Clark et al., 1989
2BBD	reduced solvent production	2-bromobutyrate^R	Clark et al., 1989
2BBR	reduced solvent production	CoA Tr$^-$, 2-bromobutyrate^R	Clark et al., 1989
34	reduced solvent production		Sass and Bennett, 1993
E. coli			
Q358	Phage propagation	*hsdR*$_k^-$, *hsdM*$_k^+$, *supF*, *Ø80*^{r}	Maniatis et al, 1982
LE392	Phage library construction	F$^-$, *hsd*R514 (r_k^-, m_k^-), *sup*E44, *sup*F58 *lac*Y1, *gal*K2, *gal*T22, *met*B1, *trp*R55, λ^-	Murray & Thompson, 1986
ER2275	Methylation	*rec*A$^-$ *mcr*BC$^-$	New England BioLabs
XL1-Blue	Subcloning	*hsdR17* ($r_k^- r_m^+$)[*F' proAB lacI*^{q} *lacZΔM15 Tn10* (*Tc*^{R})]	Bullock et al., 1987

Abbreviations: *rec*A$^-$, homologous recombination abolished; *mcr*BC$^-$, lacking methycytosine specific restriction system

Table 2.2. Bacteriophage and plasmids employed in this study.

Plasmids/phage	Function	Characteristics	Source or reference
Plasmids			
pUC19	Subcloning	ColE1 ori, Ap^R	Yanisch-Perron et al., 1985
pJC4	Integrative vector	ColE1 ori, Em^R, Tc^R	Lee et al., 1992a
pIA	Shuttle vector	p15A ori, pIM13 ori, Cm^R, Em^R	Wong, 1995
pSYL2	Shuttle vector	pCBU2 ori, ColE1 ori, Tc^R, Em^R	Lee et al., 1992b
pAN1	Methylating plasmid	p15A ori, Ø3TI, Cm^R, Tc^R	Mermelstein et al., 1993
pBA	Methylating plasmid	ColE1 ori, Ø3TI, Ap^R	Wong, 1995
pUC-AKX	Subcloning of partial *ack*	same as pUC19, AK^-, PTA^-	This study
pUC-PTAK	Subcloing of *pta* and *ack*	same as pUC19, Ap^R	This study
pIA-PTAK	Expression of *pta* and *ack*	same as pIA, Cm^-, AK^+, PTA^+	This study
pJC4-PTAK	Inactivation of *pta* and *ack*	ColE1 ori, Em^R, AK^-, PTA^-	This study
pb37	Subcloning of *hbd*	same as pUC19, $crotonase^-$, $BHBD^+$	This study
pC10	Subcloning of *BCS* operon	same as pUC19, $crotonase^+$, $BHBD^+$	This study
pSYL2-BCS	Expression of *BCS* operon	same as pSYL2, $crotonase^+$, BCD^+, $BHBD^+$	This study
Bacteriophage (EMBL3)			Frischauf et al., 1983

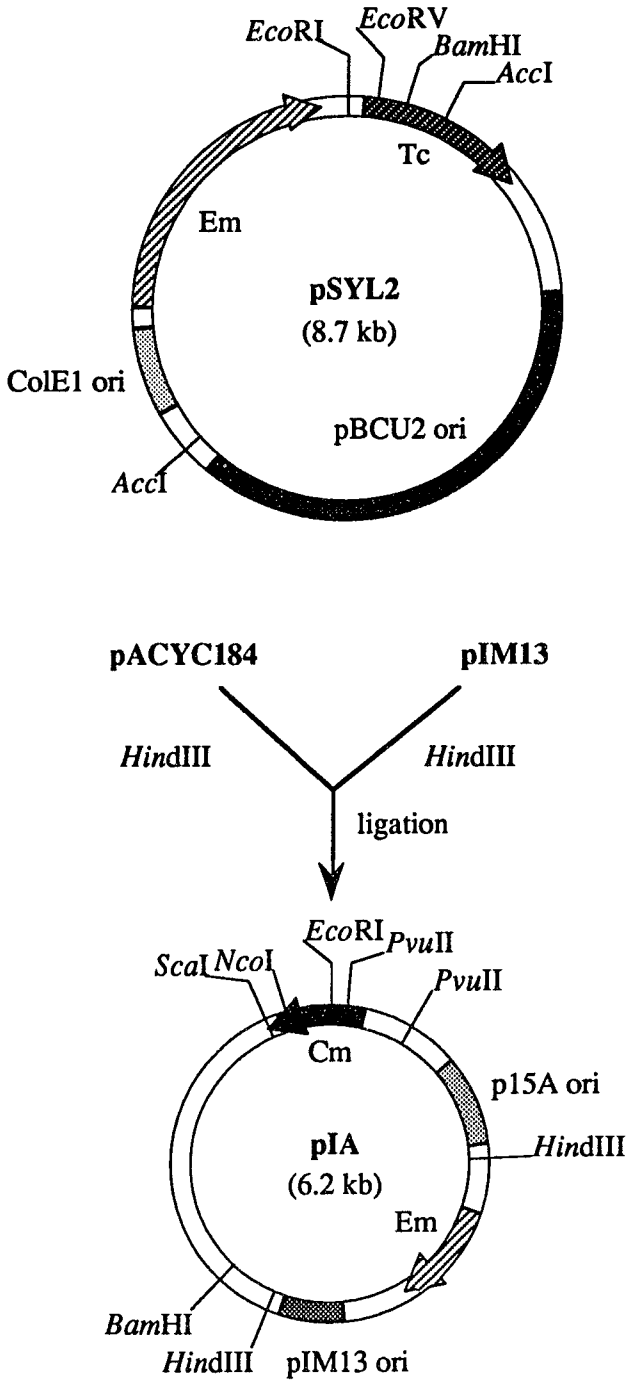

Fig. 2.1. Restriction maps of *C. acetobutylicum*/*E. coli* shuttle vectors.

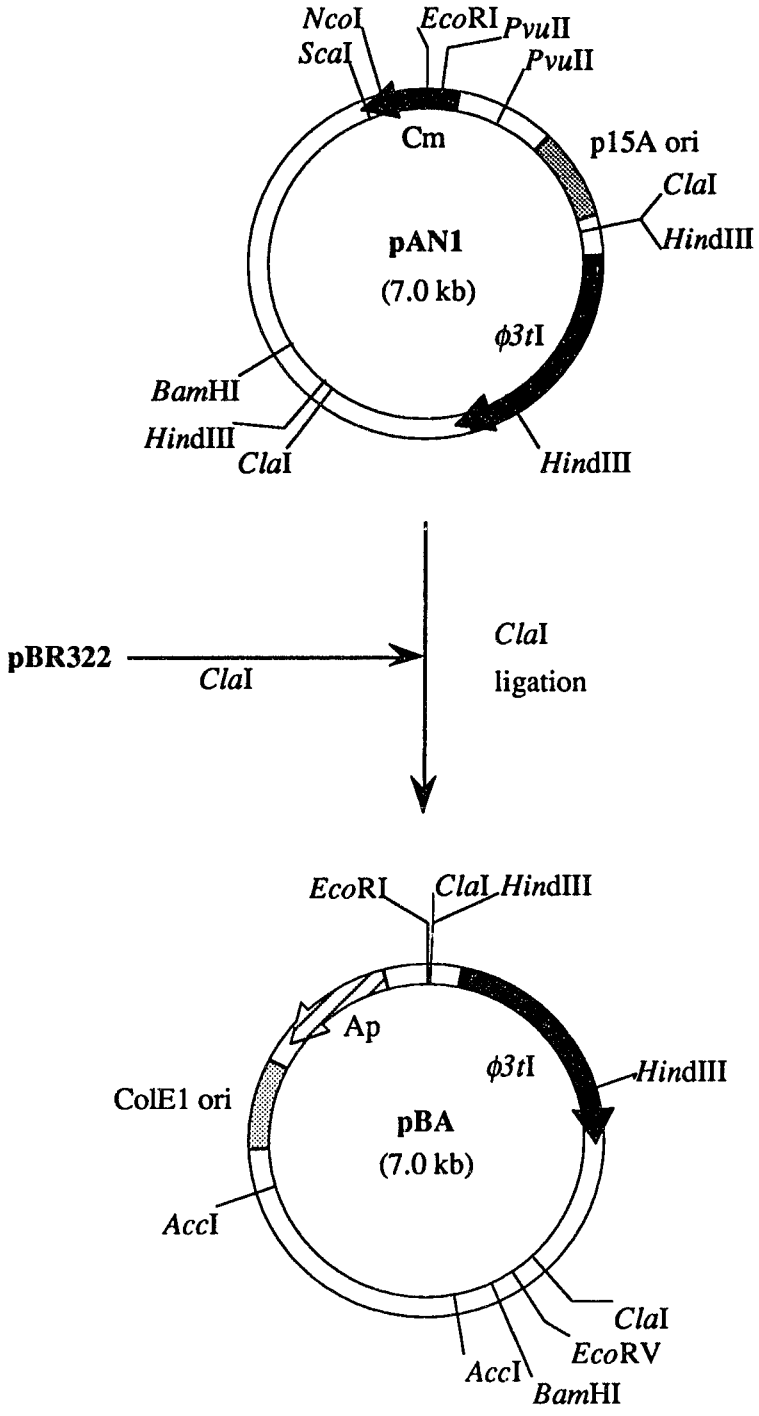

Figure 2.2. Restriction maps of methylating plasmids.

E. coli was routinely grown in a Luria-Bertani (LB, Maniatis et al., 1982) medium aerobically at 37°C. Media were supplemented with ampicillin (Ap, 50 ug/ml), erythromycin (250 ug/ml), chloramphenicol (Cm, 32 ug/ml) or tetracycline (Tc, 10 ug/ml) as required. For long term storage, strains were stored as glycerol stocks (50% V/V) at -20°C. For short term storage, strains were stored on LB plates at 4°C.

Bacteriophage was propagated using a lambda medium (Maniatis et al., 1982) containing a 1.5% bottom agar and a 0.7% top agarose. Phage lysates were collected and stored in a storage medium solution (SM, Maniatis et al., 1982) at 4°C. For long term storage, the packaged phage was aliquoted, with the addition of 5% (w/v) DMSO and 1% gelatin, and was stored at -80°C.

2.3. DNA isolation and manipulation.

2.3.1. Genomic, phage and plasmid DNA isolation. Rapid, small-scale plasmid DNA isolation was performed using the alkaline lysis method (Maniatis et al., 1982). Large-scale preparation of plasmid DNA was done using a Qiagen plasmid purification kit according to the manufacturer's instructions. Phage DNA was prepared by the rapid-plate lysate method as described (Maniatis et al., 1982). Genomic DNA was isolated using a Puregene DNA Isolation Kit (Gentra Systems, Inc), except that a phenol:chloroform:isoamyl alcohol (25:24:1) step was added to increase the purity and the stability of the genomic DNA. The DNAs were resuspended in a TE (Maniatis et al., 1982) or de-ionized water and stored at 4°C or -20°C as required.

2.3.2. Restriction digestion and DNA separation. Genomic, phage or plasmid DNAs were digested using the restriction enzymes (Promega, New England Biolabs or Stratagene) according to the manufacturer's instructions. The digested fragments were separated on a 0.8% agarose gel run in a 1xTBE buffer (Maniatis et al., 1982). The DNA was visulized after an ethidium-bromide staining as described (Maniatis et al., 1982).

2.3.3. DNA ligation and concentration. The restriction-enzyme-digested vector DNA was dephosphorylated using calf intestine phosphatase (Promega) to prevent self-religation. To prepare for the insert for DNA ligation, restriction-enzyme-digested DNA fragments were separated by a SeaPlaque low-melting-point agarose (FMC BioProducts) gel, and the desired fragments were purified away from the gel using a GELase (Epicentre Technologies) according to the manufacturer's instructions. The digestion mixture can then be concentrated and washed with the TE buffer using a Microcon-100 microconcentrators (Amicon) according to the manufaturer's instructions. The resulting DNA fragments were then ready for use in ligation. Ligation was performed using T4 DNA ligase (Promega) as described (Maniatis et al., 1982).

2.4. Construction and screening of the phage library. A *C. acetobutylicum* genomic library was constructed in λ-EMBL3 using the Packagene System from Promega. The genomic DNA was partially digested by *Sau*3AI and the 12-to-23 kb fragments were purified using Gelase and then ligated to the *Bam*HI site of the lambda vector EMBL3. A packaging efficiency of 6.7×10^6 pfu/ug DNA was achieved. The titer of the phage library was

determined and the library was screened using the lambda medium as described (Maniatis et al., 1982).

2.5. Design of oligonucleotides as primers for PCR or sequencing. The detailed strategy for designing the oligonucleotides for PCR and sequencing was as described (Peterson, 1991). The synthetic oligos were manufactured by either the department (Dept. of Biochemistry, Rice Univ.), Integrated DNA Technologies, Inc (Coralville, IA) or Retrogen (San Diego, CA). The primers used in this study are listed in Table 2.3.

2.6. PCR. The PCR reaction mixture and procedure were as recommended by the manufacturer (Perkin Elmer Cetus), except that the final concentrations of dATP and dTTP were 250 uM, whereas those for dCTP and dGTP were 150 uM. Such adjustments result from the characteristic that clostridial DNA is AT-rich. Thermal cycling was performed in a DNA cycler (Perkin Elmer Cetus). This procedure consisted of 30 cycles, each with a profile of 0.5 minute at 90°C, 1 minute at 45°C and 1 minute at 65°C, except that the first melting step was at 94°C for 4 minutes and the last elongation step was at 65°C for 8 minutes. PCR products were analyzed using agarose-gel electrophoresis and ethidium-bromide staining.

2.7. Southern hybridization. The PCR probe was radiolabelled using the random-primer DNA labeling kit (GIBCO BRL) and [α-^{32}P]dATP (ICN, 3,000 Ci/mmol). The radiolabelled probe was denatured in a 0.1 N NaOH solution and then purified through a Sephadex G-50 column.

Table 2.3. Synthetic oligonucleotides used in this study. Oligos are mainly used for sequencing unless otherwise indicated

Name	Length	Sequence (5'->3')	Comment
Primers used for genes in central fermentation pathway			
Crt-N6	17 mer	TCCTAAGCTAATAGGTC	
crotonase N5	17 mer	CGAGATTAGTACGGTAA	
crotonase C3	17 mer	TTACCGTACTAATCTCG	
crotonase N4	18 mer	GGCAGATGAAGCATTAAG	
crotonase C2	17 mer	ATGGTAACTACAGCAAC	primer ext.* (*crt*)
crotonase N3	19 mer	GTCATCCTTGAAAAGGAAG	
crotonase C1	19 mer	CTGGTTGACCAAATCTTGC	
crotonase N2	19 mer	TAGGAGGCGGATGCGAAAT	
FP-C13	18 mer	CTTAACAGCTACTGGAGC	
FP-N12	18 mer	TGCTCCAGTAGCTGTTAA	
FP-C12	19 mer	CCATCATACCATACTGACC	primer ext.* (*bcd*)
FP-N11	20 mer	AAGAGTATGGTGGCGCAGGT	
FP-N10	19 mer	ACTAATGGAGGAGTTGCAG	
FP-C11	18 mer	CCTTTAGTTCTGTCAGTC	
FP-N9	22 mer	GAAGCAAGAGCTTACATGAAGG	
FP-C10	21 mer	GGCTTCTTCCAAATTGTTTTC	
FP-N8	19 mer	GCAAGAGCTAAGCTTCATG	
FP-C9	19 mer	CCATTGCTACATTTGCCAG	
FP-N7	19 mer	TAAGAGAAGGAGTTCCATC	
FP-C8	19 mer	ATTGATGCAACTCCTTCTC	primer ext.* (*etfB*)
FP-N6	19 mer	GCTGGAAGGCAGGCTATAG	
FP-C7	19 mer	CCTGAGCTGTATCTCCATC	

Table 2.3. Continued

Name	Length	Sequence (5'->3')	Comment
FP-C6	20 mer	GTTGGTGAACCTTTAAGACC	
FP-C5	20 mer	CTACTATCTATATCATCGGC	non-annealing
FP-N5	19 mer	GAAGTTATTGATAAGCCTG	
FP-C4	19 mer	GAGACAACATATCAGCTGC	
FP-N3	21 mer	GGATTTATTATCTCATGGAGC	
FP-C3	24 mer	GCTGCTAAAACCTTATCTGCCTCC	
FP-N4	19 mer	TGTTCAGACCACAGACCAC	
FP-C2	19 mer	CATCAGAAACATTTGCATC	
FP-N1	18 mer	GGACCTTCAAGTAGGTCA	
FP-C1	22 mer	GAGTTGGTCTTACAGTTTTACC	
BHBD-N6	20 mer	GTTGTACCAGAATTAATAGC	
BHBD-C8	20 mer	TAGCAGCTTTAACTTGAGCT	
BHBD-N5	20 mer	GGTGCAGGTACTATGGGTTC	
BHBD-C7	21 mer	CCTGCACCTATAACACATACC	primer ext (*hbd*)
BHBD-C6	21 mer	ATCGCAATCAGCTGCCATATT	
BHBD-N3	23 mer	ATGCATTTCTTTAA T/C CCAGCTCC	
BHBD-C3	21 mer	GGAGCTGG G/A TTAAAGAAATGC	
BHBD-4	27 mer	CCAGGATTTGTTGTAAA CAGAATC T/A T A/T	N-terminal primer for *hbd*-specific PCR probe
BHBD-C4	19 mer	CCAACTGCTTCATTAATCATTGG	
BHBD-C	27 mer	ATAATCATAAAA T/A CCT TT T/A CC T/A GTTTT	C-terminal primer for *hbd*-specific PCR probe
BHBD-end	23 mer	GCAGGATGGCTTGGAAGAAAATC	

Table 2.3. Continued

Name	Length	Sequence (5'->3')	Comment
BHBD-end3	20 mer	GAGAATGGTAACTATATTGG	*hbd* downstream
BHBD-C10	20 mer	CCAATATAGTTACCATTCTC	*hbd* downstream
CC-1	19 mer	CAAAAGGATCCTGCCTTAA	*hbd* downstream
BHBD-end4	21 mer	CAAGGGTAAGATTTACTATGC	*hbd* downstream
BHBD-C9	22 mer	CATGAAGCTTATCTACTGTAGG	*hbd* downstream
BHBD-end5	20 mer	GGTAGCTGATTGTATAATGC	*hbd* downstream
Nonannealing primers designed for *hbd*-specific PCR probe			
BHBD-N2	21 mer	AAGACAGATCTATAGCAATAG	
BHBD-C2	19 mer	CATTGATAATGGGATCTTG	
BHBD-1	27 mer	ATCTAATTCAGCAAAAA-TTTCTTTTTT	
BHBD-3	24 mer	TTTCATAGCTGCATCGATATCTTC	
BHBD-2	27 mer	A/T A A/T GATTCTGTTTACAACAAATCCTGG	
Primers used for genes involved in acetate-production pathway			
PTA-C5	18 mer	GCTGAATACAACCAACTG	upstream of *pta*
PTA-N4	17 mer	GGTGATGAATATGTCCA	upstream of *pta*
PTA-C3	17 mer	CTCCCTTCATAATGCCA	
PTA-N3	17 mer	TGGCATTATGAAGGGAG	
PTA-C4	20 mer	GTCTTGCTTAGCACACTCCC	primer ext* (*pta*)
PTA-C6	20 mer	GCACACTCCCATATGCTTTC	primer ext* (*pta*)
PTA-C7	21 mer	CACCTTCAGCTAATATTATCC	primer ext* (*pta*)
PTA-N2	17 mer	AAGTACATCTCTAGTGC	

Table 2.3. Continued

Name	Length	Sequence (5'->3')	Comment
PTA-C2	17 mer	GTGATGTCTCTGGATCC	
PTA-N1	17 mer	GTGAAGAGGGTCTTTTA	
PTA-C1	17 mer	TCTGATGTTGGGTTAGG	
AK-C8	17 mer	GATCCGGTCTGAATTTC	
AK-N9	17 mer	G/C TTCAGCTTGATGCTGC	
AK-C7	17 mer	GATGAACTACCGCAGTT	primer ext* (*ack*)
AK-C6	17 mer	ATTCTGTGTCCTACTGC	
AK-N	28 mer	CATAGAGT A/T GT T/A CAT GG A/T GG A/T GAAAAAT	N-terminal primer for *ack*-specific PCR
AK-C	29 mer	GGCAT T/A GTTTGATGAAA T/A GC T/A GTATCAAA	C-terminal primer for *ack*-specific PCR
AK-N2	19 mer	GCATTCCATCAAACTATAC	
AK-N3	18 mer	GGAGATATGGACCCAGCA	
AK-C3	18 mer	ATCTCCACTTCTAGTTCC	
AK-N4	17 mer	CATGGATTATCTAGGAA	
AK-C4	18 mer	CCATTGGTATTCCCATAG	
AK-N7	17 mer	GGCTGCGTTAATGATTT	
AK-C5	17 mer	CATCAGCATCT A/G ACATG	non-annealing
AK-N5	17 mer	CTTATTGACTTAGGAGC	
AK-N6	17 mer	CTTATTGACTTAGGAGC	
orfX-C1	19 mer	CATACCAAGCTGAATGTCG	primer ext* (*orfX*)

* Oligonucleotides used for primer extension analysis.

Genomic, phage or plasmid DNAs were digested to completion using the desired restriction enzymes and then separated by electrophoresis. The DNA was transferred to Immobilon-N filters (Schleicher & Schuell) according to the manufacturer's instructions. Phage plaques were blotted to the nitrocellulose membranes (Schleicher & Schuell) according to the methods of Benton and Davis (1977).

Blotted filters were prehybridized in a buffer consisting of 5x SSPE (Maniatis et al., 1982), 5x Denhardt's solution, 0.5% sodium dodecyl sulfate (SDS) and 100 ug per ml of denatured, sheared salmon sperm DNA for one hour at 42°C. After prehybridization, the radiolabeled probe was added to the buffer. Following overnight incubation at the same temperature, the filters were washed at increasingly higher temperatures until a band exhibiting a strong hybridization signal could be detected. Typically, the filters were washed twice for 15 minutes each at 42°C in a 2x SSPE-0.1% SDS. A final 20-min wash in a 1x SSPE-0.1% SDS at 50°C was conducted before autoradiography at -80°C.

2.8. Cell transformation. Plasmid transformation to *E. coli* cells was routinely performed using competent cells prepared by the RbCl method of Raleigh (1984) or by the method of Chung and Miller (1988). Plasmid transformation to *C. acetobutylicum* was performed by electroporation (Wong, 1995). Prior to the transformation, plasmids were methylated by transforming the plasmids to *E. coli* ER2275 harboring the corresponding methylating plasmid (see Table 2.2), which expresses the *B. subtilis* phage 3T methytransferase and renders the plasmids resistant to the clostridial endonuclease Cac824I (Mermelstein and Papoutsakis, 1993a). The

methylated plasmid DNAs were prepared using the Qiagen method and concentrated and desalted using the Microcon-100 microconcentrators. For integration, approximately 10 ug of methylated plasmid DNA was used and for expression, approximately 0.5 ug of plasmid DNA was used.

2.9. Preparation of cell extracts. Recombinant plasmids were transformed to *E. coli* XL1-Blue or *C. acetobutylicum*. Transformants were grown in either a 50ml LB or CGM supplemented with corresponding antibiotics. After cells reached the stationary phase, transformants were harvested by centrifugation. For assays of AK, BK, PTA, PTB, BHBD and crotonase, cells were resuspended in a 10 ml of 50 mM 4-morpholine propanesulfonic acid (MOPS)-KOH pH7.0 buffer containing 1 mM 1,4-dithiothreitol (DTT). The cell suspension was sonicated in a Model W-225R sonicator (Heat Systems-Ultrasonics, Inc, Farmingdale, NY) at 60% power for 6 (for *E. coli*) or 15 (for *C. acetobutylicum*) minutes at 4°C. Cell debris was removed by centrifugation at 30,000xg for 30 minutes at 4°C.

For BCD assay, cells were resuspended in a 10 ml of anaerobic potassium phosphate buffer (100 mM, pH7.0) and DTT was omitted. The cell suspensions were treated with 1 ml of 40 mg/ml lysozyme for 30 minutes and then disrupted by vigorous vortexing for 10 minutes inside the anaerobic chamber at 0°C. The suspension was capped tightly before it was transfered out from the anaerobic chamber for centrifugation (30,000xg for 30 minutes at 4°C). After centrifugation, the supernatant was transferred into ampules and sealed tightly to prevent contact with the air. All the transfering were conducted inside the anaerobic chamber,

and all the solutions are made and left inside the chamber for at least overnight to get rid of residual oxygen.

2.10. Enzyme assays. All absorbance measurements for enzyme assays were conducted on a Gilford model 250 spectrophotometer. The enzymes, acetyl-phosphate, CoA and CoA-derivatives used for the assays were all obtained from Sigma Chemical Company. The protein concentration was measured by the dye-binding method of Bradford (1976), with 1 mg/ml bovine serum albumin as the standard (Bio-Rad) One unit of activity was defined as the amount of enzyme that converts one micromole of substrate to product per minute. Activity values were corrected against those obtained with control incubations without substrates.

BHBD activity was analyzed in the physiological direction by determining the rate of oxidation of NADH, as measured by the decrease in absorbancy at 340 nm with acetoacetyl-CoA as the substrate (Hartmanis and Gatenbeck, 1984). The reaction mixture included: 200 μM NADH, 1 mM DTT, 50 mM MOPS-KOH (pH7.0), 75 μM acetoacetyl-CoA and the enzyme extract. The reaction was initiated by the addition of either acetoacetyl-CoA or enzyme extract. The extinction coefficient used for NADH was 6.22 $mM^{-1}cm^{-1}$.

Crotonase activity was analyzed in the reverse physiological direction by observing the decreasing absorbance of crotonyl-CoA in the specific absorption band at 263 nm (Hartmanis and Gatenbeck, 1984). The 1-ml reaction mixture contained: 100 mM Tris-HCl, 150 μM crotonyl-CoA and the enzyme extract. The reaction was initiated by the addition of either

the substrate crotonyl-CoA or enzyme extract. The extinction coefficient used for crotonyl-CoA was 6.40 $mM^{-1}cm^{-1}$.

BCD activity was measured by noting the 300-nm spectral absorbance decrease, which resulted from the reduction of the ferricenium ion and demonstrated an extinction coefficient of 4,300 $M^{-1}cm^{-1}$ (Lehman et al., 1990). The assay mixture contained: 100 mM Hepes pH 7.6 buffer, 200 μM ferricenium hexafluorophosphate ($Fc^+PF_6^-$) and 50 μM butyryl-CoA. The addition of the enzyme extract initiated the reaction.

BK and AK activities were analyzed in the acyl-phosphate forming direction as described by Rose (1955), with the addition of the crude extract initiating the reaction. The BK assay was also described in detail by Peterson (1991). For AK activity, potassium acetate was used instead of potassium butyrate. The PTB activity was assayed by using 5,5′-dithiobis-2-nitro-benzoic acid (DTNB, Sigma), which reacts with the sulfhydryl form of CoA (Wiesenborn et al., 1989). The PTA activity was analyzed by monitoring the conversion of acetyl-phosphate to acetyl-CoA coupled to NADH formation through malic dehydrogenase and citrate synthase, as described by Brown et al. (1977). The reaction mixture contained: 100 mM Tris-HCl pH8.0, 5 mM $MgCl_2$, 500 μM NAD^+, 500 μM CoA, 5 mM L-malate, 10 mM lithium acetyl-phosphate, 50 mM β-mercaptoethanol, 1 U/ml malate dehydrogenase, 1 U/ml citrate synthase and crude extract. The extinction coefficient for NADH is 6.22 $mM^{-1}cm^{-1}$.

2.11. Crotonase purification and sequencing. Initially, cloning of the crotonase encoding gene from *C. acetobutylicum* ATCC 824 was attempted

by a researcher in this laboratory through screening of a plasmid library constructed in pBR322. However, that screening was unsuccessful. Therefore, a new approach was used in which the crotonase was first purified and then the N-terminal amino acid sequence was conducted. From the peptide sequencing data, an oligonucleotide was designed and then used as the probe for screening the genomic library constructed on phage EMBL3.

The purification procedure for crotonase was primarily adopted from Waterson et al. (1972), with minor variations. Briefly, *C. acetobutylicum* was grown to late-stationary phase and separated by standard centrifugation. The cells were then sonicated, and the crude extract was processed in the following sequential steps: (1) acid heat treatment (2) acetone precipitation (3) Sephadex G-200 chromatography (4) DEAE-Sephadex chromatography (twice), and finally SDS-PAGE gel separation. After purification, samples were loaded onto a 12% SDS-polyacrylamide Ready gel for the Mini-PROTEAN II Cell (Bio-Rad), and the desired protein band was excised and processed for sequencing as described (Cary et al., 1990). The N-terminal amino acid sequencing data were collected by Richard G. Cook, Baylor College of Medicine, Houston, TX.

2.12. DNA sequence analysis. Recombinant plasmid DNA was prepared for sequencing using a Qiagen purification kit. DNA sequencing of both strands was conducted using the dideoxy-chain termination method (Sanger et al., 1977). The DNA was radiolabeled with [^{35}S]dATP (ICN) and primed with oligonucleotides using a Sequenase Version 2.0 sequencing kit (U.S. Biochemicals) as specified by the manufacturer.

2.13. RNA isolation and primer extension. Total RNA was isolated either using the method as described (Walter et al., 1992), or using RNA Stat-60 (Tel-Test "B") according to the manufacturer's instructions. The purified RNA was dissolved into diethyl pyrocarbonate-treated water and stored at -80°C. For genes involved in the central fermentation pathway, RNA was isolated from stationary phase *C. acetobutylicum* cultures. For genes involved in the acetate-producing pathway, RNA was isolated from the exponential-phase cultures.

Primer extension analyses were performed essentially as described (Gerischer and Dürre, 1992), with minor changes. Basically, oligonucleotides were radiolabelled with gamma ^{32}P (ICN) using a T4-polynucleotide kinase (Promega) according to Promega's procedure. RNA (10 to 20 µg) and 0.2 pmole of the radiolabeled primer were then hybridized in a 10 µl of 1 M KCl-40 mM Tris-HCl (pH7.9) buffer, with the addition of 12.5 U RNasin (Promega). The hybridization was performed by heating the mixture to 80°C for 5 minutes and then incubated at room temperature overnight. After annealing, 10 µl of 5x AMV reverse transcriptase buffer, 5 µl of dNTP mix (5 mM dATP, 5 mM dGTP, 5 mM dCTP and 5 mM dTTP), 20 µl of H_2O and 5 µl (40 Units) of AMV reverse transcriptase were added to the hybridization mixture. The reverse transcription reaction was conducted for two hours at 37°C, with all the reagents used purchased from Promega. The primer extension product was purified and concentrated to 4 µl by using the Microcon-100 microconcentrator, followed by the addition of 4 µl of gel-loading buffer (U.S. Biochemicals) prior to loading on a polyacrylamide sequencing gel.

2.14. Analysis of fermentation products. *C. acetobutylicum* was grown anaerobically in a small-scale 10 ml CGM tube culture. All fermentations using recombinant 824 strains were carried out in the presence of 100 ug/ml of erythromycin to maintain the plasmid DNA. Cultures at exponential or stationary phases were centrifuged, and the supernatant, which contained the fermentation products acetate, acetone, ethanol, butyrate and butanol, was analyzed by gas chromatography using a Hewlett-Packard 5890 Series II Gas Chromatograph with a flame ionization detector and reporting integrator, as previously described (Green and Bennett, 1996). Briefly, a standard solution which contains 10 mM ethanol, 20 mM acetone, 40 mM butan-1-ol, 30 mM acetate and 30 mM butyrate was used for calibration. Samples of culture supernatant and the standard solution were acidified using an equal volume of 20% (v/v) phosphoric acid before each run, and a 5 µl of injection volume was maintained through all the runs. The GC program was: 135°C for 8 min, 135°C to 195°C ramp at 30°C/min, 195°C for 10 min. The injector and detector temperatures were 245°C and 215°C, respectively. The carrier gas was nitrogen, and a flow rate of 25 ml/min was maintained.

2.15. Computer programs and sequence accession number. Searches were performed using the Genetics Computer Group sequence analysis package, version 8.0 (Wisconsin). The employed search programs include Blast, tFastA, Bestfit, Pileup and Prettyplot. The complete nucleotide and amino acid sequences of the *pta* and *ack* genes have been submitted to GenBank and assigned the accession number U38234. The complete nucleotide and amino acid sequences of the *BCS* operon have been assigned the accession number U17110. The sequence alignment was conducted using SeqVu™

program version 1.0.1 (The GarVan Institute of Medical Research, Sidney, Australia).

Chapter 3. Genes Involved in the Butyryl-CoA Synthesis

The genes encoding enzymes in the central clostridial fermentation pathway constitute the focus of the discussion which follows. It begins with an introduction of the enzymes involved in butyryl-CoA synthesis from acetoacetyl-CoA: BHBD, crotonase, BCD and related electron-transfer flavoproteins. A description then follows of how the genes were cloned through genomic library screening, using a PCR-generated BHBD-gene-specific screening probe. The subcloning to various vectors and the mapping and sequencing are then described. The results from the primer-extension analysis which suggests these genes form an operon are presented together with a discussion of the expression of this cloned operon in both *E. coli* and *C. acetobutylicum*. The chapter ends with a discussion of the sequence analysis of the cloned genes, based on the amino-acid alignment data, and recommendations for future studies.

3.1. Introduction: enzymes involved in the butyryl-CoA synthesis

The central fermentation pathway in *C. acetobutylicum* involves eight enzymes, which play key roles in both acid and solvent production (Jones and Woods, 1986). Four of these enzymes, responsible for the conversion of acetyl-CoA to butyryl-CoA, are thiolase, β-hydroxybutyryl-CoA dehydrogenase (BHBD), crotonase and butyryl-CoA dehydrogenase (BCD). A similar enzyme configuration of thiolase, 3-hydroxyacyl-CoA dehydroganase (HAD), enoyl-CoA hydratase (ECH) and acyl-CoA dehydrogenase (ACD), is involved in the β-oxidation of fatty acids in eucaryotes (see Fig. 3.1), suggesting possible structural and mechanistically

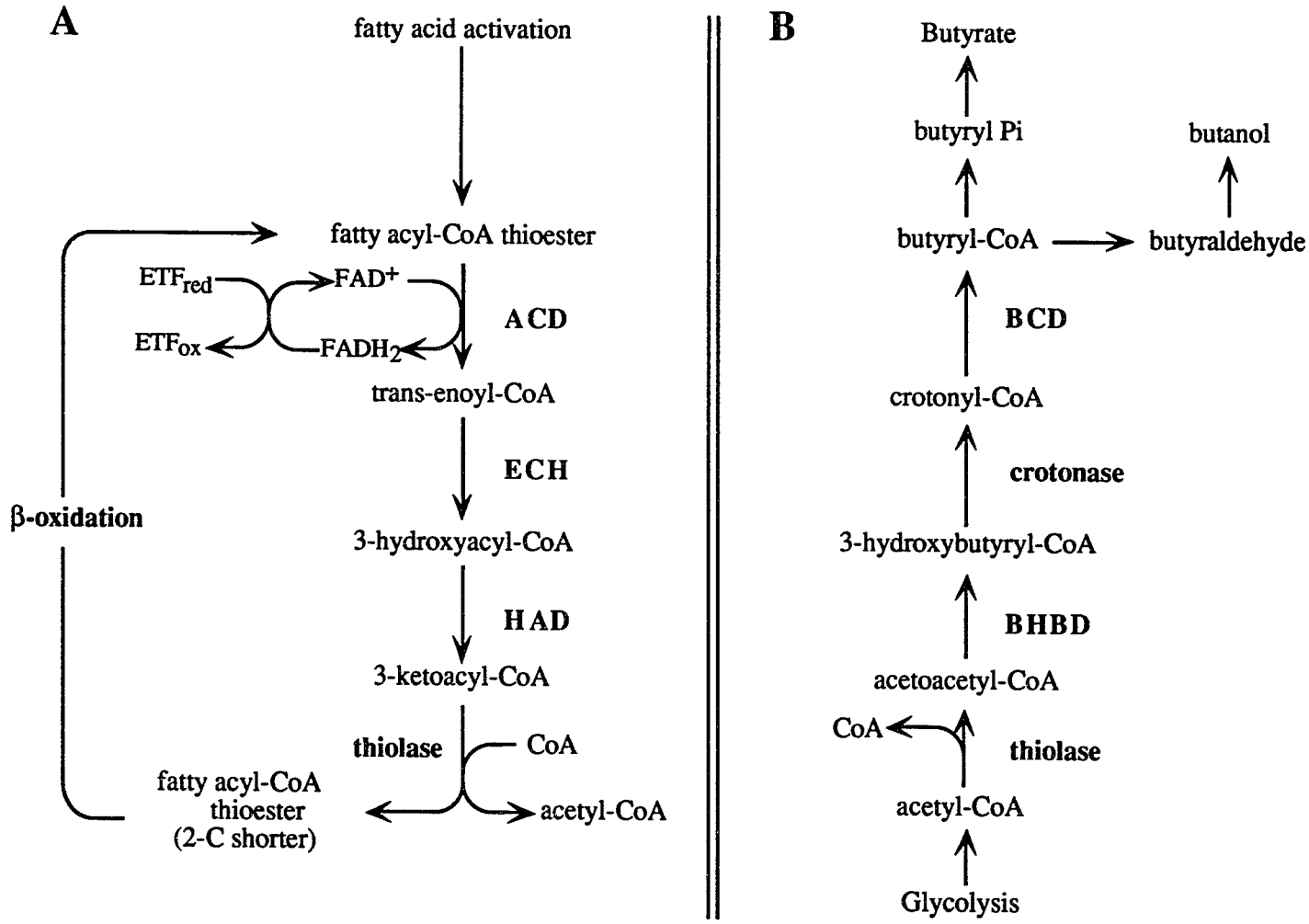

Fig. 3.1. Comparison of the metabolic pathways utilized for the (A) β-oxidation of fatty acids in eucaryotes and (B) butyrate/butanol synthesis in *C. acetobutylicum*.

conserved elements. In addition, a multifunctional enzyme complex, comprising thiolase, HAD, ECH, epimerase and isomerase is encoded by the fatty-acid degradative operon, *fadBA*, found in *E. coli* (Pramanik et al., 1979, Yang et al., 1991, Yang et al., 1993).

3.1.1. β-hydroxybutyryl-CoA dehydrogenase (BHBD)

BHBD (EC 1.1.1.35) in clostridia catalyzes the reduction of acetoacetyl-CoA by NAD(P)H. This subprocess is the initial and necessary step toward the ultimate production of butyrate and butanol. The *hbd* gene, encoding BHBD from *C. acetobutylicum* P262 and *C. difficile,* has already been cloned in *E. coli* and sequenced (Youngleson et al., 1989, Mullany et al., 1994). For *C. acetobutylicum* P262, *hbd* encodes a protein of 282 amino acids with a calculated molecular mass (Mr) of 31 kDa, and is located upstream of the *adh-1* gene (encoding an alcohol dehydrogenase). For *C. difficile, hbd* encodes a protein of 281 residues with a 31 kDa Mr. The deduced primary amino acid sequence for *hbd* shows a 46% similarity to the equivalent fatty-acid β-oxidation enzyme from the pig (Bitar et al., 1980) and a 38% similarity to the HAD part of the bifunctional enzyme (HAD:ECH) from rat peroxisomes (Osumi et al., 1985).

BHBD has been purified and characterized from *C. beijerinckii* NRRL B593 (Colby and Chen, 1992) and *C. Kluyveri* (Madan et al., 1973). BHBD from *C. beijerinckii* exhibited a native molecular weight of 213 kDa and a subunit Mr of 31 kDa, which is similar in value to BHBD from *C. kluyveri,* where a native Mr of about 220 kDa with eight subunits per enzyme complex was found (Madan et al., 1973). However, BHBD from *C.*

Kluyveri is NADP(H)-dependent whereas BHBD from *C. beijerinckii* could use either NAD(H) or NADP(H) as a cofactor, even though the enzyme demonstrated much more activity toward NAD(H). Interestingly, the enzyme from *C. beijerinckii* was found to be inhibited by acetoacetyl-CoA at low concentration of NADH.

3.1.2 Crotonase

Crotonase from *C. acetobutylicum* is a bacterial analog of enoyl-CoA hydratase (ECH, EC 4.2.1.17), which catalyzes the reversible, stereospecific hydration of unsaturated fatty acyl-CoA derivatives to the corresponding β-hydroxyacyl-CoA in the mitochondrial oxidation of fatty acids (see Fig. 3.1). The enzyme is commonly referred to as crotonase because it is most active with crotonyl-CoA as its substrate. Crotonase from *C. acetobutylicum* NRRL-B-527 has been previously purified and characterized (Waterson et al., 1972). Unlike the crotonase from bovine liver, which is a hexamer with a subunit Mr of 27.3 kDa (Waterson and Hill, 1972), the native enzyme from *C. acetobutylicum* is composed of four identical subunits, each with an approximate Mr of 40 kDa and 370 amino acid residues. The enzyme activity is inhibited by acetoacetyl-CoA, whereas CoA, butyryl-CoA and acetyl-CoA demonstrate no such effect. In contrast to the broad substrate specificity (C4-C16) shown from bovine source, the crotonase from *C. acetobutylicum* exhibits a narrower specificity with respect to fatty acyl-CoA compounds, with only crotonyl-CoA and hexenoyl-CoA being hydrated. In addition, bacterial crotonase is very sensitive to a high concentration of crotonyl-CoA, whereas no

inhibition was found with the bovine enzyme (Waterson and Hill, 1972, Waterson et al., 1972).

Many genes encoding ECH from eucaryotic sources as well as bacteria have been cloned. However, until recently, no literature has been reported on the cloning of the crotonase-encoding gene from *C. acetobutylicum*. A putative gene encoding crotonase from *C. difficile* has been incompletely cloned and sequenced (Mullany et al., 1994). This gene is located upstream of the *hbd* gene and is followed by an inverted-repeat-termination structure. The gene was defined by its sequence homology with the known enoy-CoA hydratase genes and no gene expression data is available from this report.

3.1.3. Butyryl-CoA Dehydrogenase (BCD)

BCD from *C. acetobutylicum* is a bacterial analog of short-chain acyl-CoA dehydrogenase (ACD, EC 1.3.99.2) from mammalian mitochondria (see Fig. 3.1). Mammalian BCD is a member of the fatty-acid acyl-CoA dehydrogenase group, each of which catalyzes the α,β-desaturation of acyl-CoA substrates (Engel and Massey, 1971). ACDs have recently received increasing attention, because it was found that ACD deficiencies have caused genetic disorders demonstrating serious symptoms, such as coma and violent vomiting. Severe hypoglycemia is observed in most cases. In addition, it is speculated that ACD defects play a role in "sudden infant death syndrome" (Matsubara et al., 1989, Schiffer et al., 1989).

Three soluble fatty acyl-CoA dehydrogenases have been described with different but overlapping specificities for short, medium and long acyl chains (Beinert, 1963). BCD is specific for short-chain (C4-C6) acyl-CoA substrates, with optimum specificity for butyryl-CoA (Kim et al., 1994, Williamson and Engel, 1984). Like other acyl-CoA dehydrogenases, BCD contains FAD as a cofactor which is tightly bound to the apoenzyme. It should also be noted that various acyl-CoA dehydrogenases share many identical and conserved amino acid residues throughout their sequence, except for the leader peptide and in the N-terminal region (Kelly et al., 1987, Matsubara et al., 1987, Matsubara et al., 1989). Each acyl-CoA dehydrogenase is a tetramer with a subunit Mr from 41.7 to 44.5 kDa, and with a function requiring an electron-transfer flavoprotein (ETF) as an electron donor/acceptor.

In *C. acetobutylicum*, BCD acts in the reverse direction from fatty acid degradation to produce the reduced butyryl-CoA. The characterization of this enzyme from *C. acetobutylicum* has not yet been reported. However, BCDs were purified from the butyrate-producing anaerobes *Megasphaera elsdenii* (Engel, 1981, Van Berkel et al., 1988) and *Peptostreptococcus elsdenii* (Engel and Massey, 1971a) and their properties characterized (Engel and Massey, 1971b, Williamson and Engel, 1984). Moreover, the 3-dimensional structure of BCD from *M. elsdenii* has been defined (Djordjevic et al., 1995) and its encoding gene cloned and sequenced (Becker et al, 1993). Many properties of the bacterial BCD are similar to those of the corresponding enzyme obtained from mammalian mitochondria, and the encoding gene exhibited high amino acid similarity to its mammalian counterpart. The molecular weight of the BCD enzyme from *M. elsdenii*

is approximately 175 kDa, with one molecule of FAD noncovalently bound per subunit, and with a tetramer structure having a subunit Mr of approximately 43 kDa (Williamson and Engel, 1982). Like mitochondrial flavoenzymes, its function requires an ETF for electron transport.

3.1.4. Electron-transfer flavoprotein (ETF)

ETF plays an important role in the β-oxidation of fatty acids and in oxidative demethylation reactions by coupling primary flavoprotein dehydrogenase to the electron-transport chain (Komuniecki et al., 1989, Nagao and Tanaka, 1992). ETFs have been extensively studied from mammalian sources, mainly because the defects in ETF or ETF-dehydrogenase (also called ETF:ubiquinone oxidoreductase, an iron-sulfur flavoprotein, Ruzicka and Beinert, 1977) in humans result in glutaric acidemia type II, a potentially fatal metabolic disease (Bedzyk et al., 1993, Ikeda et al., 1986). However, ETF or ETF-like proteins have also been isolated from a variety of bacteria, such as *P. elsdenii* (Whitfield and Mayhew, 1974), *M. elsdenii* (Pace and Stankovich, 1987) and *Paracoccus denitrificans* (Husain and Steenkamp, 1985, Watmough et al., 1992). The last bacterium is used in the study of many redox proteins, because it can synthesize an electron transport system containing proteins similar to those of the mammalian respiratory system (Stouthamer, 1980).

The electron flow of ETF from anaerobes is reversed to that in mammalian system. In anaerobic bacteria, ETF functions as the electron acceptor for flavoproteins as acyl-CoA dehydrogenase. In mitochondria and aerobic bacteria, it donates reducing equivalents to the ETF-

dehydrogenase which, in turn, transfers an electron pair to the mitochondrial electron-transport chain by reducing coenzyme Q (Ruzicka and Beinert, 1977, Husain and Steenkamp, 1985). A proposed scheme which illustrates the electron transport from acyl-CoA thioesters through dehydrogenases into ETF in bacteria and enkaryotes is showm in Fig. 3.2.

ETF from a mammalian source is a heterodimer consisting of an α- and a β-subunit (Finocchiaro et al., 1988 and 1993, Husain and Steenkamp, 1983). The molecular size of α-ETF for human is 32 kDa, with a precursor Mr of 35 kDa. The Mr of the β-subunit is 27 kDa for both the precursor and mature protein. ETF from mammalian and *P. denitrificans* (Husain and Steenkamp, 1985) sources contains one FAD per dimer, with β-ETF binding to the FAD and interacting directly with acyl-CoA dehydrogenase. However, the ETF from the anaerobes *M. elsdenii* and *P. elsdenii* contains two FADs per heterodimer, with one FAD-binding site on each subunit (Onualláin and Mayhew, 1986, Whitfield and Mayhew, 1974).

Neither BCD nor ETF has been purified from strains of *C. acetobutylicum*. In fact, it was not until recently that the presence of a BCD-related ETF in solvent-producing clostridia was suggested (Chen, 1993). This presence was suggested primarily because of the isolation of NAD(P)H-specific ETFs from either anaerobic bacteria (Dietrichs et al., 1990, Pace and Stankovich, 1987, Stanton, 1989, Whitfield and Mayhew, 1974) or anaerobic mitochondria (Komuniecki et al., 1989). In contrast to the bacterial ETF, the corresponding mammalian enzyme does not oxidize NADH (Beinert, 1963, Frisell et al., 1966). However, eukaryotic and bacterial studies show striking similarities in the electrochemical

Bacterial (*M. elsdenii*)

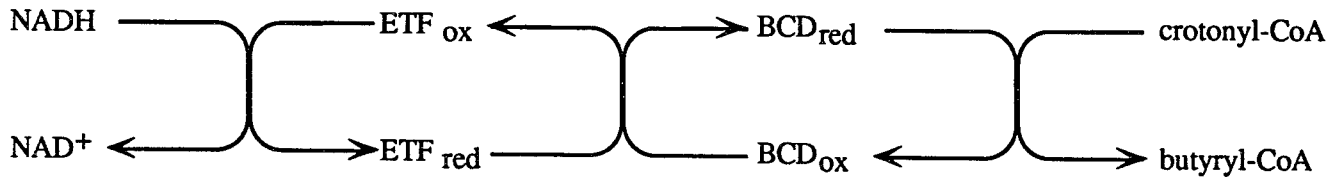

Mammalian (porcine liver)

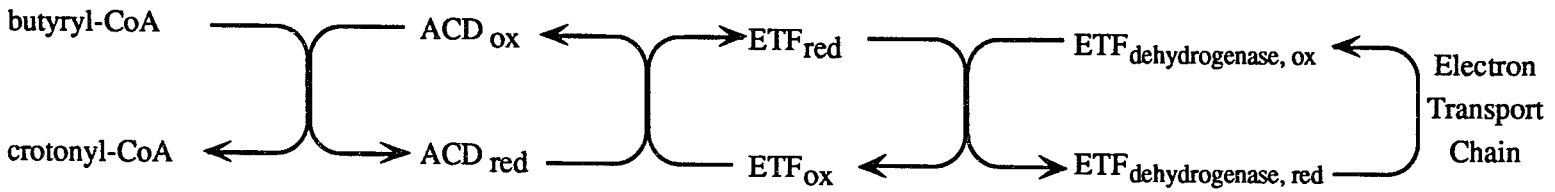

Fig. 3.2. Delivery of electrons through the fatty acid oxidation cycle in eukaryotes and butyryl-CoA synthesis in bacteria. (modified from a scheme proposed by Stankovich and Soltysik, 1987 based on reported midpoint potentials)

behavior and peptide sequences of BCD or ETF between mammalian and bacterial enzymes (Watmough et al, 1992). Because of these homologies, structural and mechanistic similarities would therefore be expected.

Interestingly, the nucleotide sequences of α-ETF and β-ETF also show a marked similarity to the *fixB* and the *fixA* genes, respectively. Such genes were originally identified within the *fixABCX* operon derived from different rhizobia and non-symbiotic bacteria such as *Azorhizobium caulinodans* (Arigoni et al., 1991). Three ORFs of this operon, *fixA, fixB and fixC,* encode hypothetical proteins with sequence similarities to the beta and alpha subunits of ETF and ETF:ubiquinone oxidoreductase, respectively (Arigoni et al., 1991, Bedzyk et al., 1993). So far, no specific biochemical function has yet been identified for the *fixABCX* gene products, but it has been suggested that such products are involved in the electron transport to nitrogenase (Arigoni et al., 1991).

A list of functions and biochemical properties of ETFs or ETF-related proteins from different sources is shown in Table 3.1. A list of redox potentials of enzymes, substrates and cofactors involved in the ETF reactions is shown in Table 3.2. It has been found that upon the binding of substrate/product couple, the redox properties of various ACDs are modulated to allow the reaction to proceed thermodynamically (Lenn et al., 1990). Specifically, the reduction potential of substrate/product-bound ACD shifts in the positive direction, which allows isopotential electron transfer to occur from substrate to enzyme (Table 3.2). It can also be seen that the midpoint redox potential of ETF from anaerobic bacteria is much more negative than that of mammalian enzyme, therefore it is consistent

Table 3.1. Electron Transfer Flavoproteins

Source	Structure	Mr (kDa)	Cofactor	Action	Reference
Human	hetero-dimer	32 (α) 27 (β)	 FAD	acyl-CoA dehydrogenase electron donor/acceptor	Ikeda et al., 1988
A. caulinodans	FixB FixA	40 30		Redox in N2 fixation??	Arigoni et al., 1991
R. meliloti	FixB FixA	38 31		Redox in N2 fixation??	Earl et al., 1987
M. elsdenii	hetero-dimer	38 32	FAD FAD	BCD, NADH or lactate dehydrogenase	Pace & Stankovich 1987
P. elsdenii	hetero-dimer	33 41	FAD FAD	BCD, NADH or lactate dehydrogenase	Whitfield & Mayhew 1974
P. denitrificans	hetero-dimer	32 28	FAD*	glutaryl-CoA dehydrogenase BCD (pig)	Husain & Steenkamp 1985
C. sticklandii	homo-dimer	35	FAD FAD	NADPH-glycine proline reductase	Dietrichs et al., 1990
Ascaris suum	hetero-dimer	37 32		NADH 2-methyl-enoyl-CoA reductase	Komuniecki et al., 1988

* Contain only one FAD per enzyme molecule, but it is not sure which subunit binds FAD.

Table 3.2. Comparison of electrochemcal properties of ETF between bacteria and mammalian.

	Redox Potentials[a] (mV)						
Source	butyryl-CoA/ crotonyl-CoA	Complexed BCD[b]	Free BCD	ETF	ETF:ubiquinone oxidoreductase	NADH	Refernece
M. elsdenii	-13[c] -126[e]	-19	-79	-259	N/A[d]	-320	Pace & Stankovich, 1987 Fink et al., 1986 Stankovich & Soltysik, 1987
porcine liver	-126[e] -13[c]	-26	-139	-25	-15 (flavin) +40 (iron-sulfur)	N/A[d]	Gustafson et al., 1986 Husain et al., 1984 Lenn et al., 1990

a. Midpoint potential at pH 7.0-to-7.1, versus standard hydrogen electrode.

b. BCD bound to natural substrate/product couple.

c. From Stankovich and Soltysik, 1987.

d. N/A: not applied. Mammalian enzyme does not oxidize NADH, and the ETF from *M. elsdenii* does not interact with ETF:ubiquinone oxidoreductase.

e. From Gustafson et al, 1986.

with the behavior that ETF functions as the electron donor in the bacterial system (NADH-> ETF -> BCD). On the other hand, the Em of mammalian BCD is more negative than its ETF, therefore allows BCD to transfer reducing equivalents to ETF and subsequently to ETF:ubiquinone oxidoreductase.

Even though the DNA sequences from both subunits of ETF of human and *P. denitrificans* had been known (Bedzky et al., 1993, Finocchiaro et al., 1988 and 1993), no information regarding the functional domains has been obtained from the primary structures. However, mammalian and bacterial ETF seem to have structural similarities, as examplified by the likelihood of identical redox potentials for the flavins (Watmough et al., 1992). In addition, similarities of the hydrogen bonding and polarity of the environments of the isoalloxazine ring of FAD had been demonstrated. It has also been shown that ETF from *P. denitrificans* can serve as an electron acceptor for porcine SACD and MACD (Husain and Steenkamp, 1983 and 1985). Despite these similarities, major differences also exist. The flavin in bacterial ETF is not highly fluorescent, and the circular dichroism spectrum of the bacterial ETF flavin is much more intense than that of the mammalian flavin, suggesting a minor difference in the microenvironment of the flavin ring (Watmough et al., 1992).

3.2. Results

3.2.1. PCR. The *hbd* gene from *C. acetobutylicum* P262 had already been cloned and sequenced (Youngleson et al, 1989). Based on those sequencing data, six sets of primer pairs were designed for the PCR so as to generate the necessary screening probe. Of these pairs, the most successful set was generated from nucleotide positions of 547 to 574 (BHBD-4 of Table 2.3) and from nucleotides complementary to positions of 820 to 847 (BHBD-C of Table 2.3) (Fig. 2 of Youngleson et al., 1989). A DNA fragment of the expected ~300 bp size was amplified. Thus, the 300-bp PCR product was chosen as the probe for λ-phage-library screening.

3.2.2. Specificity of the PCR probe. Prior to screening the EMBL3 phage library, the specificity and the hybridization conditions of the screening probe was determined by hybridizing the probe to Southern blots of genomic DNA digested by various restriction enzymes. Only the chromosomal DNA exhibited a signal with the PCR probe, which hybridized to a 1.0 kb *Hind*III- and a 3.6 kb *Eco*RV-digested genomic DNA fragment (Fig. 3.3).

3.2.3. Screening of the phage library. A λ library of *C. acetobutylicum* was previously constructed by Cary et al (Cary et al., 1988) in this laboratory. The phage library stock was diluted to produce ~1,000 plaques per plate. After screening six plates, 49 plaques exhibited homology with the probe. Eight of these plaques were isolated for further analysis. After tertiary screening, two distinct phage DNAs were isolated from two (B4 and B7) of the eight plaques using the rapid plate-lysate method.

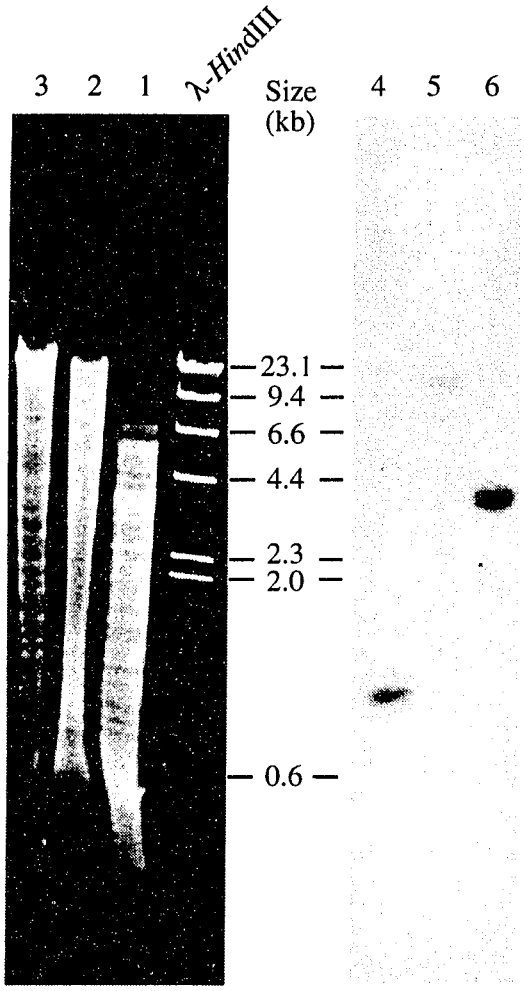

Fig. 3.3. Southern blot analysis of restriction-enzyme-digested *C. acetobutylicum* DNA hybridized to the radiolabelled BHBD-screening probe. lanes:

1-3. *Hind*III, *Eco*RI and *Eco*RV digests of genomic DNA, respectively.

4-6. Autoradiogram of lanes 1-3 after Southern transfer and hybridization to the ^{32}P-labelled BHBD-screening probe.

The genomic and positive-phage-B4 DNAs were digested with *Hin*dIII, *Eco*RV and *Ban*II and then blotted to the membranes for Southern hybridization. Fragments of a 1.0 kb *Hin*dIII-, a 3.6 kb *Eco*RV- and a ~12 kb *Ban*II-digested phage DNA were hybridized to the probe, the same size as those from the corresponding genomic DNA digests (Fig. 3.4). This data suggested that the expected chromosomal region containing a *hbd* gene is located on the recombinant phage. This result also suggested that only one copy of the *hbd* gene is present in the chromosome.

3.2.4. Subcloning and enzyme activity. The 3.6 kb *Eco*RV-cleaved phage DNA fragment was purified away from the gel and ligated with a *Sma*I-cleaved pUC19-vector. The ligation mixture was then used to transform *E. coli* XL1-Blue cells, with the transformation mixture plating onto the indicated medium. The transformants demonstrating the insertional inactivation of the β-galactosidase gene were the white colonies chosen to be screened. One of the colonies, hybridized successfully with the probe, was designated as pb37.

BHBD and crotonase assays were performed using crude extracts of XL1-Blue transformants containing pUC19 (control) and pb37 (pUC19 with a possible *hbd* gene insert). The cells were grown aerobically and to the stationary phase. The results are shown in Table 3.3. *E. coli* cells harboring pb37 exhibited an NADH-dependent BHBD activity approximately sixty times greater than the control strain.

However, no crotonase activity was detected in transformant containing the pb37. Therefore, an attempt was made to subclone a much

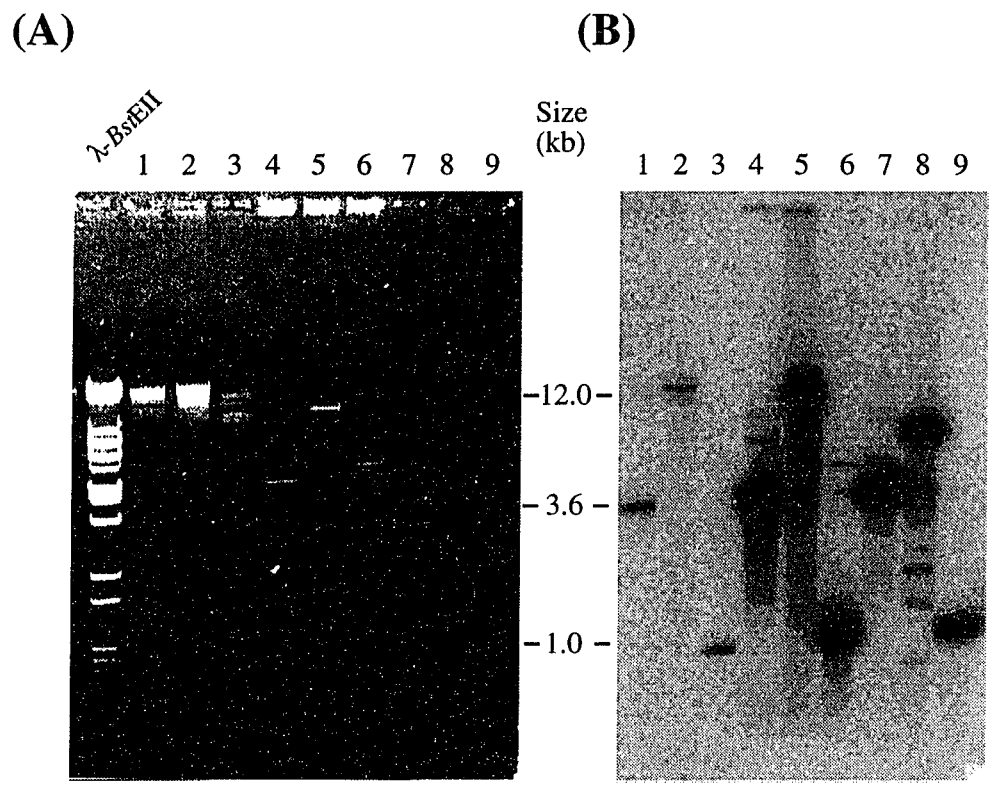

Fig. 3.4. Southern blot analysis of restriction-enzyme-digested genomic, phage B4 and plasmid pC10 DNAs.

(A) Samples were electrophoresed on an 0.8% agarose gel and stained with ethidium bromide. lanes:

1-3. *Eco*RV, *Ban*II and *Hin*dIII digests of genomic DNA, respectively.

4-6. *Eco*RV, *Ban*II and *Hin*dIII digests of recombinant phage isolate B4, respectively.

7-9. *Eco*RV, *Ban*II and *Hin*dIII digests of recombinant plasmid pC10, respectively.

(B) Autoradiogram of lanes 1-9 after Southern transfer and hybridization to the ^{32}P-labeled BHBD-screening probe.

Table 3.3. Enzyme activities of recombinant *E. coli* and *C. acetobutylicum* strains.

Organisms and Plasmids	Specific Activities (mean value[a]) (U[b]/mg)		
	Crotonase	BHBD	BCD
Aerobically-grown *E. coli*			
pUC19	0.1	0.1	**
pb37	0.1	5.6	**
pC10	13.7	7.4	**
pSYL2	0.3	0.1	**
pSYL2-BCS	46.5	11.6	**
Anaerobically-grown *E. coli*			
pSYL2	0.1	<0.03	**
pSYL2-BCS	187.5	8.6	**
C. acetobutylicum			
pSYL2	67.0	6.6	1.2
pSYL2-BCS	128.6	11.0	3.3

a. Data shown are based on at least two independently prepared extracts and are reproducible within 15% of the value given.

b. One unit is defined as the amount of enzyme that converts one micromole substrate to product per minute.

** Undetectable; minimum measurable limit for BCD is ~0.04 U/mg.

longer 9.7 kb *Bgl* II-digested phage B4 fragment to the *Bam*HI-cleaved pUC19 vector. After transforming to XL1-Blue and then performing the enzyme assay as described, both BHBD and crotonase activities were successfully detected from crude extract of this new transformant. The recombinant plasmid was designated pC10. *E. coli* cells harboring pC10 exhibited over 70 times greater BHBD activity and about 140 times higher crotonase activity than the control strain (Table 3.3). In addition, the activity values from the *E. coli* cells harboring the pb37 and pC10 plasmids are comparable to those obtained from the wild-type *clostridium* cells at the stationary phase, where the maximal activity levels are observed (Hartmanis and Gatenbeck, 1984).

3.2.5. Restriction mapping. Various restriction enzymes were used to generate the physical maps of the recombinant plasmids pb37 and pC10 and the maps of the subcloned segments in plasmids pb37 and pC10 are shown in Fig. 3.5. It is seen that the 3.6 kb *Eco*RV-insert of pb37 is situated within the 9.7 kb *Bgl*II-insert of the pC10 plasmid. Since no crotonase activity was detected from the pb37 transformant, and since the estimated crotonase encoding gene contains 337 residues with a nucleotide length of more than 1 kb (Waterson et al., 1972), the region downstream of the pb37 3′ *Eco*RV site is only about 0.8 kb, and therefore not large enough to contain the crotonase encoding gene. Thus, the gene encoding crotonase, and possibly BCD, could only be located upstream of the *hbd* gene.

Three restriction sites each were found for *Eco*RV and *Hinc*II, two sites were found for *Ban*II, and one site each was found for *Eco*RI, *Sac*I,

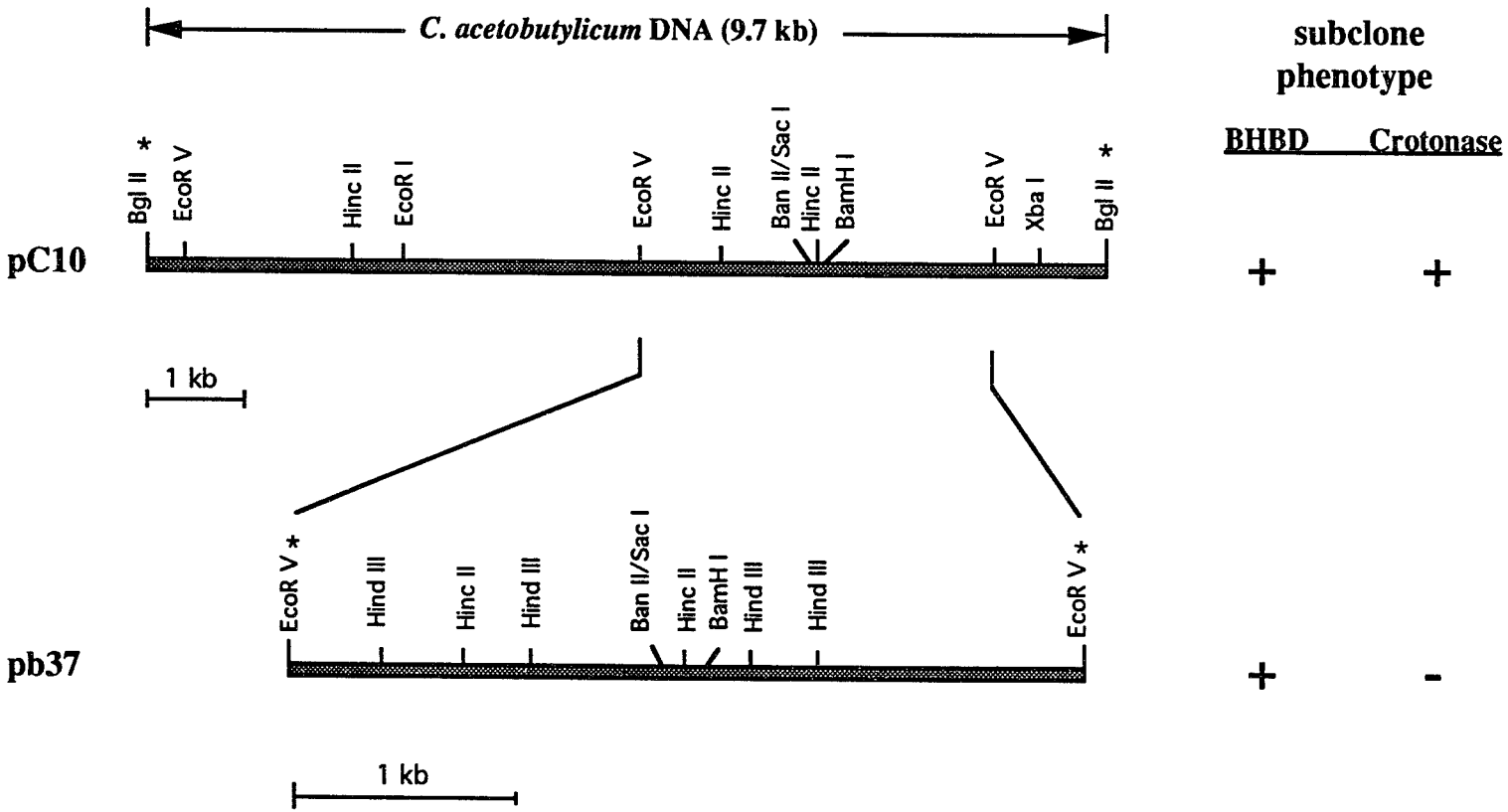

Fig. 3.5. Restriction maps of BHBD subclones. The restriction sites of the insert for the recombinant pb37 and pC10 are shown. An asterisk indicates the loss of the *Bgl*II sites for the pC10 insert and of the *Eco*RV sites for the pb37 insert due to ligation with the *Bam*HI and *Sma*I digested pUC19 vectors, respectively. The *Hin*dIII sites for the pC10 insert are omitted to simplify the map. The presence (+) or absence (-) of enzyme activity in *E. coli* XL1-Blue cells bearing the corrsponding plasmids is indicated at right.

*Bam*HI and *Xba*I. No restriction sites were found for *Kpn*I, *Pst*I, *Sma*I, *Sal*I and *Nco*I (Fig. 3.5).

The integrity of the 9.7 kb-*Bgl*II-insert was tested through a Southern blot experiment using genomic DNA from *C. acetobutylicum* and recombinant DNA from phage B4 and from plasmid pC10, all of which were digested using *Eco*RV, *Hinc*II and *Ban*II individually. The ~0.5 kb *Hinc*II/*Eco*RI fragment of pC10 was purified and labeled as the Southern probe (Fig. 3.6). The fragments exhibiting homology from recombinant phage and plasmid DNA aligned nicely with those from the chromosomal DNA. Specifically, the probe hybridized to a 4.8 kb *Eco*RV- and a 3.8 kb *Hinc*II-digested fragment from genomic, phage and plasmid DNA. Moreover, the probe also demonstrated a signal to the 9.7 kb *Bgl*II-digested fragment from both chromosomal and phage B4 DNA. Therefore, all the fragments corresponded in size to those anticipated from the physical map of the 9.7 kb insert (Fig. 3.6)

3.2.6. DNA sequencing. Nucleotide sequencing of the inserts for both subclones was initially conducted using the PCR primers previously mentioned. The gene *hbd*, encoding BHBD of 282 amino acid residues and a 30.5 kDa Mr from *C. acetobutylicum* ATCC 824, was located at the 3′ end of the pC10 insert. The gene was preceded by a putative Shine-Dalgarno (S.D.) site with the sequence AGGGAGG located 8 bp upstream of the ATG start codon. A stem-loop sequence existed 9 bp downstream of the TAA stop codon (Fig. 3.7).

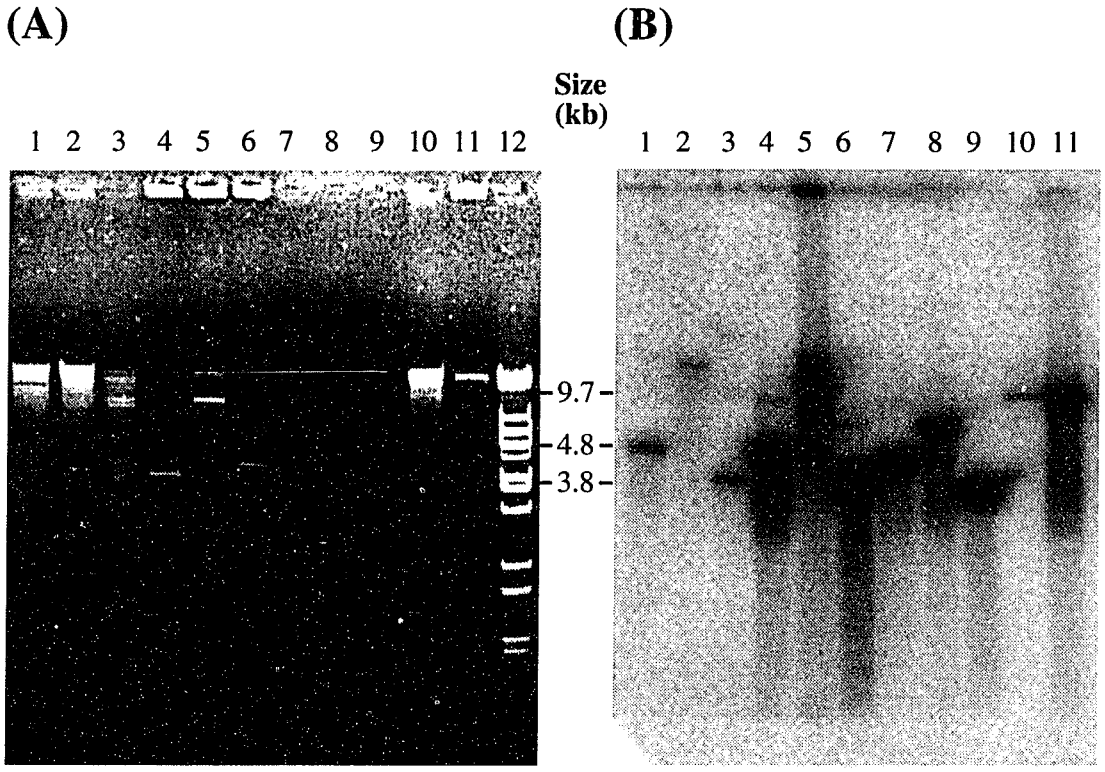

Fig. 3.6. Southern blot analysis of restriction-enzyme-digested genomic, phage B4 and plasmid pC10 DNAs.

(A) Samples were electrophoresed on an 0.8% agarose gel and stained with ethidium bromide. lanes:

1-3. *Eco*RV, *Ban*II and *Hin*dIII digests of genomic DNA, respectively.

4-6. *Eco*RV, *Ban*II and *Hin*dIII digests of recombinant phage isolate B4, respectively.

7-9. *Eco*RV, *Ban*II and *Hin*dIII digests of recombinant plasmid pC10, respectively.

10-11. *Bgl*II digests of genomic and phage B4 DNAs, respectively.

12. λ/*Bst*EII molecular size marker.

(B) Autoradiogram of lanes 1-11 after Southern transfer and hybridization to the ^{32}P-labelled crotonase-gene-specific probe.

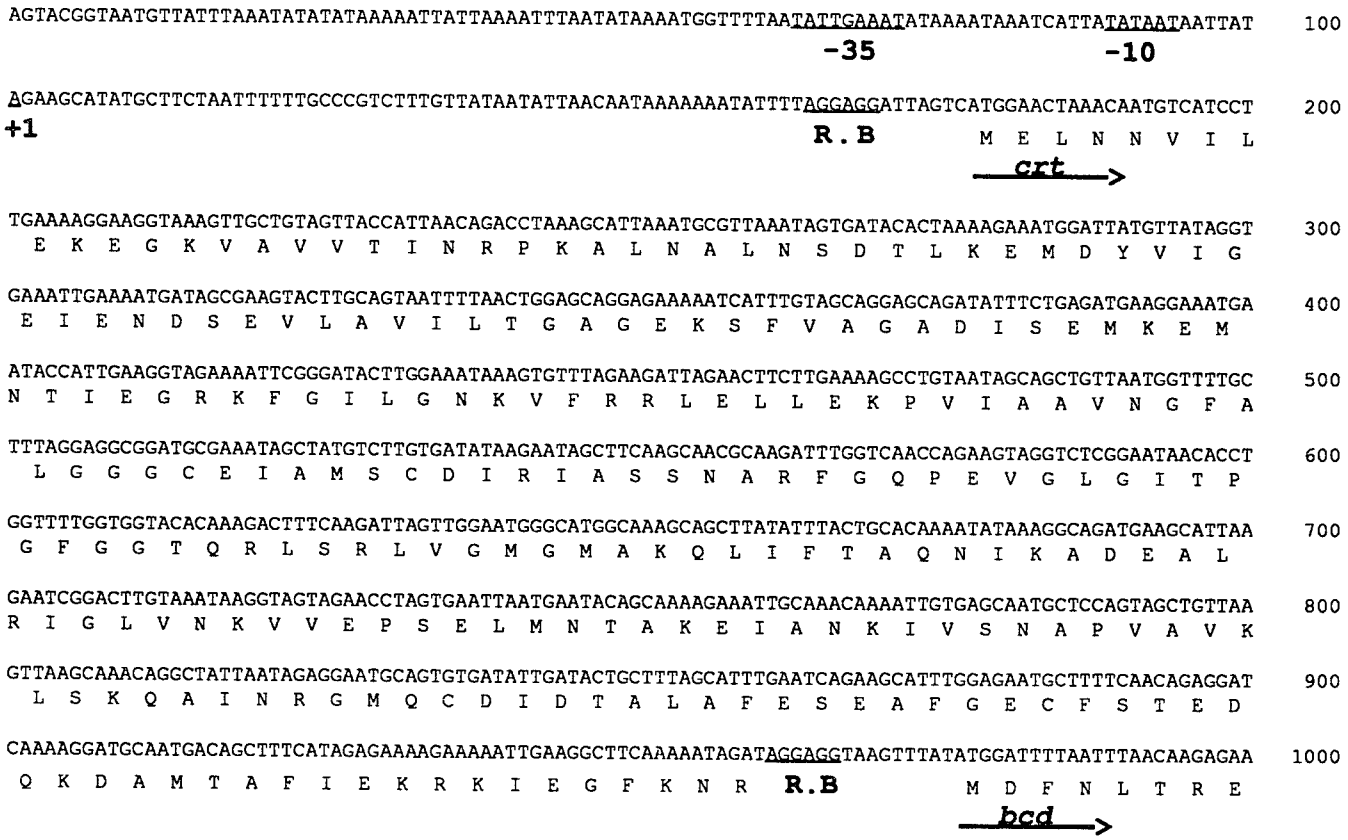

Fig. 3.7. Nucleotide and the deduced amino acid sequences of the genes in the *BCS* operon. Standard one-letter amino acid abbreviations are listed under the second nucleotide of each codon. The putative ribosome-binding (R.B.) site, the promoter sequence -35 and -10 regions and the transcriptional start site (+1) are underlined. A potential transcriptional terminator is indicated by convergent arrows. The putative NAD-binding site for the *hbd* gene is marked with asterisks (*).

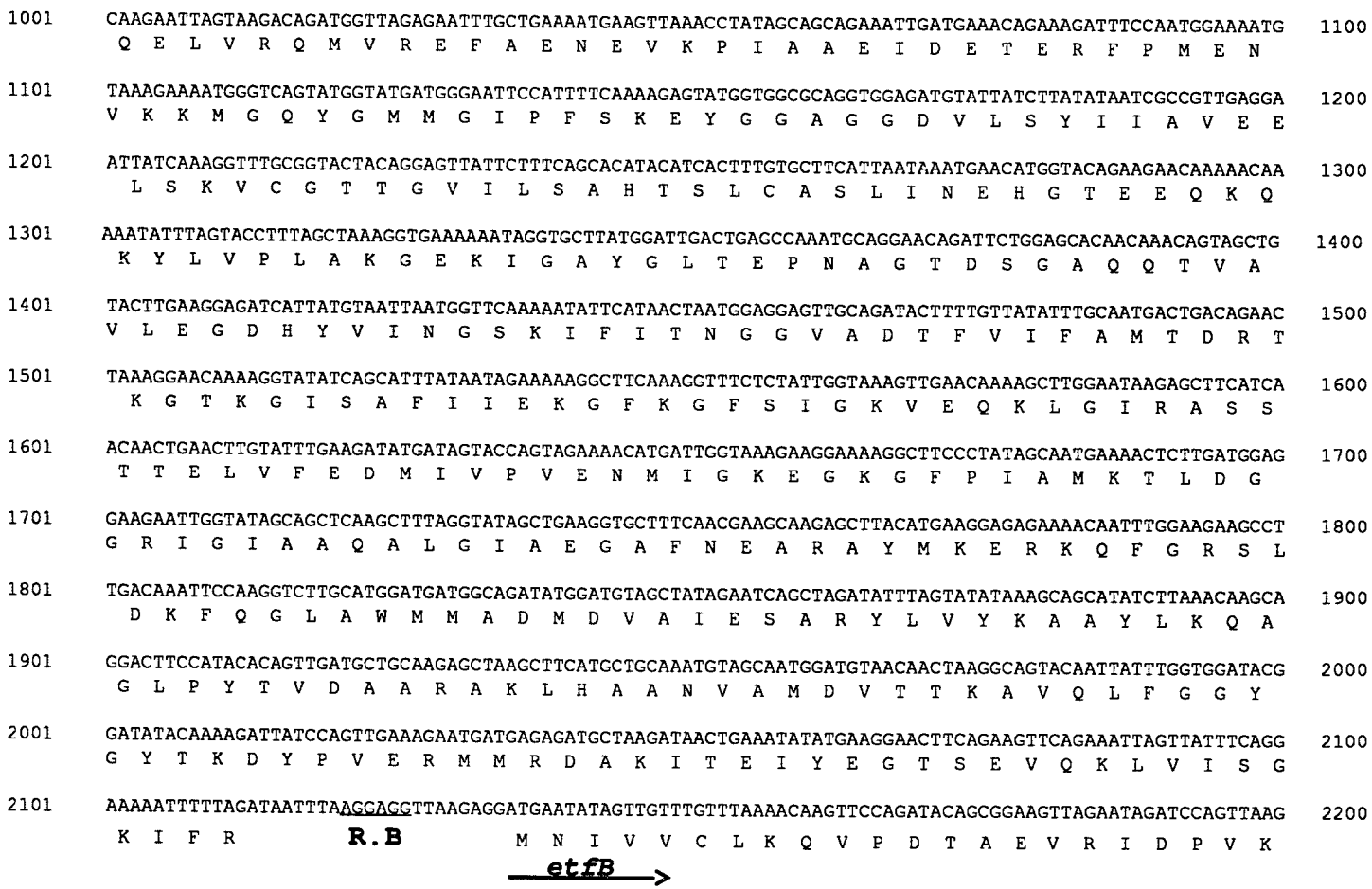

Fig. 3.7. Continued.

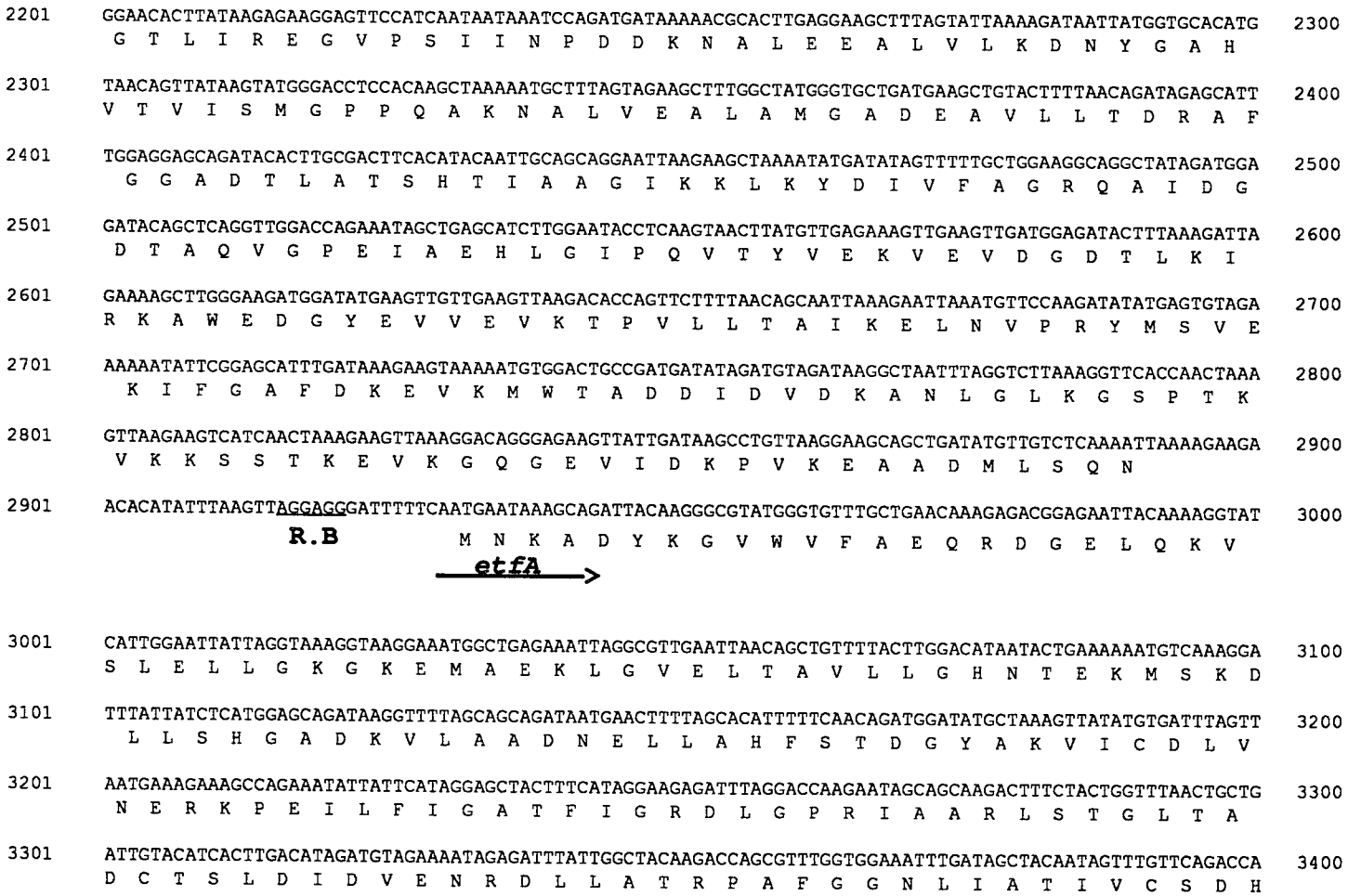

Fig. 3.7. Continued.

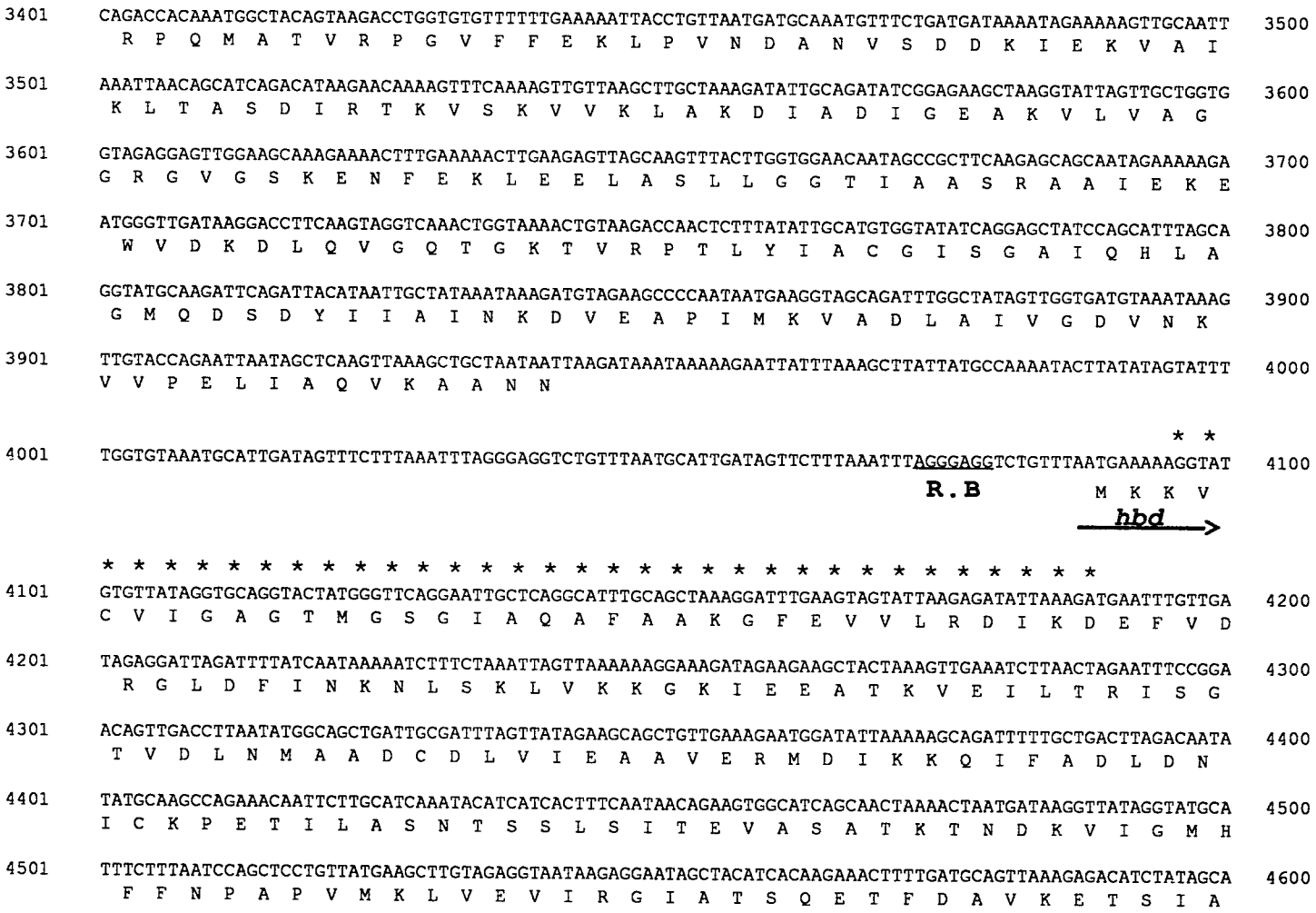

Fig. 3.7. Continued.

```
4601    ATAGGAAAAGATCCTGTAGAAGTAGCAGAAGCACCAGGATTTGTTGTAAATAGAATATTAATACCAATGATTAATGAAGCAGTTGGTATATTAGCAGAAG   4700
          I  G  K  D  P  V  E  V  A  E  A  P  G  F  V  V  N  R  I  L  I  P  M  I  N  E  A  V  G  I  L  A  E

4701    GAATAGCTTCAGTAGAAGACATAGATAAAGCTATGAAACTTGGAGCTAATCACCCAATGGGACCATTAGAATTAGGTGATTTTATAGGTCTTGATATATG   4800
        G  I  A  S  V  E  D  I  D  K  A  M  K  L  G  A  N  H  P  M  G  P  L  E  L  G  D  F  I  G  L  D  I  C

4801    TCTTGCTATAATGGATGTTTTATACTCAGAAACTGGAGATTCTAAGTATAGACCACATACATTACTTAAGAAGTATGTAAGAGCAGGATGGCTTGGAAGA   4900
          L  A  I  M  D  V  L  Y  S  E  T  G  D  S  K  Y  R  P  H  T  L  L  K  K  Y  V  R  A  G  W  L  G  R

4901    AAATCAGGAAAAGGTTTCTACGATTATTCAAAATAAGTTTACAAGAATCCCCATTATCAAATGGGGATTTTTTATATATAATATAATTTTAGA
          K  S  G  K  G  F  Y  D  Y  S  K                  ------->  <-------
```

Fig. 3.7. Continued.

Further nucleotide sequencing of the region upstream of *hbd* revealed a second open reading frame (ORF) located 143 bp upstream of *hbd*, encoding a protein of 337 amino acids and a 36.1 kDa Mr (Fig. 3.7). A search of protein-sequence data banks revealed that the deduced amino acid sequence of this ORF had a very high degree of homology with those for the *fixB* genes from *C. acetobutylicum* P262 (Youngleson et al., 1994), *Azorhizobium caulinodans* (Arigoni et al., 1991) and *Rhizobium meliloti* (Earl et al., 1987) and with the α-subunit of ETFs from human (Finocchiaro et al., 1988), rat (Shinzawa et al., 1988) and the bacteria *Paracoccus denitrificans* (Bedzyk et al., 1993). This gene is designated as *etfA* and it is also preceded by a putative S.D. sequence (AGGAGG), located 9 bp upstream of the methionine start codon.

A third ORF containing 252 amino acid codons was found (27.2 kDa) and located 37 bp upstream of *etfA* (Fig. 3.7). A computer search of the deduced peptide sequence demonstrated direct similarities between this gene product and the β-subunit of ETF from human (Finocchiaro et al., 1993) and *P. denitrificans* (Bedzyk et al., 1993) sources, and between this same product and that for the *fixA* genes from *A. caulinodans* (Arigoni et al., 1991) and *R. meliloti* (Earl et al., 1987). This gene, designated *etfB*, is preceded by the putative S.D. sequence AGGAGG and an 8-bp spacing.

A fourth ORF of 379 residues was located 17 bp upstream of *etfB* (Fig. 3.7), and a computer search revealed a high peptide similarity of this gene product with those of various acyl-CoA dehydrogenases (Kelly et al., 1987, Matsubara et al., 1987, 1989, Naito et al., 1989). Because of the nature of BCD, which reacts with its related ETF, it is highly probable that this ORF

represents the structural gene that encodes BCD and is therefore designated as *bcd*. The putative S.D. sequence AGGAGG is located 9 bp upstream of the *bcd* Met start codon.

A fifth ORF was located 13 bp upstream of *bcd*, encoding a polypeptide of 261 residues with an Mr of 28.2 kDa (Fig. 3.7). The sequencing data for this ORF show homology with the incompletely cloned crotonase gene from *C. difficile* (Mullany et al., 1994), and with various enoyl-CoA hydratase from rat (Minami-Ishii et al., 1989), *Caenorhabditis elegans* (Wilson et al., 1994), and with the enoyl-CoA hydratase part of the fatty oxidation complex (Yang and Elzinga, 1993) from *E. coli*. Therefore, this ORF appears to be that for the *crt* gene, encoding a crotonase of 28.2 kDa from *C. acetobutylicum* ATCC 824.

Further sequencing up to a point 500 bp upstream of *crt* and 1.2 kb downstream of *hbd* revealed no obvious ORFs which would encode metabolically related enzymes in the clostridial pathway. No transcriptional termination sequences were found in the intergenic regions between the five genes cloned in this study.

3.2.7. Primer extension. Primer extension experiments were conducted using primers homologous to the N-terminal nucleotide sequences of the *hbd*, *etfA/B*, *bcd* and *crt* genes (listed in Table 2.3) to identify the transcriptional start site for this gene cluster. One single transcriptional start site (see Fig. 3.8) was determined and located 77 bp upstream of the *crt* start codon. The corresponding -10 and -35 regions for this site matched closely with the consensus promoter sequences. No other

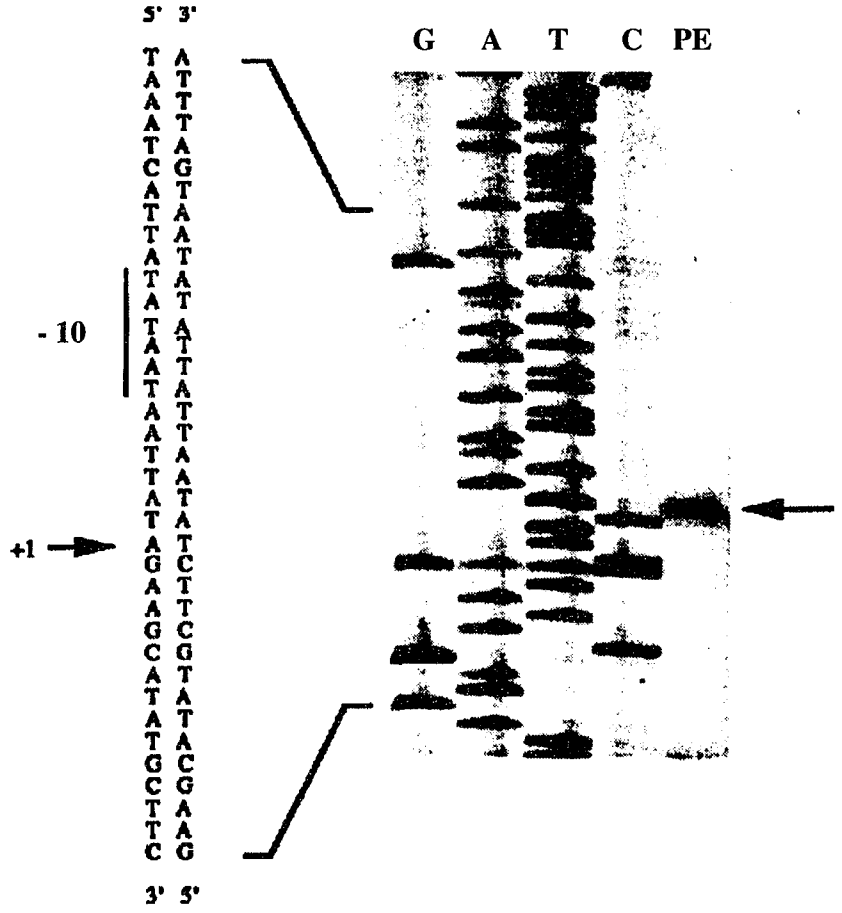

Fig. 3.8. Determination of the transcription start site of the *BCS* operon by primer extension analysis. An oligonucleotide complementary to the *crt* sequence (from nucleotide positions 217 to 233, Fig. 3.7) was hybridized to RNA isolated from the stationary phase culture of *C. acetobutylicum* and extended by reverse transcriptase. Lane PE represents the primer extension product. Lanes G, A, T and C represent the sequencing reaction products using the same oligonucleotide as primer and the recombinant plasmid pC10 as template.

transcriptional start sites were found within 150 bp of the start codon of all remaining genes, suggesting that the clustered genes were transcribed as a single unit to form an operon, designated as *BCS* (butyryl-CoA synthesis). The transcriptional organization within the gene cluster is summarized in Fig. 3.9.

3.2.8. Expression in *E. coli* and *C. acetobutylicum*. BHBD or crotonase were overproduced in crude extracts of *E. coli* XL1-Blue containing either pb37 or pC10, as shown in Table 3.3. The assay analysis for BCD activity was also conducted, using *E. coli* extracts made from cells grown either aerobically or anaerobically, as described in Materials and Methods. The *E. coli* was grown anaerobically due to the fact that BCD might be air sensitive. However, the BCD activity was undetected from either source.

A 6.8 kb *Ban*II fragment, containing the entire *BCS* operon was therefore subcloned to an *E. coli*/*C. acetobutylicum* shuttle vector pSYL2, which contains both *E. coli* and clostridial origins of replication (Lee et al., 1992a and 1992b). The subclone was designated as pSYL2-BCS (see physical map in Fig. 3.9). Both pSYL2 and pSYL2-BCS were used to transform either *E. coli* XL1-Blue or *C. acetobutylicum*, as described in Materials and Methods. Crude extracts from cultures containing either pSYL2 (control) or pSYL2-BCS were assayed for BHBD, crotonase and BCD activities, and the results are also shown in Table 3.3. During the stationary phase, the BHBD and crotonase activities were elevated significantly in *E. coli* harboring the pSYL2-BCS plasmid. However, the BCD activity was still undetected from *E. coli* extracts, probably because of the instability of this enzyme. For *C. acetobutylicum*, the BHBD, crotonase

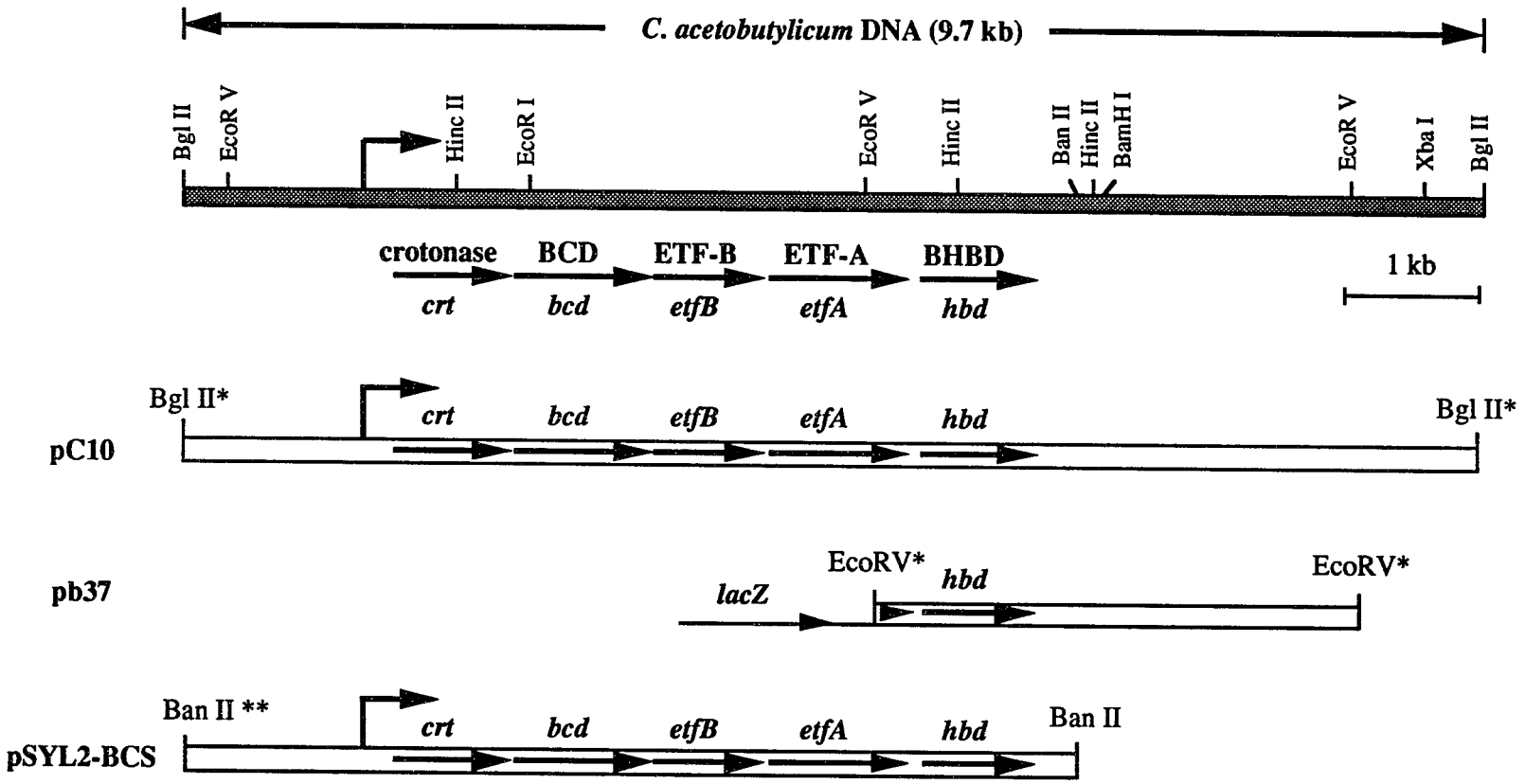

Fig. 3.9. Transcriptional organization within the clustered genes encoding the enzymes involved in the butyryl-CoA synthesis. Open boxed regions represent the cloned insert. The arrow upstream of the *crt* gene represents the transcriptional initiation site. Two asterisks indicate that the *Ban*II is derived from the polylinker cloning site of pUC19.

and BCD activity levels increase 2-to-3 fold when harboring the subclone pSYL2-BCS (Table 3.3).

3.2.9. Crotonase purification. The crotonase was purified and samples were loaded onto a 12% SDS-polyacrylamide gel as described in Materials and Methods. The purification table was shown in Table 3.4. Two bands, one in the range of 29 kDa and the other in 14 kDa, were present (see Fig. 3.10). The observed 29-kDa band was processed for its N-terminal amino acid sequence, and the first ten amino acid residues were as follows: Lys/Thr-Glu-Leu-Asn-Asn-Val-Ile-Leu-Glu-Lys. The purified crotonase exhibited an Mr size much smaller than reported (29 kDa vesus 43 kDa, Waterson et al., 1972). However, the N-terminal sequencing data from the purified crotonase agree closely with the deduced peptide sequence from its encoding gene, except that the first methionine residue was ambiguous from the N-terminal sequencing data. In addition, the estimated Mr of 28.2 kDa for crotonase from the DNA sequencing data also match closely with the observed 29-kDa size. The reason for the somewhat smaller crotonase Mr size is not known. However, this subunit is quite similar in size to the corresponding purified bovine enzyme (Waterson and Hill, 1972).

3.2.10. Protein sequence analysis and alignment. The alignment of the deduced polypeptide sequences of *hbd*, *etfA/B*, *bcd* and *crt* from *C. acetobutylicum* ATCC 824 with those from their functionally related proteins are shown in Figs. 3.11-3.15 for each gene, respectively. A summary of the peptide similarity and identity of these cloned gene products with those from other sources is shown in Table 3.5.

Table 3.4. Purification of *C. acetobutylicum* crotonase

Step	Total Activity (U*)	Specific Activity (U/mg)	Fold Purification
1. Crude extract	4.27×10^6	2.28×10	1
2. Acid-heat treatment		**	**
3. 0 to 50% acetone precipitation		1.42×10^3	62
4. G-200 chromatography		4.11×10^3	180
5. DEAE-Sephadex chromatography		1.23×10^5	5394
6. DEAE-Sephadex chromatography		1.89×10^5	8289

* 1 unit = 1 micromole hydrated per min.

** not quantified

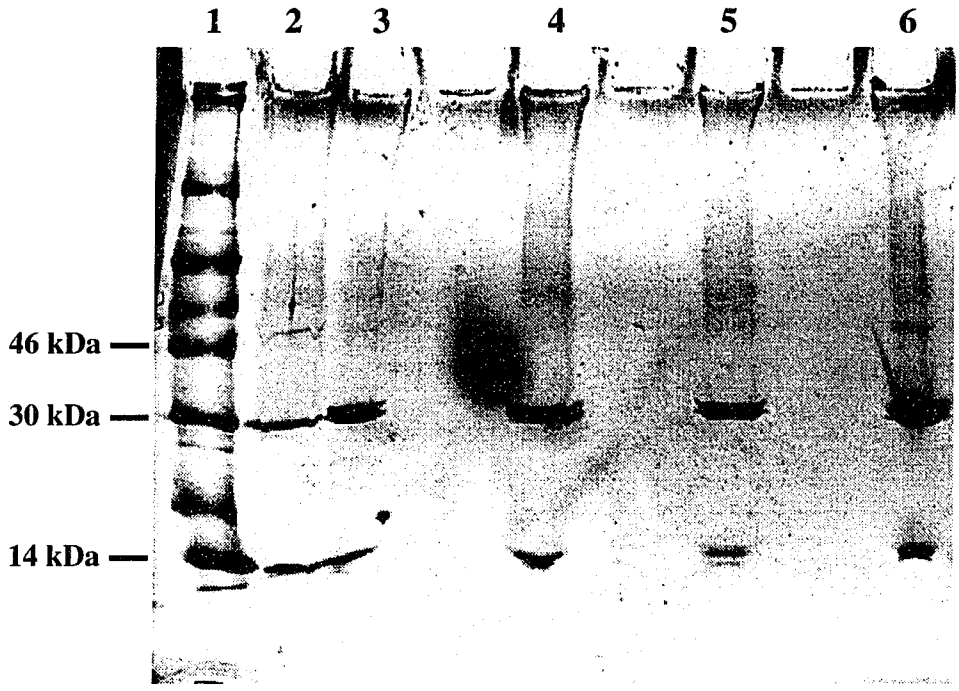

Fig. 3.10. SDS-PAGE analysis of *C. acetobutylicum* crotonase. Lanes:

1. Molecular weight markers.
2-5. Samples obtained after second ion-exchange chromatography.
   2. Fraction from the peak front.
   3. Fraction from the front-to-middle peak.
   4. Fraction from the middle-to-tail peak.
   5. Fraction from the peak tail.
6. Sample obtained after first ion-exchange chromatography.

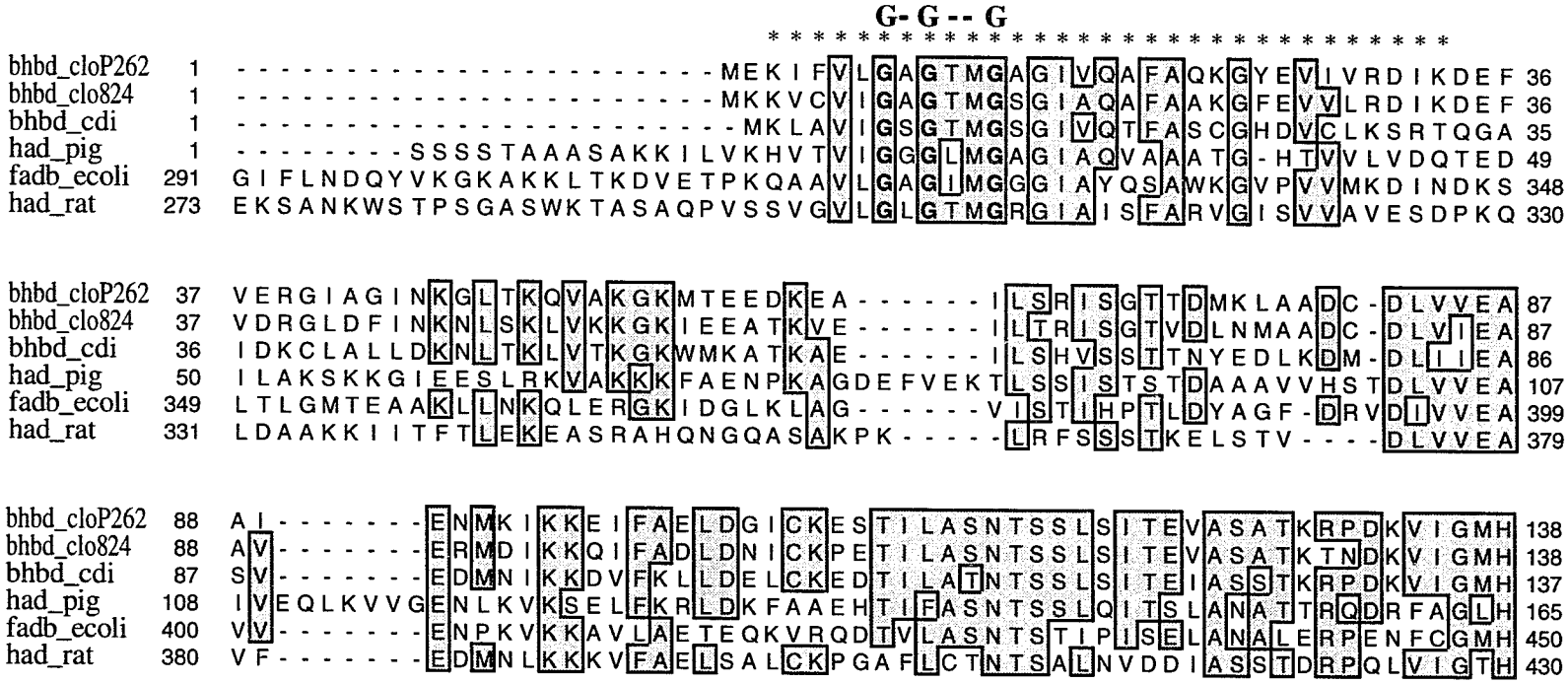

Fig. 3.11. Alignment of the amino acid sequence of *C. acetobutylicum* ATCC 824 BHBD and its functionally related enzymes. The putative NAD-binding site is marked with asterisks (*). The amino acid sequence numbers for each enzyme are shown on both the left and the right of the plot. Abbreviations: bhbd_cloP262, bhbd_clo824 and bhbd_cdi, BHBD from *C. acetobutylicum* P262, ATCC 824 and *C. difficile*, respectively; had_pig, fadb_ecoli and had_rat, HAD from pig, *E. coli* and rat, respectively. For FADB and HAD from *E. coli* and rat, only the region corresponding to HAD activity are aligned to conserve space.

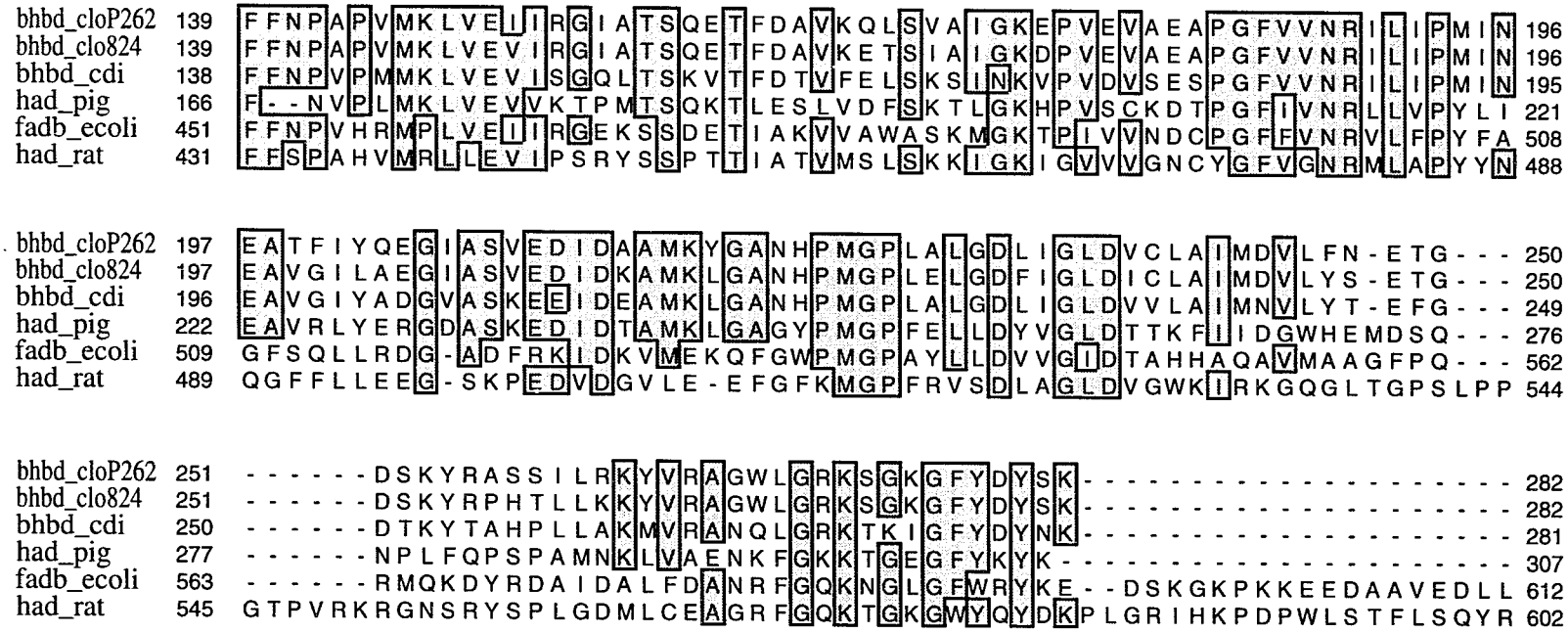

Fig. 3.11. Continued.

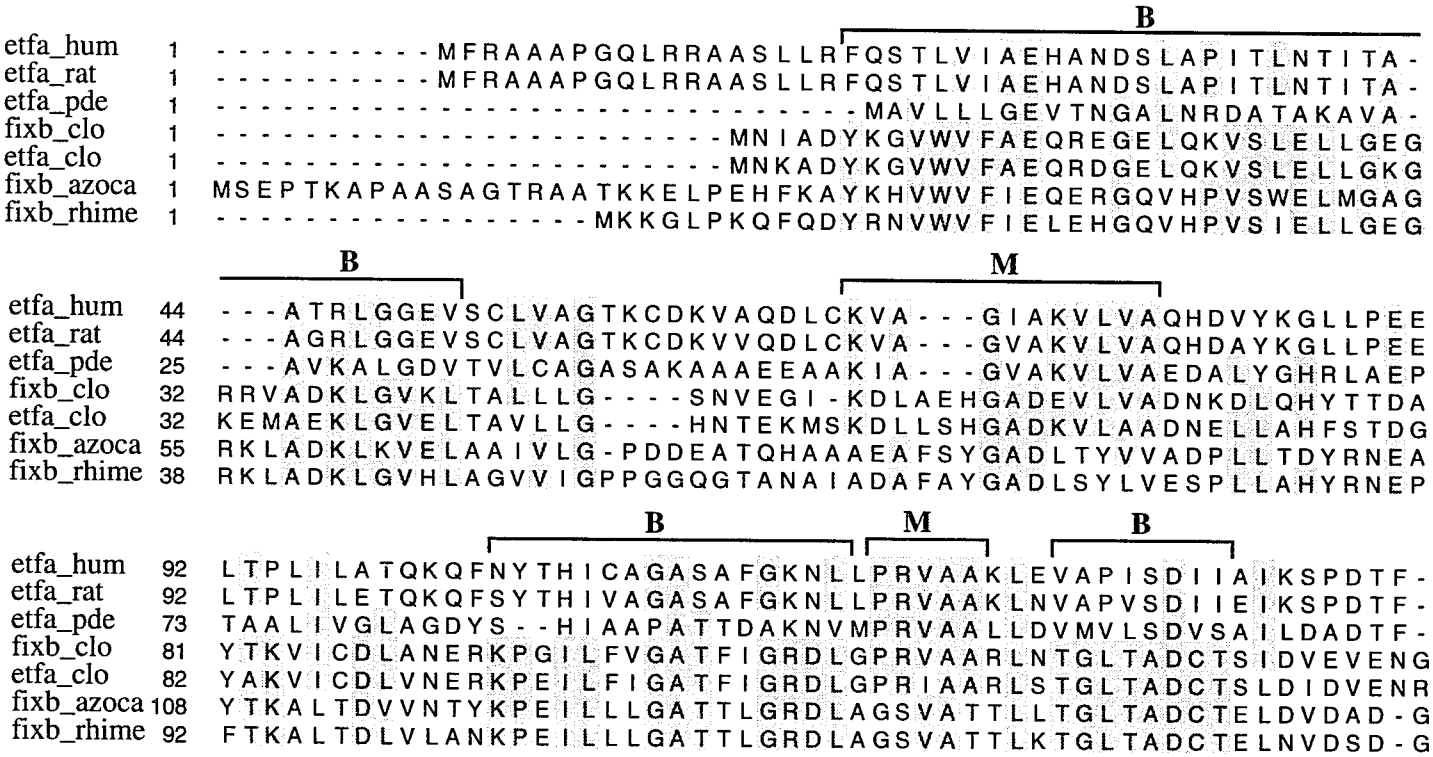

Fig. 3.12. Alignment of the amino acid sequence of *C. acetobutylicum* ATCC 824 ETF-A and its functionally related enzymes. The amino acid sequence numbers for each enzyme are shown on the left of the plot. Abbreviations: etfa_hum, etfa_rat, etfa_pde and etfa_clo, α-subunit of ETF from human, rat, *P. denitrificans* and *C. acetobutylicum* ATCC 824, respectively; fixb_clo, fixb_azoca and fixb_rhime, *fixB* gene products from *C. acetobutylicum* P262, *A. caulinodans* and *R. meliloti*, respectively. The conserved regions shown indicate a higher homology to either the bacterial *fixB* gene products (marked with a 'B') or to the mammalian α-ETF (marked with an 'M'). The C-terminal region showing a high homology to both bacterial and mammalian counterparts is indicated by 'All Homology'.

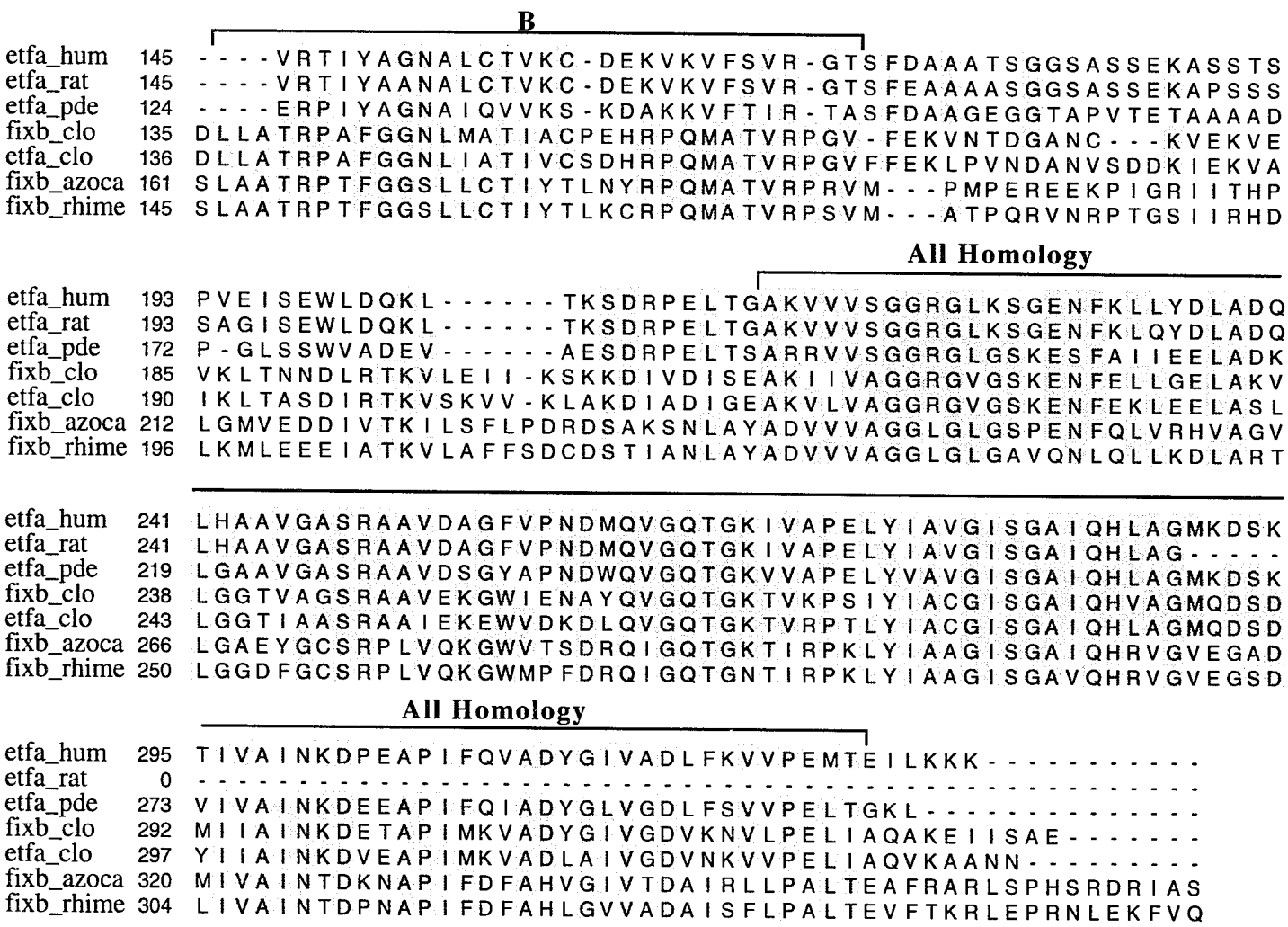

Fig. 3.12. Continued.

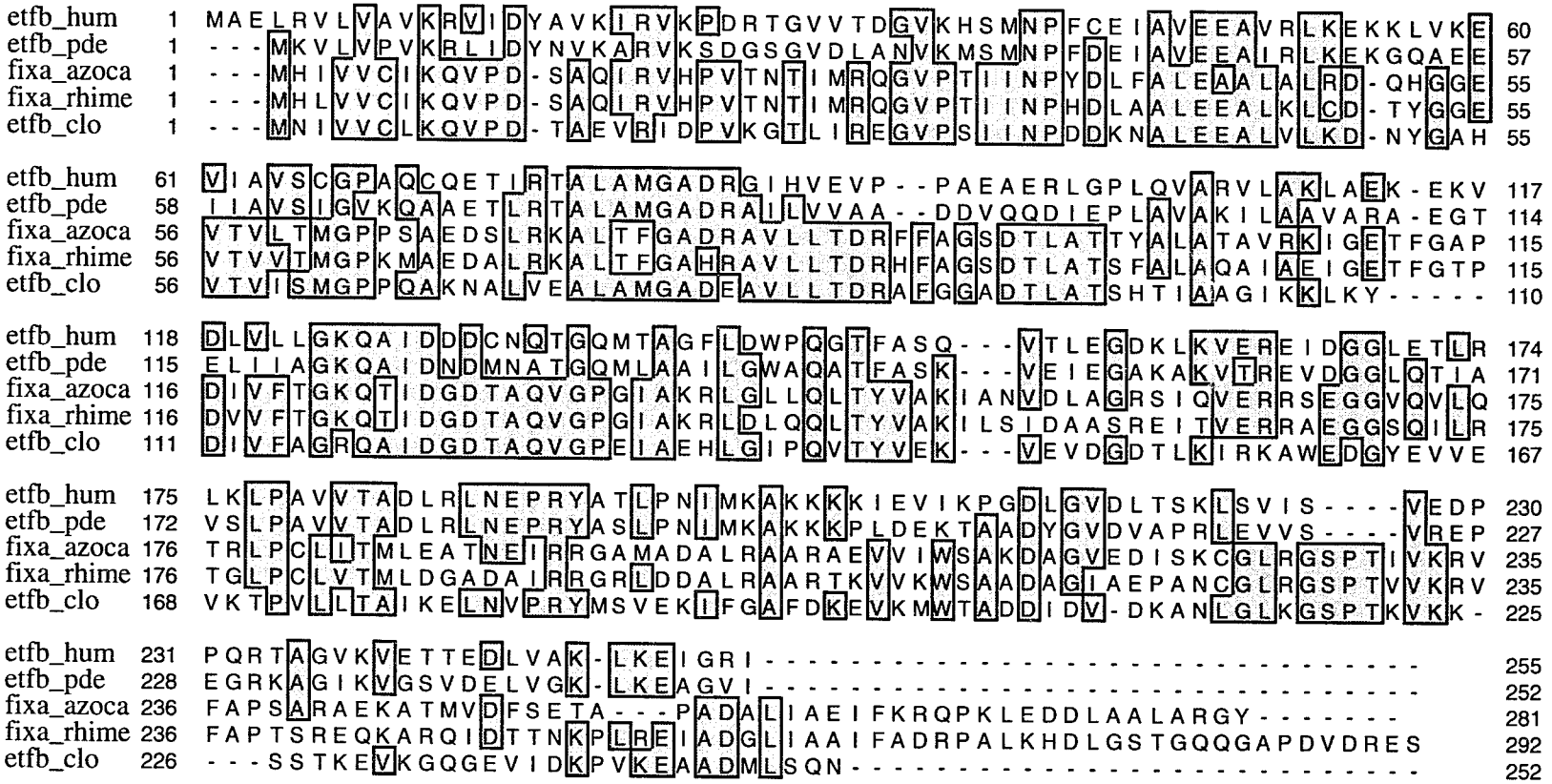

Fig. 3.13. Alignment of the amino acid sequence of *C. acetobutylicum* ATCC 824 ETF-B and its functionally related enzymes. The amino acid sequence numbers for each enzyme are shown on both the left and the right of the plot. Abbreviations: etfb_hum, etfb_pde and etfb_clo, β-subunit of ETF from human, *P. denitrificans* and *C. acetobutylicum* ATCC 824; fixa_azoca and fixa_rhime, *fixA* gene products from *A. caulinodans* and *R. meliloti*, respectively.

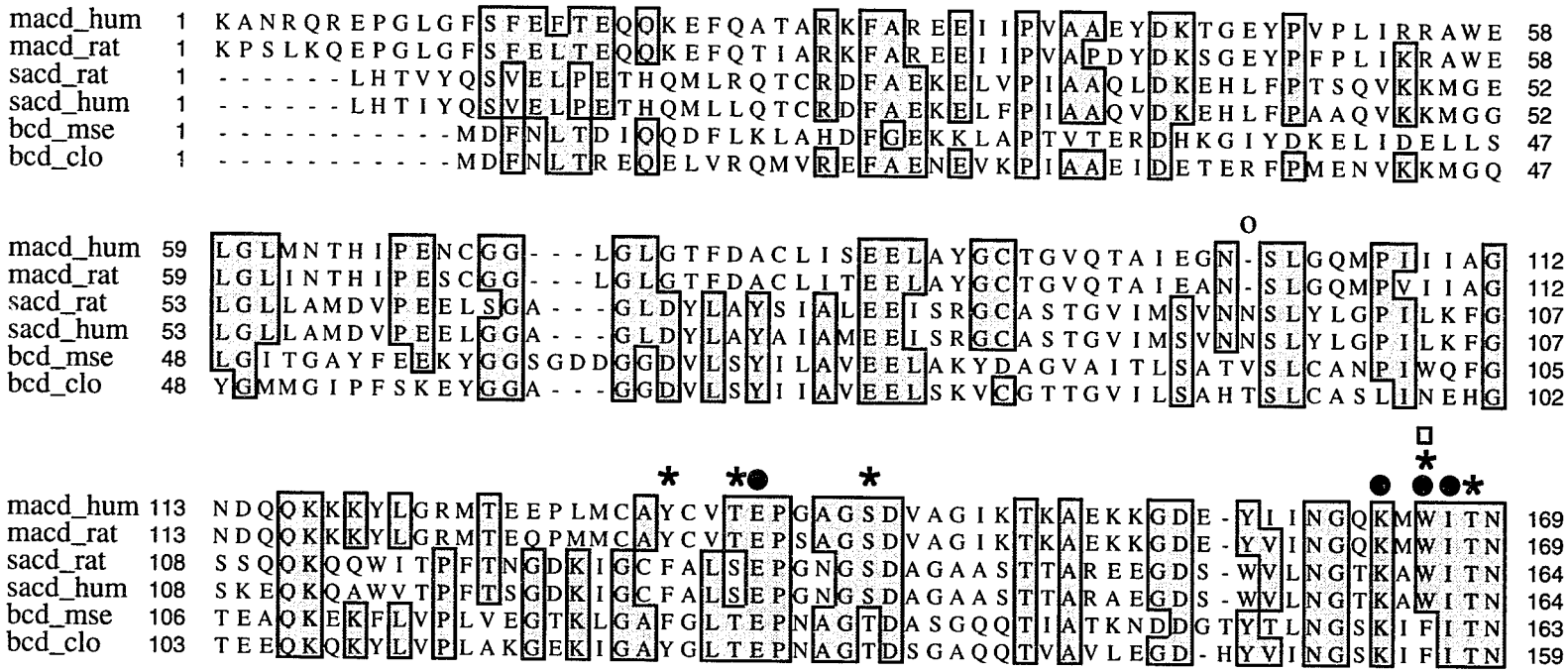

Fig. 3.14. Alignment of the amino acid sequence of *C. acetobutylicum* BCD and its functionally related enzymes. The amino acid sequence numbers for each enzyme are shown on left and right of the plot. Abbreviations: sacd_rat, sacd_hum, SACD from rat and human; macd_rat and macd_hum, MACD from rat and human; bcd_mse and bcd_clo, BCD from *M. elsdenii* and *C. acetobutylicum*, respectively. The Glu, suggested to be in catalysis, is marked with a plus sign (+). The residues that are suggested to be involved in the short-chain specificity are marked with open circles (o). The residue that is suggested to contribute to oxygen sensitivity is marked with a square (□). The residues that are suggested to be involved in the FAD-binding are marked with asterisks (*). The residues that are suggested to interact with the ETF are marked with dots (●).

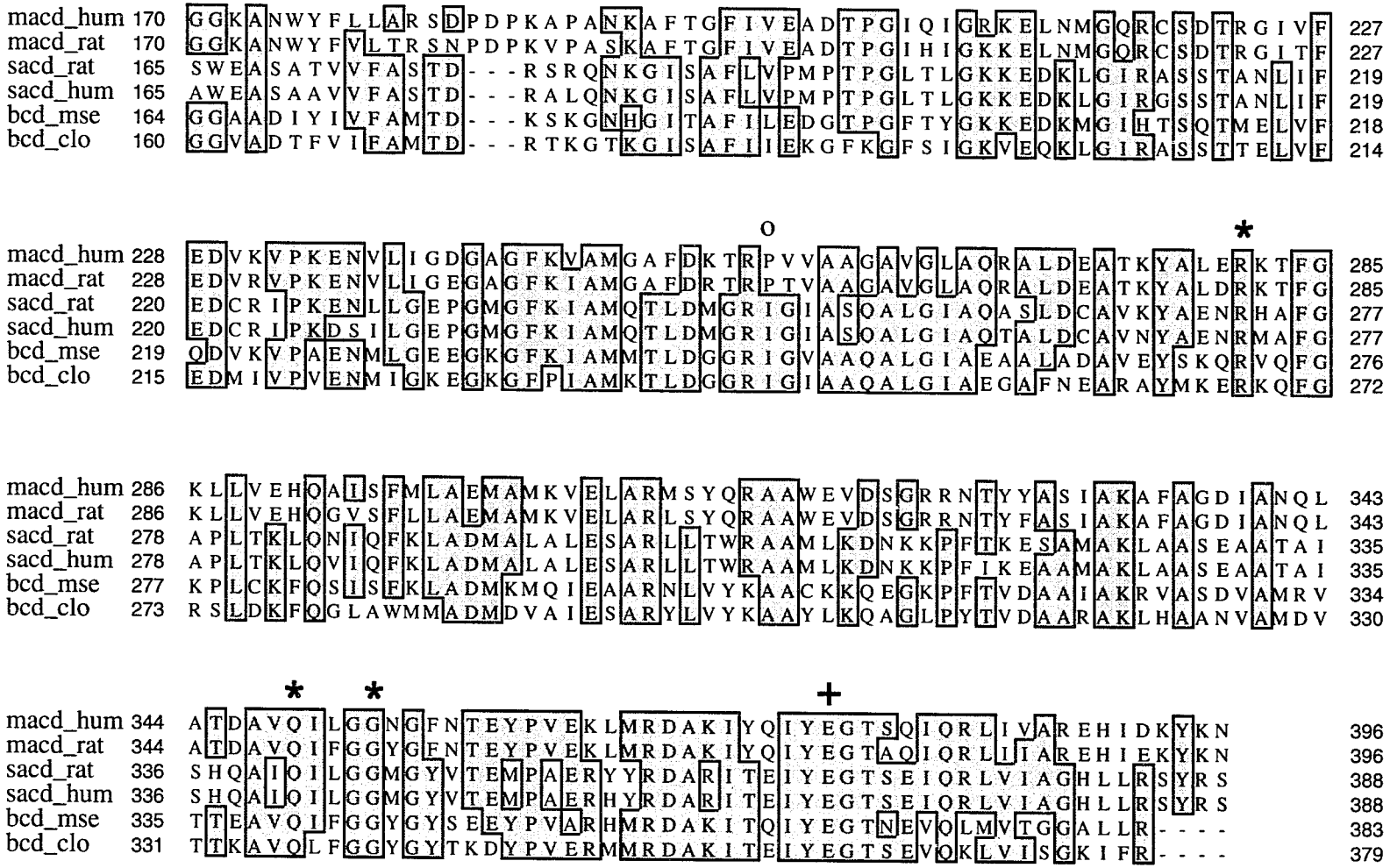

Fig. 3.14. Continued.

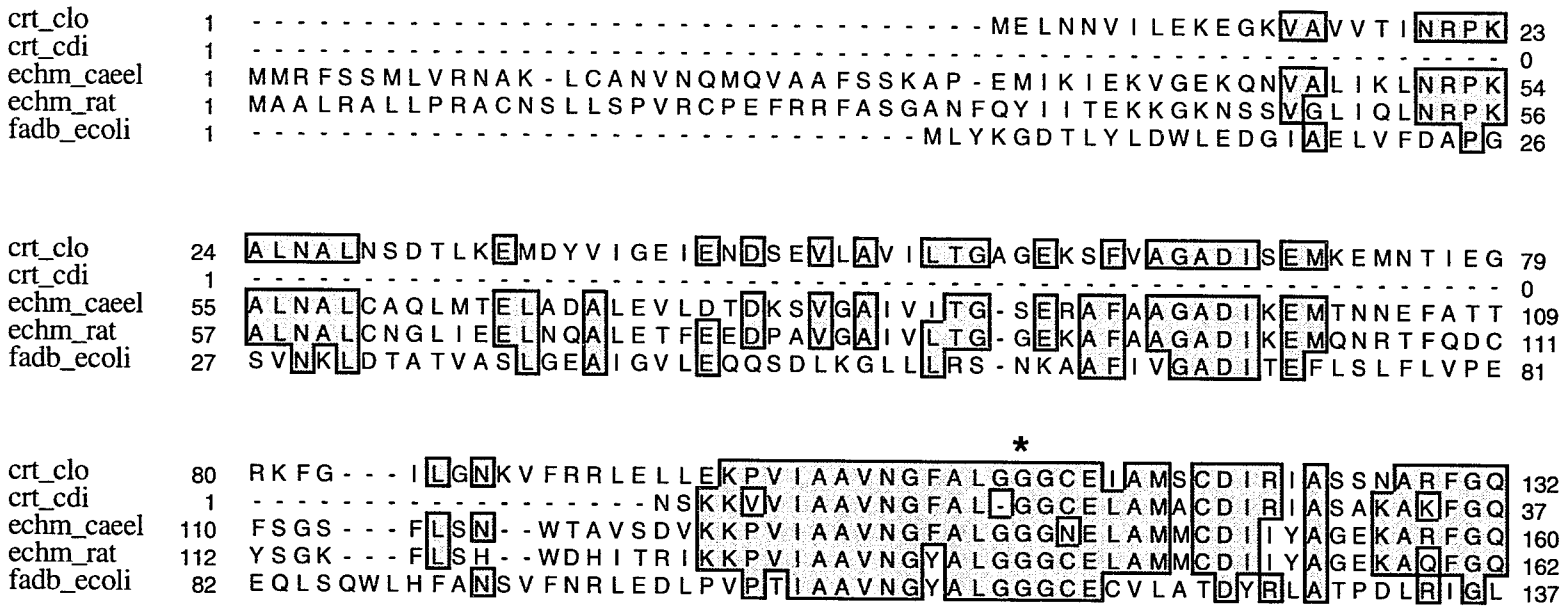

Fig. 3.15. Alignment of the amino acid sequence of *C. acetobutylicum* crotonase and its functionally related enzymes. The amino acid sequence numbers for each enzyme are shown on both left and right of the plot. The glycine residue that was suggested to be important for catalysis is marked with an asterisk (*). Abbreviations: crt_clo and crt_cdi, crotonase from *C. acetobutylicum* and *C. difficile;* echm_caeel, echm_rat and fadb_ecoli, ECH from *C. elegans,* rat, and *E. coli,* respectively. For fadb_ecoli, only the region corresponding to ECH activity are aligned to conserve space. For crt_cdi, only the available cloned sequences are aligned.

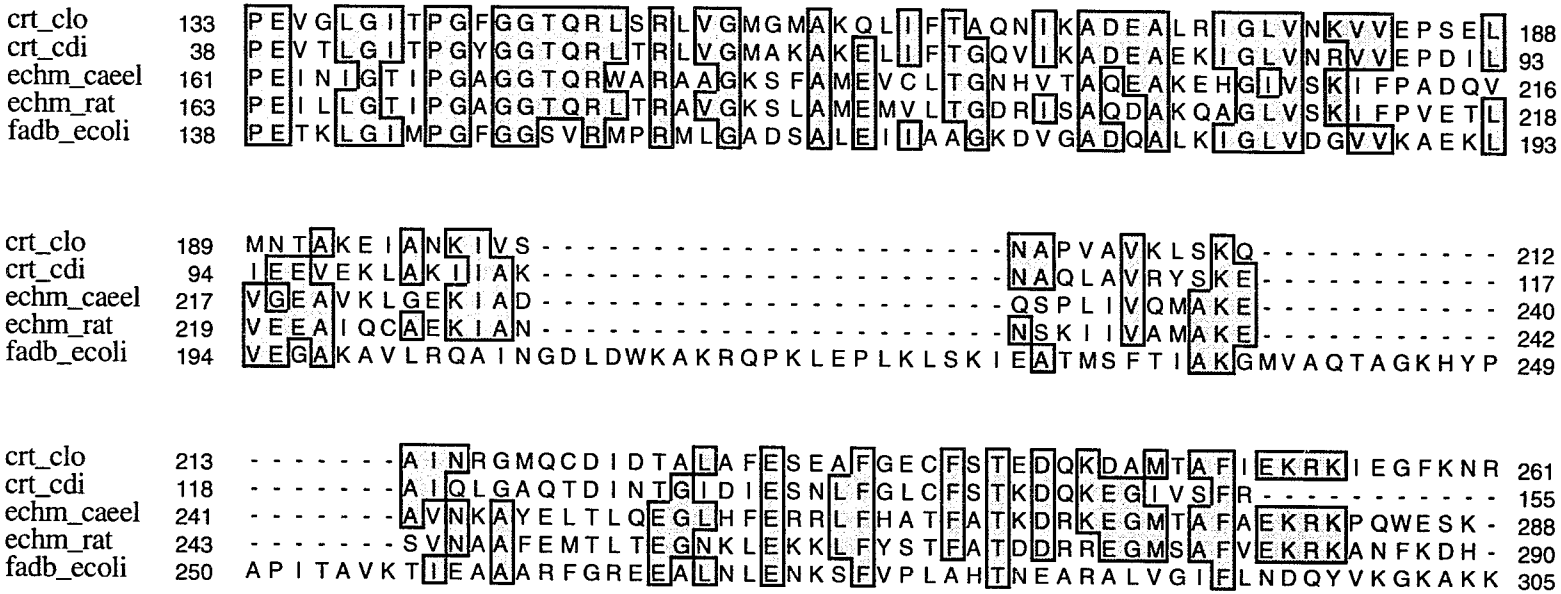

Fig. 3.15. Continued.

Table 3.5. Sequence comparison of *BCS* operon encoded enzymes and their functionally related enzymes

Enzyme[a]	Source	Length (aa)[b]	Mr (kDa)	Similarity %	Identity %	Reference
Crotonase	*C. acetobutylicum*	261	28.2	100	100	This work
Crotonase	*C. difficile*	155[c]		79	64	Mullany et al., 1994
ECHM	Rat	290	31.5	66	41	Minami-Ishii et al., 1989
ECHM	*C. elegans*	288	31.2	65	40	Wilson et al., 1994
FADB	*E. coli*	729	79.6	59	34	Yang et al., 1991
BCD	*C. acetobutylicum*	379	41.4	100	100	This work
SACD	*M. elsdenii*	383	41.9	73	56	Becker et al., 1993
SACD	Rat	388	42.2	68	48	Matsubara et al., 1989
SACD	Human	388	42.2	66	48	Naito et al., 1989
MACD	Human	396	43.7	62	38	Kelly et al., 1987
MACD	Rat	396	43.7	60	37	Matsubara et al., 1987
ETF-B	*C. acetobutylicum*	252	27.2	100	100	This work
FixA	*R. meliloti*	292	31.1	67	46	Earl et al., 1987
FixA	*A. caulinodans*	281	30.1	66	46	Arigoni et al., 1991
β-ETF	*P. denitrificans*	252	27.2	55	32	Bedzyk et al., 1993
β-ETF	Human	255	27.5	56	30	Finocchiaro et al., 1993

Table 3.5. Continued.

Enzyme[a]	Source	Length (aa)[b]	Mr (kDa)	Similarity %	Identity %	Reference
ETF-A	*C. acetobutylicum* ATCC 824	337	36.1	100	100	This work
FixB	*C. acetobutylicum* P262	334	36.4	86	74	Youngleson et al., 1994
FixB	*A. caulinodans*	369	39.7	67	45	Arigoni et al., 1991
FixB	*R. meliloti*	353	37.8	65	46	Earl et al., 1987
α-ETF	Human	333	35.1	61	39	Finocchiaro et al., 1988
α-ETF	*P. denitrificans*	308	33.0	58	36	Bedzyk et al., 1993
α-ETF	Rat	289	30.0	59	35	Shinzawa et al., 1988
BHBD	*C. acetobutylicum* ATCC 824	282	30.5	100	100	This work
BHBD	*C. acetobutylicum* P262	282	31.4	87	78	Youngleson et al., 1989
HAD	Pig	307	33.3	61	44	Bitar et al., 1980
HAD	Rat	721	78.5	56	38	Osumi et al., 1985
FADB	*E. coli*	729	79.6	55	37	Yang et al., 1991

a. Abbreviations: ECHM, mitochondrial precursor of ECH; FADB, fatty oxidation complex alpha subunit.

b. Length of the amino acid residues.

c. Incompletely cloned, comparison was based on the known 155 amino acids.

3.3. Discussion

In the central acetone-butanol fermentation pathway, BHBD, crotonase and BCD catalyze the conversion of one key intermediate, acetoacetyl-CoA, to another key intermediate, butyryl-CoA. There has not yet been reports of the purification and characterization of all of the enzymes responsible for this conversion. The cloning of the genes encoding these enzymes has therefore provided new information concerning gene regulation and significantly improved the understanding of the genetic structures and other elements in the butyryl-CoA synthesis.

3.3.1. Operon arrangement. It has been known that the genes encoding functionally related enzymes in *C. acetobutylicum* tend to cluster. BHBD, crotonase and BCD are involved in the production of butyryl-CoA from acetoacetyl-CoA, and previous research had shown that the specific activity levels of BHBD and crotonase in *C. acetobutylicum* followed similar patterns throughout the course of fermentation (Hartmanis and Gatenbeck, 1984). From the gene structure and arrangement (Fig. 3.9), it is quite probable that these genes form an operon, which correspond to a regulatory unit of associated functions. This suggestion was further confirmed through primer extension experiments (Fig. 3.8). A single transcriptional start site was identified upstream of *crt* but none was identified upstream of any other gene in the cluster. However, even though the thiolase is also in the central fermentation pathway involved in the formation of butyryl-CoA from acetyl-CoA, the gene encoding the thiolase is not in the vicinity of the *BCS* gene cluster, probably because of the presence of the acetone-production pathway.

3.3.2. Gene expression in *E. coli* and *C. acetobutylicum*. The crotonase and BHBD activities are highly expressed in *E. coli* (Table 3.3). However, the BCD activity is detected only in extract of *C. acetobutylicum* but not of *E. coli*, even when *E. coli* is grown under anaerobic condition. The reason for this phenomenon is not known but may result from the expressed protein being improperly folded and not functioning in *E. coli*. Although BHBD, crotonase and BCD activities are elevated in *C. acetobutylicum* harboring the pSYL2-BCS, the elevated levels are not as high as for those in *E. coli*. The reason for this result could be that the specific activity levels of BHBD, crotonase and BCD in *C. acetobutylicum* are already extremely high (Hartmanis and Gatenbeck, 1984, Waterson et al., 1972). An increased gene dosage might not exhibit a dramatic effect on the enzyme activity level as in *E. coli*, where the basal activity of BHBD, crotonase or BCD is at a very low level (Table 3.3). Alternatively, perhaps an autoregulatory control exists.

3.3.3. Coenzyme- and substrate-binding sites for BHBD. Various dehydrogenases are characterized by two major domains. One domain is involved in coenzyme binding and the other in substrate binding (Rosemann et al., 1975). The common structure of the NAD-binding site in many dehydrogenases is a βαβ-fold, centered around a conserved sequence G-x-G-x-x-G (Wierenga et al., 1986). The first glycine is located on the end of the first β-sheet, the second is the beginning of the α-helix, and the third is needed to provide space for a close interaction between the β-sheets and the α-helix. There is a putative NAD-binding site, which contains a conserved glycine-rich region of GxGxxG, from amino-acid

residues 3 to 33 in BHBD from *C. acetobutylicum* P262 (Youngleson et al., 1989). The binding site is derived from the comparisons of deduced amino acid sequences of *hbd* with other NAD-dependent enzymes. Thirteen out of 31 residues for BHBD from strain P262 were identical to residues in the two HAD enzymes from pig and rat.

A similar supersecondary structure was observed based on the alignment of the BHBD enzyme from strain ATCC 824 with the HAD enzymes from rat and pig (see Fig. 3.11.). In fact, of the aligned 31 residues from position 3 to 33, 18 of these showed an identity with the porcine HAD and 15 with the HAD portion of the rat bifunctional enzyme. Therefore, the putative NAD-binding site of BHBD from *C. acetobutylicum* ATCC 824 might also be located from residues 3 to 33. This observation is in agreement with an X-ray crystallographic study of crystallized porcine HAD at 2.8 Å, which suggests that the NAD-binding site of this enzyme locates within the amino-terminal domain (Birktoft et al., 1987). In the study by Birktoft et al., possible modes of substrate-enzyme interaction were suggested; however, the resolution was not high enough to provide sufficient information about amino acid side chains. Therefore, the active center and the substrate binding site are yet to be defined.

3.3.4. Electron-transfer flavoprotein. The cloning of the *etfA/B* genes provides insight into important, but previously unidentified, elements in the clostridial butyryl-CoA synthesis pathway. Neither ETF nor its related BCD has been purified from any strain of *C. acetobutylicum*. The *etfA* gene from *C. acetobutylicum* ATCC 824 is located 143 bp upstream of *hbd*. Its deduced peptide sequence shared a marked similarity to the alpha

subunits of ETF from human, rat and *P. denitrificans*, and to various *fixB* gene products. Interestingly, the nucleotide sequence of *etfA* also exhibited a close homology with the *fixB* gene, located upstream of *hbd* from *C. acetobutylicum* P262 (Youngleson et al., 1994). From the gene structure and arrangement, it is probable that the two are homologous genes from different clostridial strains. Therefore, the gene products of *etfA* from strain ATCC 824 and of *fixB* from P262 should perform the same function.

The *etfA* gene is then immediately preceded by an *etfB* gene, which encodes the putative β-subunit of ETF in *C. acetobutylicum*. The deduced peptide sequence of this gene shared a high similarity and identity with the β-subunit of ETF from the human and *P. denitrificans* sources (Table 3.5). This sequence also shared a ~66% similarity and a 46% identity with *fixA* from rhizobia and azorhizobia. The alignment of sequences from the ETF-B of clostridia, with its functionally related enzymes from other organisms, showed highly conserved sequences near the amino-terminals and internal regions (Fig. 3.13). In addition, it appears that ETF-B from clostridia shows a much closer homology to the bacterial *fixA* product than to mammalian β-ETF across the entire sequence. The alignment of sequences from the ETF-A of clostridia (Fig. 3.12), also with functionally related enzymes, only shows a partial in-sequence preference to the bacterial *fixB* product, with some conserved blocks showing a higher homology to mammalian α-ETF. Most noticeably, the C-terminal of the ETF-A shows extensively conserved regions to both the bacterial *fixA* product and mammalian α-ETF. However, attempts to identify the probable dinucleotide-binding sites for either FAD or NAD (GxGxxGx

patches), based on the alignment of *etfA* and *etfB*, did not reveal a clear identification for any of them.

There are two reasons for the gene designations as *'etfA/B'* (*C. acetobutylicum* ATCC 824) instead of *'fixB/A'*(*C. acetobutylicum* P262, Youngleson et al., 1994). First, ETF from *P. denitrificans* has been purified and characterized, and its encoding gene cloned and expressed. BCD-related ETF has also been purified and characterized from the anaerobic bacteria *M. elsdenii* and *P. elsdenii*. The *etfA/B* gene from *P. denitrificans* shows a close homology to the *etfA/B* gene from *C. acetobutylicum* ATCC 824 (Table 3.5). Secondly, from the arrangements of the *etfA/B* and *bcd* gene structures of *C. acetobutylicum* ATCC 824 (Figs. 3.8 and 3.9), it is reasonable to propose that ETF-A and ETF-B form the two subunits of an ETF-like heterodimer. This heterodimer is proposed to be involved in the electron transfer to BCD, just as for the mitochondrial α- and β-ETF functions. Finally, the *fixA/B* designation from *C. acetobutylicum* P262 was based on the sequence homology (Youngleson et al., 1994) without the knowledge of the location of the *bcd* structural gene and the experimental confirmation of the enzyme functions. Therefore, *etfA/B* may serve to designate these genes better and provide a more succinct explanation of the functions of their corresponding enzymes.

3.3.5. Butyryl-CoA dehydrogenase (BCD)

3.3.5.1. Catalytic site. Alignment of the deduced amino acid sequences of BCD with functionally related enzymes (Fig. 3.14) showed that, in *C. acetobutylicum*, Glu-363 is the residue homologous to the Glu-376 in

medium-chain acyl-CoA dehydrogenase (MACD), the Glu-368 in short-chain acyl-CoA dehydrogenase (SACD) and the Glu-367 in BCD from *M. elsdenii*. Early work using suicide inhibitors suggested that a glutamic acid residue was responsible for the α, β-dehydrogenation, specifically the α-proton abstraction (Fendrich and Abeles, 1982). The three dimensional structure of MACD showed that Glu-376 indeed is placed adjacent to the substrate α-H, supporting the catalytic mechanism this reference proposes (Kim et al., 1992 and 1993, Kim and Wu, 1988). Exchange of this residue with Gln in human MACD results in a mutant with less than 0.02% catalytic activity, confirming the role of this glutamate (Bross et al., 1990). In BCD from *M. elsdenii*, Glu-367 is the Glu376-homolog residue, and site-directed mutagenesis of the Glu367Gln resulted in a mutant that had less than 0.03% of the activity seen in the normal cloned BCD (Becker et al., 1993). Recently, the catalytic site for substrate binding has also been confirmed by crystal-structure analysis of BCD from *M. elsdenii* (Djordjevic et al., 1995) and rat SACD (Glu-368, Kim et al., 1994, Lundberg and Thorpe, 1993). Since in *C. acetobutylicum*, Glu-363 is the residue homologous to the noted catalytic sites (Fig. 3.14), it is highly probable that this residue is active in such catalysis.

3.3.5.2. Substrate-binding and specificity. The acyl-CoA substrate binding sites of BCD from *M. elsdenii* and the porcine MACD have already been carefully demonstrated (Djordjevic et al., 1995, Kim et al., 1993). In both studies, the fatty acyl chain of the acyl-CoA ligand is found to be deeply buried inside the protein. The phosphopantetheine portion of the CoA moiety has no direct interaction with the enzyme, and the 3'-AMP is positioned at the surface of the tetrameric enzyme molecule. The C_α-C_β

bond of the bound ligand is located between the carboxylate of the catalytic glutamic acid residue and the flavin ring. Several residues that can form potential hydrogen bonds to the CoA moiety of the substrate, for example, Arg-324, Arg-256 and Ser-191 in porcine MACD, and Thr-135 and Arg-247 in BCD from *M. elsdenii*, are suggested in each structure analysis (Djordjevic et al., 1995, Kim et al., 1993). Based on the alignment data (Fig. 3.13), it can be seen that except for an arginine (corresponds to Arg-256 of MACD, Arg-247 of BCD from *M. elsdenii*, and Arg-243 in *C. acetobutylicum*), most of the residues shown are not conserved or replaced by chemically similar residues. The reason for these differences probably involves the substrate specificity in different ACDs, since a weak sequence homology within regions interacting with substrates has been shown to be a determining factor in substrate specificity (Djordjevic et al., 1995). It probably also involves the fact that primary structure is insufficient to determine the residues involved in substrate recognition.

Comparison between the 3-D structures of porcine MACD and *M. elsdenii* BCD reveal distinct factors that contribute to the substrate specificity. The reason for substrate specifity between MACD and BCD might be the binding cavity for a different length of substrate (Djordjevic et al., 1995). The relatively shallow cavity for BCD from *M. elsdenii* results from the insertion of a single amino acid, Val-94. This insertion distorts the helix that binds the substrate, thereby bringing it closer to the substrate. Another reason for the deeper cavity for MACD is the side-chain of residue Pro-257, which results in a helix that is less aligned and farther removed from the substrate. From the alignment data (Fig. 3.14), it is evident that various ACDs, including BCD from *C. acetobutylicum*,

also contain an additional residue (Thr-91 for *C. acetobutylicum*) at the same position as observed in BCD from *M. elsdenii*. In addition, the proline in MACD is replaced by isoleucine in various SACD, including Ile-244 in *C. acetobutylicum*. It is therefore expected that the BCD from *C. acetobutylicum* might also exhibit a shallow substrate-binding cavity, thus explaining the short-chain specificity of this enzyme.

3.3.5.3. FAD-polypeptide interaction. The amino acid sequence alignment of the ACDs from rat, human and bacterial sources (Fig. 3.14) showed no region that has the clear homology to the FAD-binding sites (GxGxxGx patches) found in the other FAD-binding enzymes. This observation is consistent with the results from three-dimensional studies, which showed that no classical nucleotide binding domain (βαβ secondary structure) has been observed in the vicinity of the FAD-binding site (Kim and Wu, 1988). This phenomenon is also consistent with the knowlege that ACDs require an ETF as the electron donor/acceptor and therefore might not contain a binding site for NAD or NADP.

Some of the amino acids in the FAD-binding site identified in the X-ray crystal structure of MACD (Kim et al., 1993) and BCD from *M. elsdenii* (Djordjevic et al., 1995) are either identical or chemically similar to those from *C. acetobutylicum* (Fig. 3.14). For example, Thr-168, Tyr-133 and Thr-136, which had been identified to be involved in the flavin-ring binding in porcine MACD, are also present in *C. acetobutylicum* (corresponding to Thr-158, Tyr-123 and Thr-126 in BCD, respectively). But Ser-142 and Trp-166, which are also involved in hydrogen bonding with the flavin ring in MACD, are replaced by chemically similar threonine

and phenylalanine residues, respectively, in BCD from both *C. acetobutylicum* (corresponding to Thr-132 and Phe-156) and *M. elsdenii*. Arg-281, Gly-353 and Gln-349 make contact with the ADP moiety of FAD in porcine MACD, and these residues are highly conserved in all aligned sequences, including BCD from *C. acetobutylicum* (Arg-268, Gly-340 and Gln-336, respectively).

3.3.5.4. Structure difference for oxygen sensitivity. One of the main differences between the bacterial BCD and the mammalian ACD is the oxygen sensitivity. Bacterial BCD reacts rapidly with oxygen, which is not true for the mammalian counterpart (Engel, 1981, Engel and Massey, 1971). While *C. acetobutylicum* and *M. elsdenii* are strictly anaerobes, mammalian enzymes transfer reducing equivalents efficiently to the natural acceptor ETF in an aerobic environment. The reason for this difference is explained by 3-D structures of BCD from *M. elsdenii* (Djordjevic et al., 1995) and MACD from rat (Kim et al., 1993, Kim and Wu, 1988). The si-face of the FAD in BCD is more exposed to solvent than that in MCAD, primarily bacause of the substitution of a phenylalanine (Phe-160 in BCD from *M. elsdenii*) for Trp-166 in MACD. The increased exposure of the flavin to solvent results in a stabilized superoxide anion and significantly increased the rate of oxidation of the reduced flavin in bacterial enzyme (Djordjevic et al., 1995). From the alignment data (Fig. 3.14), it is shown that in BCD from *C. acetobutylicum*, Trp-166 of MACD is also replaced by a phenylalanine (Phe-156), consistent with the result from that for *M. elsdenii*. Therefore, Phe-156 might also be a contributor for the high oxygen sensitivity of BCD from *C. actobutylicum*.

The different oxygen reactivity between mammalian and bacterial BCD might reflect a genetic adaptation of mammalian enzymes to prevent access of oxygen to flavin. Another possibility for the oxygen sensitivity of bacterial BCD might be that the enzyme contains an iron-sulfur center, which can easily react with molecular oxygen (Voet and Voet, 1990). However, the putative iron-sulfur binding motifs, which contain multiple cysteine residues arranged in clusters (CxxCxxC or CxC), were not apparent (Chow et al., 1995, Phillips et al., 1987). In fact, there is only a single cysteine residue (Cys-94) throughout the entire peptide sequence of BCD from *C. acetobutylicum*. Therefore, BCD from *C. acetobutylicum* is unlikely an iron-sulfur flavoprotein.

3.3.5.5. ETF-binding site. From the 3-D structures of porcine MACD (Kim et al., 1993) and *M. elsdenii* BCD (Djordjevic et al., 1995), it is suggested that ETF interacts with ACD through the sinister side of the flavin, and Trp-166 and Met-165 in MACD might play a role in the transfer of electrons between the two flavoproteins. It is also shown that many polar residues, such as Glu-137, Arg-210, Glu-212, and Arg-164, are at the surface of the MACD molecule around the Trp-166, where ETF might bind the enzymes through electrostatic interactions. From the alignment data (Fig. 3.14), it is shown that in *C. acetobutylicum*, Met-165 and Trp-166 are replaced by the chemically comparable residues isoleucine (Ile-155) and phenylalanine (Phe-156), respectively. The surrounding residues are also either conserved (Glu-127 and Glu-199 in clostridia are Glu-137 and Glu-212 analogs, respectively) or replaced by lysine (Lys-197 for Arg-210 and Lys-154 for Arg-164, respectively), which maintains a positively charged side chain. Obviously, the primary sequence comparison is not sufficient for

identifying the exact interaction site between the BCD and ETF, and further information about the X-ray structures of different ACDs and ETFs is required.

3.3.6. Crotonase. The gene encoding crotonase, *crt*, is immediately upstream of *bcd*, with only a 13 bp between the two genes. From the comparison of the primary structure (Fig. 3.15), it is seen that most of the conserved blocks are located in the central region, with variations in both N-terminal and C-terminal sequences. Because no X-ray crystallographic structure has been defined for any ECH, the location of the active sites has not been established. However, site-directed mutagenesis had been conducted on *fadB* from *E. coli*. A change of Gly-116 to phenylalanine resulted in an undetectable level of ECH (encoded by the N-terminal of *fadB*) and 3-hydroxyacyl-CoA isomerase activity. In contrast, the hydroxyacyl-CoA dehydrogenase activity, which is encoded by the C-terminal of *fadB*, is maintained at the same level as the wild type (Yang and Elzinga, 1993). From the alignment data, it is noted that the amino acid sequence around the substitued glycine is quite well conserved, suggesting that this region is of great importance to the catalytic function of crotonase.

There was no obvious CoA-binding site found based on the peptide sequence alignment of crotonase with its related enzymes. This deficiency is in contrast to thiolase, which showed a clear putative CoA-binding site with the concensus sequence x_1-x-x-Cys-x-Ser-x-x (Thompson et al., 1989). Cys has been identified in the thiolase as the thiol nucleophile in the substrate binding site, and the x_1 residue is either Asn or Thr.

Nevertheless, further analysis of the alignment of crotonase, as well as BHBD and BCD from *C. acetobutylicum* with their functionally related enzymes, is required. Additional information about the 3-D crystallographic structure and from enzymological studies should reveal homologous domains that are essential for the catalytic functions commonly shared by these enzymes, as well as revealing divergent domains that determine their catalytic specificity.

3.3.7. Gene arrangement and evolution. In *C. acetobutylicum* P262, *hbd* is downstream of *fixB* and upstream of *adh-1*, an alcohol dehydrogenase gene (Youngleson et al., 1989 and 1994). There was no transcription termination sequence between any two pairs of these three genes. In *C. difficile*, *hbd* is downstream of a crotonase encoding gene and upstream of a thiolase gene, with a termination sequence between the crotonase and *hbd* genes but no such sequence between the *hbd* and the thiolase gene (Mullany et al., 1994). In *C. acetobutylicum* ATCC 824, *hbd* is downstream of the *etfA* gene and is followed by a stem-loop structure after its stop codon (Figs. 3.7 and 3.9). Sequencing data for the 1.2 kb downstream region of *hbd* revealed no obvious ORF that could correspond to an alcohol dehydrogenase or a thiolase.

It is noted that functionally identical *hbd* genes from *C. acetobutylicum* ATCC 824 and from strain P262 and *C. difficile* did not share a close identity with each other. This phenomenon was also exhibited in the *etfA/fixB* genes of this study. The functionally identical *etfA* and *fixB* gene products only shared an 86% similarity and a 74% identity to each other. A number of other genes cloned from different

strains of *C. acetobutylicum* also demonstrate such characteristic divergence. The genes encoding butyrate kinase and PTB, *buk* and *ptb* respectively, had been cloned from both ATCC 824 (Cary et al., 1988, Walter et al., 1994b) and NCIMB 8052 strains (Oultram et al., 1993). The deduced amino acid sequence of *buk* showed an 80% similarity and a 64% identity to each other. For *ptb*, the corresponding values were 84% and 69%, respectively.

It is interesting that the deduced amino-acid sequences of the *BCS* operon genes all share close similarity with the equivalent enzymes involved in fatty-acid β-oxidation. This characteristic suggests that a common origin and mechanism exists for the fatty-acid β-oxidation pathway of mammalian mitochondria and the butanol/butyrate synthesis pathway of bacteria.

3.4. Conclusions and recommendations

In this work, five genes encoding enzymes involved in the production of butyryl-CoA from acetoacetyl-CoA were cloned, sequenced and expressed. These genes are clustered in the clostridial genome and form an operon. In addition, a previously unidentified element in this path, ETF with a possible α and a β-subunit, was suggested as being involved in butyryl-CoA synthesis.

None of the enzymes in this path, especially BCD and ETF, have been purified or characterized in *C. acetobutylicum* ATCC 824. In fact, except for the BCD study using *M. elsdenii*, little work has been done with BCD

derived from any other bacteria. The cloning of genes encoding enzymes involved in butyryl-CoA synthesis will help researchers in this laboratory to develop the procedures for enzyme purification and for later enzyme analysis. Such knowledge would be of great importance in understanding the regulation of the central fermentation pathway. BCD from *C. acetobutylicum* may offer many advantages over the mammalian model in studying this pathway. Unlike the mammalian counterpart, which is very difficult to purify, *C. acetobutylicum* might have only one fatty acyl-CoA dehydrogenase present (BCD), thereby allowing for easier purification and a higher protein yield without contamination by other ACDs and greatly reducing the effort required in the purification process.

It would also be interesting to examine the redox properties of BCD and ETF from *C. acetobutylicum*, since the electron flow could be in the opposite direction to that from the mammalian system. In addition, the fatty-acid oxidation cycle is a vital energy production pathway, and an understanding of the electron-transferring properties of this class of enzymes is necessary to an understanding of the regulation mechanism. Because of the complex mixture of enzyme species present, the available data related to redox potentials of BCD and ETF often differ markedly (Gustafson et al., 1986, Fink et al., 1986, Lenn et al., 1990, Stankovich and Soltysik, 1987). Additional study using a simpler model is necessary. The redox processes from the mammalian and bacterial enzymes might be regulated by significantly different mechanisms. This property might permit the researcher to design novel antibiotics which could possess the proper potential to block bacterial metabolism without affecting that of the host organism.

This study also provides materials for gene inactivation, permitting the generation of mutants with improved product characteristics. The recent development of a gene-inactivation system, via integrational plasmids (Edward and Bennett, 1996, Wilkinson and Young, 1994) has allowed these cloned genes to be specifically used to inactivate their counterparts in wild-type strains, and their physiological roles in clostridial strains can then be studied. For example, the *hbd* gene could be specifically inactivated and the acetone production of the mutant might thereby be improved, since the mutant produces neither butanol nor butyrate. This mutant might be of interest if the cost of separation for acetone and butanol is of industrial concern. Alternatively, the generated mutant could also be used for either complementation or pathway metabolite studies.

Some of the more important residues, such as Glu-367 and Thr-91 of BCD in *C. acetobutylicum*, identified based on peptide sequence alignment data (Fig. 3.14), can be used in site-directed mutagenesis studies. The catalytic or physiological roles of these residues could then be evaluated. Such studies would also make it possible to examine further the evolution of the enzymes involved in bacterial butyrate/butanol production and in the mammalian fatty acid β-oxidation pathway. Should these enzymes evolve from a common origin, the catalytic machinery required for a specific reaction would be maintained while some functional groups responsible for substrate specificity could be changed.

Chapter 4. Genes Involved in the Acetate-Production Pathway

The cloning, sequencing and characterization of genes encoding the acetate-production enzymes, PTA and AK in *C. acetobutylicum,* are discussed. These genes were first cloned using a PCR probe derived from the conserved regions of the known AK-encoding genes. The gene cloning results presented herein were confirmed through DNA sequencing and gene expression studies. These genes were then inactivated in the clostridial genome through integration techniques. The interesting results derived from the mutant study are also discussed in detail.

4.1. Introduction

Acetyl-CoA resides at a major branch point in the acid- and solvent-producing pathways. During acidogenesis, acetate kinase (AK) and phosphotransacetylase (PTA) convert acetyl-CoA to acetate, with the production of ATP as an important energy source. During solventogenesis, the activity levels of AK and PTA decrease, suggesting the uptake of acetate may not generally occur through a reversal of these enzymes, which have unclear roles in this stage (Chen, 1993, Hartmanis and Gatenbeck, 1984, Hartmanis et al., 1984).

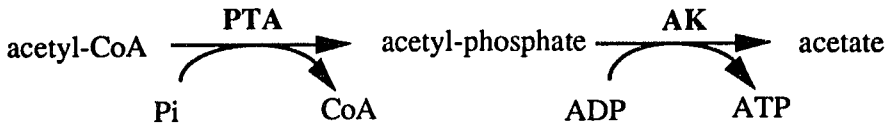

Despite the importance of PTA and AK in the carbon cycling and energy metabolism of both aerobes and anaerobes, only a few molecular

biology studies of these enzymes have been conducted. To date, the *ackA* gene, encoding AK, has only been cloned, sequenced and characterized from *E. coli* (Matsuyama et al., 1989), *Methanosarcina thermophila* (Latimer and Ferry, 1993) and *Bacillus subtilis* (Grundy et al., 1993). The PTA-encoding gene, *pta*, has only been cloned and characterized from *M. thermophila* (Latimer and Ferry, 1993) and *E. coli* (Kakuda et al., 1994, Matsuyama et al, 1989, Yamamoto-Otake et al, 1990). Even though the sequences for *pta* from *Paracoccus denitrificans* (Van Spanning et al., 1994), *B. subtilis* (Glaser et al., 1993) and *Mycoplasma genitalium* (Fraser et al., 1995), and for *ackA* from *Haemophilus influenzae* (Fleischmann et al., 1995) and *M. genitalium* (Fraser et al., 1995) are available in the genome database, these genes are defined only by sequence homolgy and therefore can not be considered as being well characterized.

PTA and AK have not been purified, nor have their genes been cloned from *C. acetobutylicum* ATCC 824. However, PTA purified from the anaerobic archaobacterium *M. thermophila* (Lundie and Ferry, 1989) exists as a monomer with a native Mr of from 42-to-52 kDa. PTA has also been isolated and partially characterized in three other species of clostridia. The Mr value for PTA was found to be 88 kDa in *C. thermoaceticum* (Drake et al., 1981), 63 kDa and 75 kDa in *C. acidiurici* (Robinson and Sagers, 1972) and 60 kDa in *C. kluyveri* (Stadtman, 1955).

The AK enzyme has been purified from *M. thermophila* (Aceti and Ferry, 1988), *C. thermoaceticum* (Schaupp and Ljungdahi, 1974), *Salmonella typhimurium* and *E. coli* (Fox and Roseman, 1986). AK from *E. coli* and *S. typhimurium* are each homodimers with the same subunit

Mr of 40 Kda (Fox and Roseman, 1986). AK from C. *thermoaceticum* has a subunit Mr of 60 Kda (Schaupp and Ljungdahi, 1974), and for AK from *M. thermophila,* a homodimer with a native Mr of 94 kDa was found (Aceti and Ferry, 1988).

The commercial potential of clostridial fermentation for solvent production has grown because of new developments in genetic and metabolic engineering (Mermelstein et al., 1994). However, successful genetic manipulation still requires a better understanding of gene regulation. For example, attempts to redirect carbon flux toward solvent production, thereby increasing yields, require a thorough understanding of the genetic basis of acid production, particularly the genes encoding AK and PTA. Additionally, the factors influencing the production of two-carbon- versus four-carbon-derived products must be more fully understood. To follow is a report of the cloning, sequencing and characterization of genes encoding PTA and AK in C. *acetobutylicum.* A possible promoter for these genes has been identified, and the chromosomal copy of the PTA-encoding gene has been inactivated. The acid and solvent yields using such manipulated strains were carefully measured to determine their relative-efficiency contributions. The engineered mutants therefore provide further information about these important gene functions and yield-enhancing possibilities through genetic manipulation.

4.2. Results

4.2.1. PCR probe. The acetate kinase-encoding gene, *ack*, had already been cloned and sequenced from *E. coli*, *B. subtilis* and *M. thermophila*. Oligonucleotides were designed based on the alignment of the known *ack* gene sequences. An amplification was conducted using the *C. acetobutylicum* genomic DNA as the template and specifically designed oligos as primers (see Table 2.3 for specific sequences), as described in Materials and Methods. A DNA fragment of an expected size of 200 bp was amplified and cloned into a PCR vector (Invitrogen) and then sequenced. The deduced amino acid sequence showed a 77% similarity and a 62% identity in a 68-aa overlap with *ackA* from *E. coli*, an 85% similarity and a 68% identity with *ackA* from *B. subtilis*, and a 79% similarity and a 70% identity with *ack* from *M. thermophila*. The alignment of the deduced peptide sequence from this PCR product with the known *ack* gene sequences is shown in Fig. 4.1. Thus, the 200-bp PCR product was chosen as the acetate kinase-specific probe for λ-phage-library screening.

4.2.2. Screening of the phage library. Prior to the library screening, the specificity and the hybridization conditions were determined by hybridizing the radiolabelled PCR probe with the Southern blots of the genomic DNA, which was digested with restriction enzymes *Eco*RV, *Hinc*II, *Nco*I and *Pvu*II. The results are shown in Fig. 4.2. Fragments of a 3.5 kb *Eco*RV, a 6.0 kb *Hinc*II and a 1.0 kb *Pvu*II demonstrated hybridization signals with the radiolabelled probe.

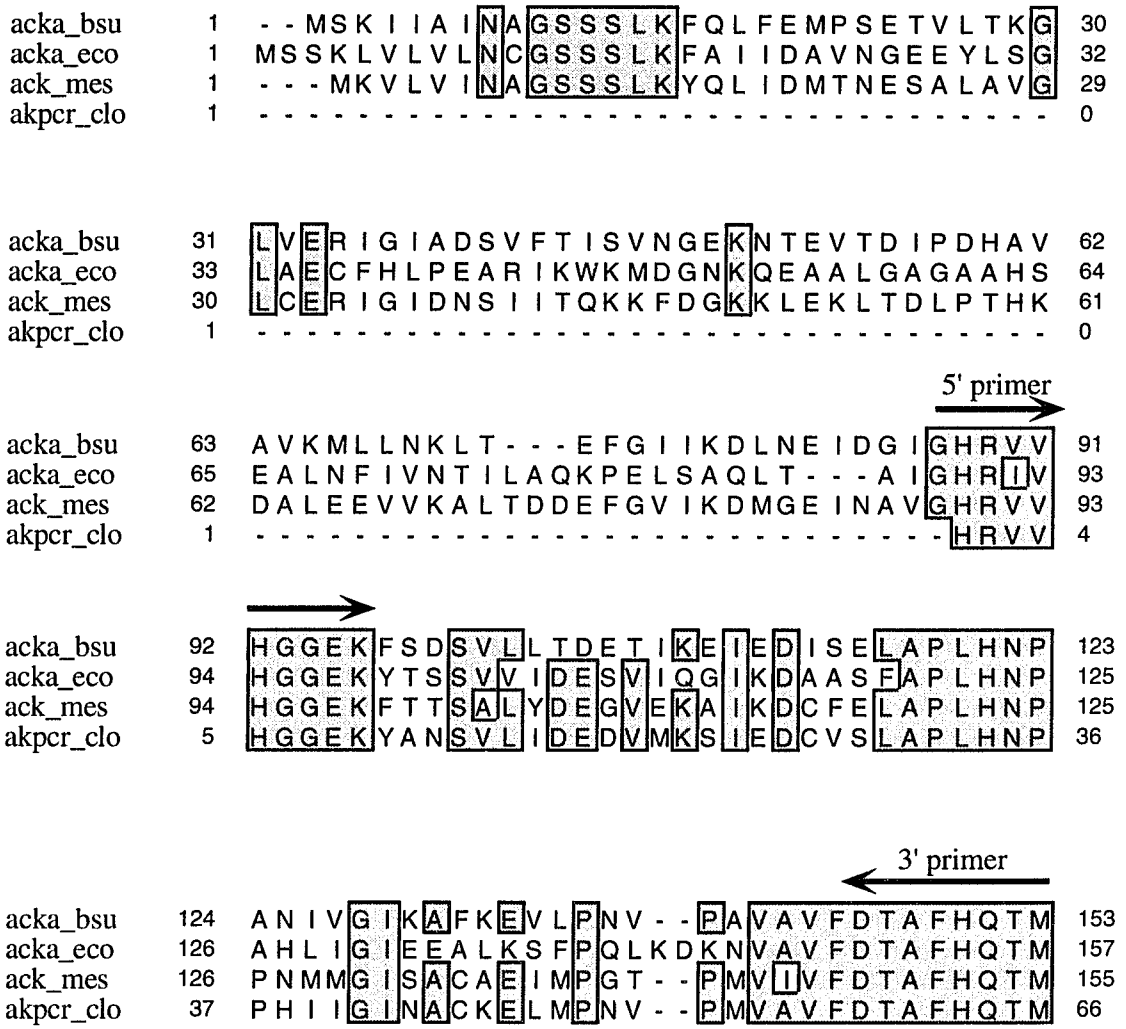

Fig. 4.1. Alignment of the deduced amino acid sequences of the amplified PCR fragment with the known acetate kinase gene sequences. The amino acid sequence numbers for each enzyme are shown on both the left and right of the plot. Abbreviations: akpcr_clo, the amplified PCR fragment from *C. acetobutylicum* ATCC 824; ack_mes, AK from *M. thermophila*; acka_bsu, AK from *B. subtilis*, acka_eco, AK from *E. coli*, respectively. Only the N-terminal residues are shown to save the space.

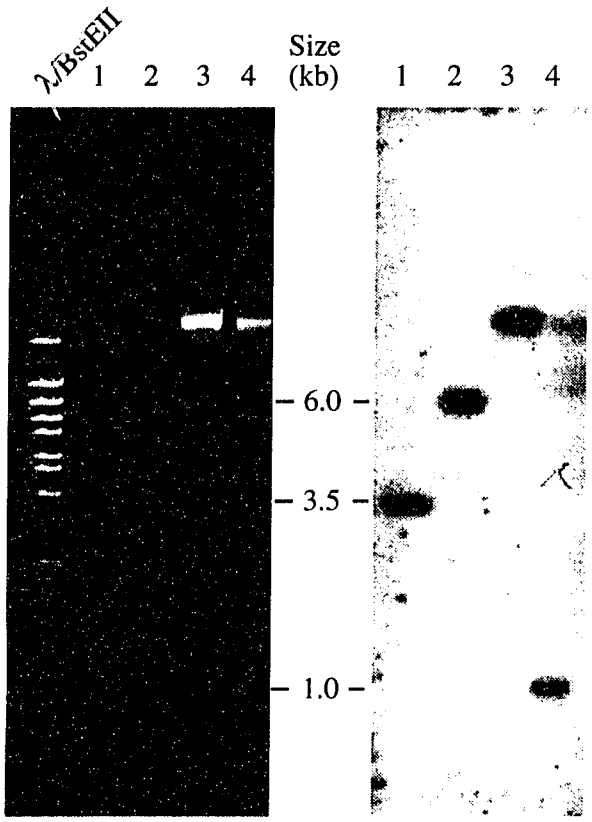

Fig. 4.2. Southern blot analysis of restriction-enzyme-digested *C. acetobutylicum* DNA hybridized to the radiolabelled PCR-screening probe.

(A) Samples were electrophoresed on an 0.8% agarose gel and stained with ethidium bromide.

Lanes 1-4. *Eco*RV, *Hinc*II, *Nco*I and *Pvu*II digests of genomic DNA, respectively.

(B) Autoradiogram of lanes 1-4 after Southern transfer and hybridization to the ^{32}P-labelled PCR-screening probe.

The phage library was diluted to generate 5,000 to 10,000 phage per plate, and six plates were screened. Six candidates were isolated. Compared with the other plaques, the plaque generated from the positive phage was very small, and its size would not increase even after long incubation. After tertiary screening, two distinct phage DNAs were isolated using the plate lysate methods. The genomic and phage DNAs were digested with *Hin*dIII, *Hinc*II, *Eco*RV and *Pvu*II and then blotted to the membranes for southern hybridization. Fragments of a 1.6 kb *Hin*dIII, a 3.5 kb *Eco*RV, a 6.0 kb *Hinc*II and a 1.0 kb *Pvu*II digested phage DNA were hybridized to the probe, the same size as those from the corresonding genomic DNA digests (Fig. 4.3). A ~5.0 kb *Pvu*II fragment also demonstrated a hybridization signal, probably caused by an incomplete digestion. These data suggest that the expected chromosomal region containing the AK encoding gene is located on the recombinant phage. This result also suggests that only one copy of an acetate kinase encoding gene is present in the chromosome. A restriction map of this region of the *C. acetobutylicum* chromosomal fragment is shown in Fig. 4.4.

4.2.3. Subcloning, sequencing and mapping. The 1.6 kb *Hin*dIII-fragment of the positive phage DNA was subcloned into the pUC19 vector. The plasmid was designated as pUC-AKX. The insert of this plasmid was sequenced initially by using the PCR primers previously mentioned. Sequencing data revealed that an incomplete ORF, which showed high similarity with the known *ackA* gene sequences, was contained in this construct. Downstream of this ORF is another incomplete ORF, designated *orfX*, which is preceeded by a putative Shine-Dalgarno (S.D.) sequence TTAGGAGC (Fig. 4.5.). A Blast search in the GenBank database

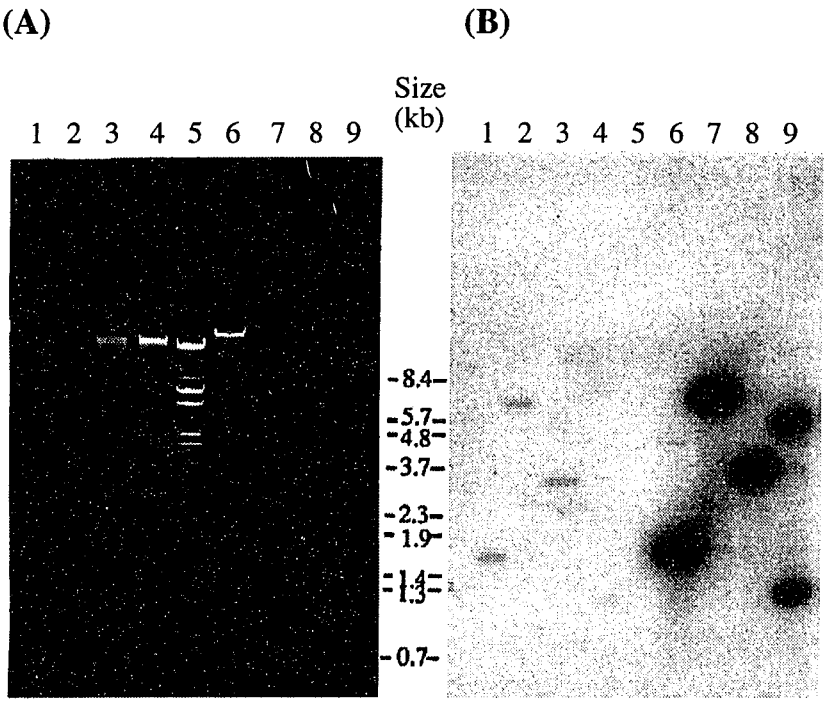

Fig. 4.3. Southern blot analysis of restriction-enzyme-digested genomic and phage DNA using the AK-gene-specific screening probe.

(A) Samples were electrophoresed on an 0.8% agarose gel and stained with ethidium bromide. Lanes:

1-4. *Hind*III, *Hinc*II, *Eco*RV and *Pvu*II digests of genomic DNA, respectively.

5. Size standard.

6-9. *Hind*III, *Hinc*II, *Eco*RV and *Pvu*II digests of phage DNA, respectively.

(B) Autoradiogram of lanes 1-9 after Southern transfer and hybridization to the ^{32}P-labelled PCR-screening probe.

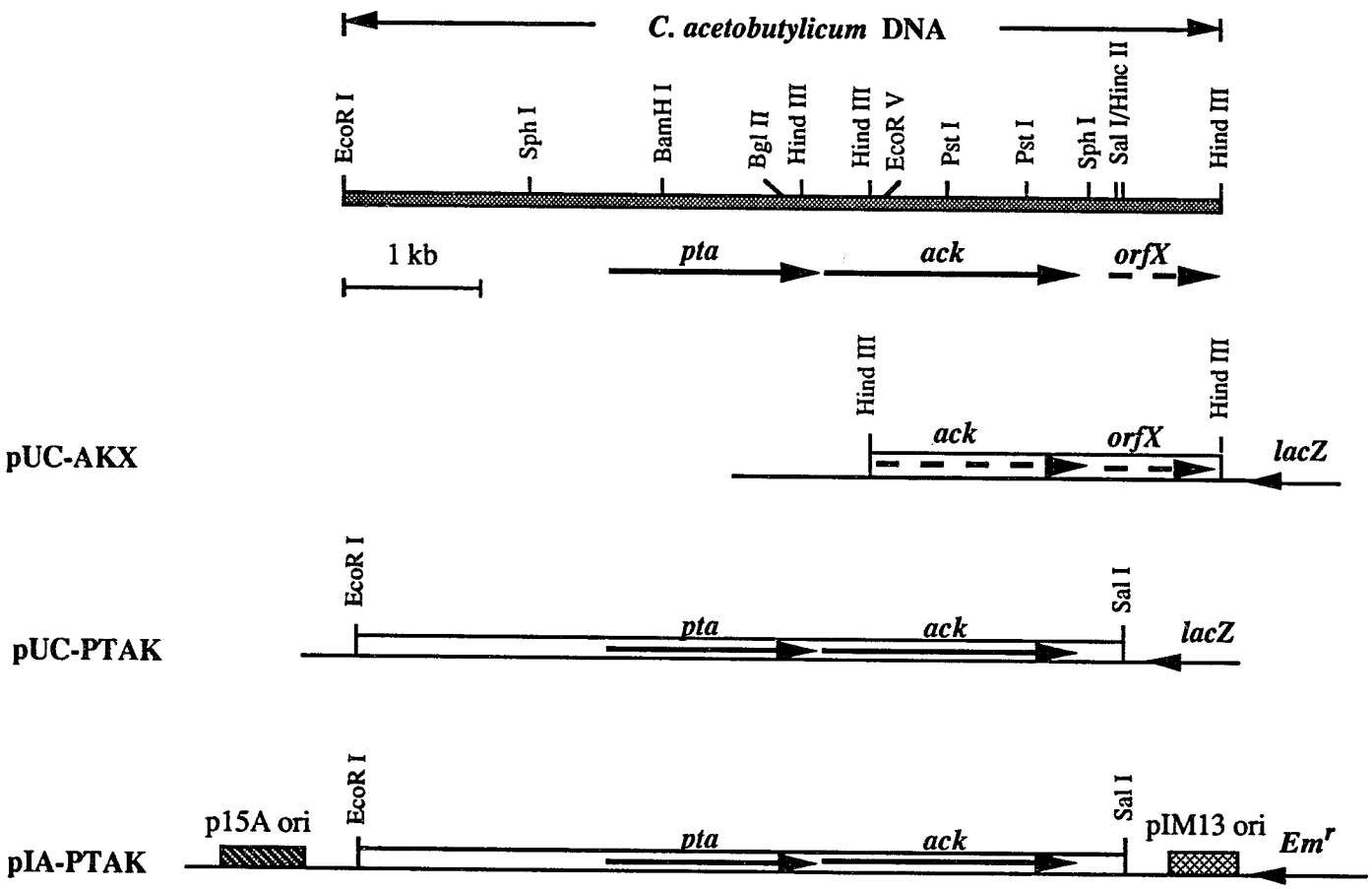

Fig. 4.4. Physical maps of PTA-AK subclones. Open boxed regions represent the cloned insert. The orientations of inserts are indicated by the direction of transcription of *lacZ* and erythromycin resistant gene (Em^r) on vectors.

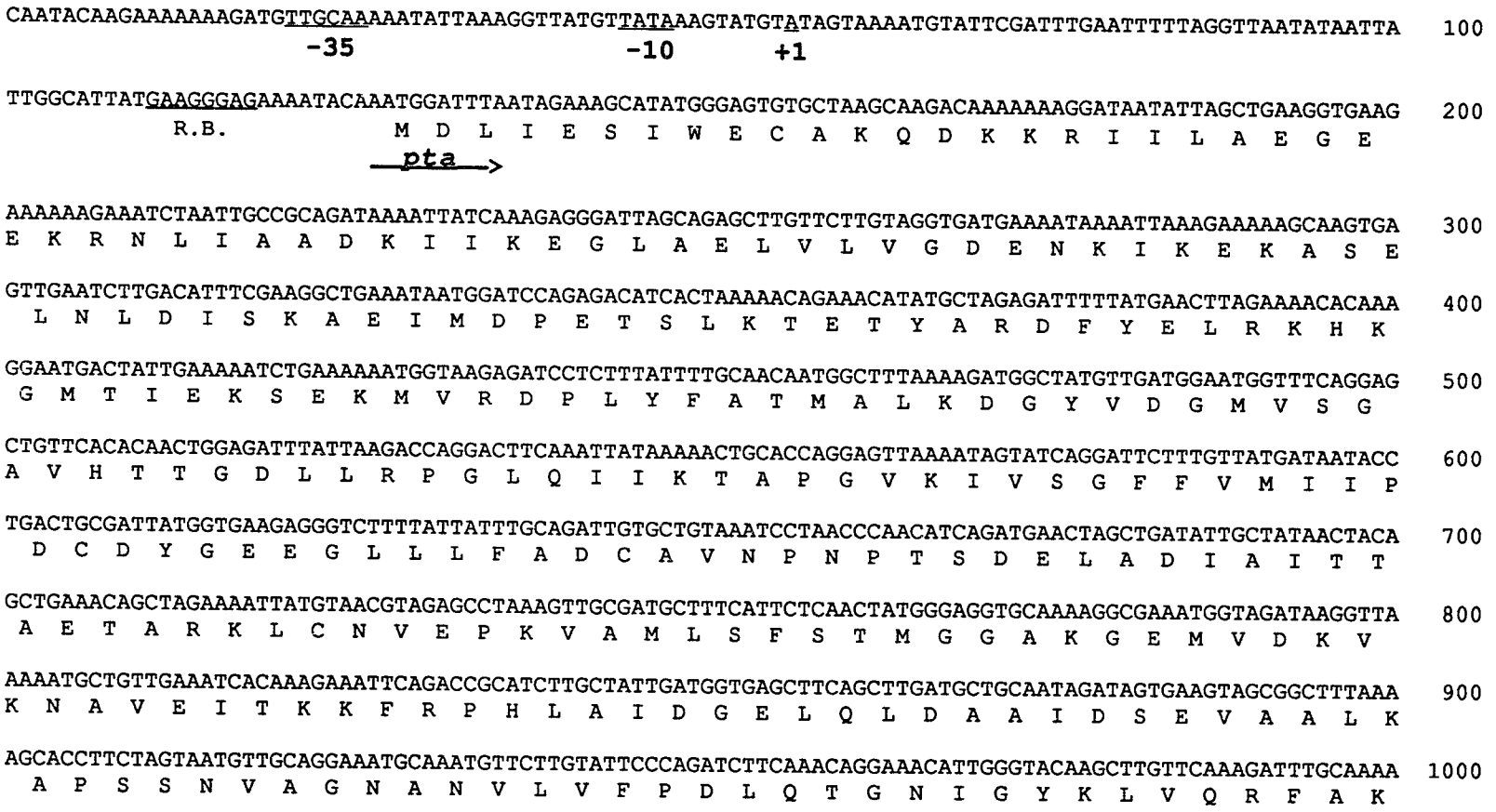

Fig. 4.5. Nucleotide and the deduced amino acid sequences of the genes encoding PTA and AK. Standard one-letter amino acid abbreviations are listed under the second nucleotide of each codon. The putative ribosome-binding site (R.B.), the promoter sequence -35 and -10 regions and the transcriptional start site (+1) are underlined.

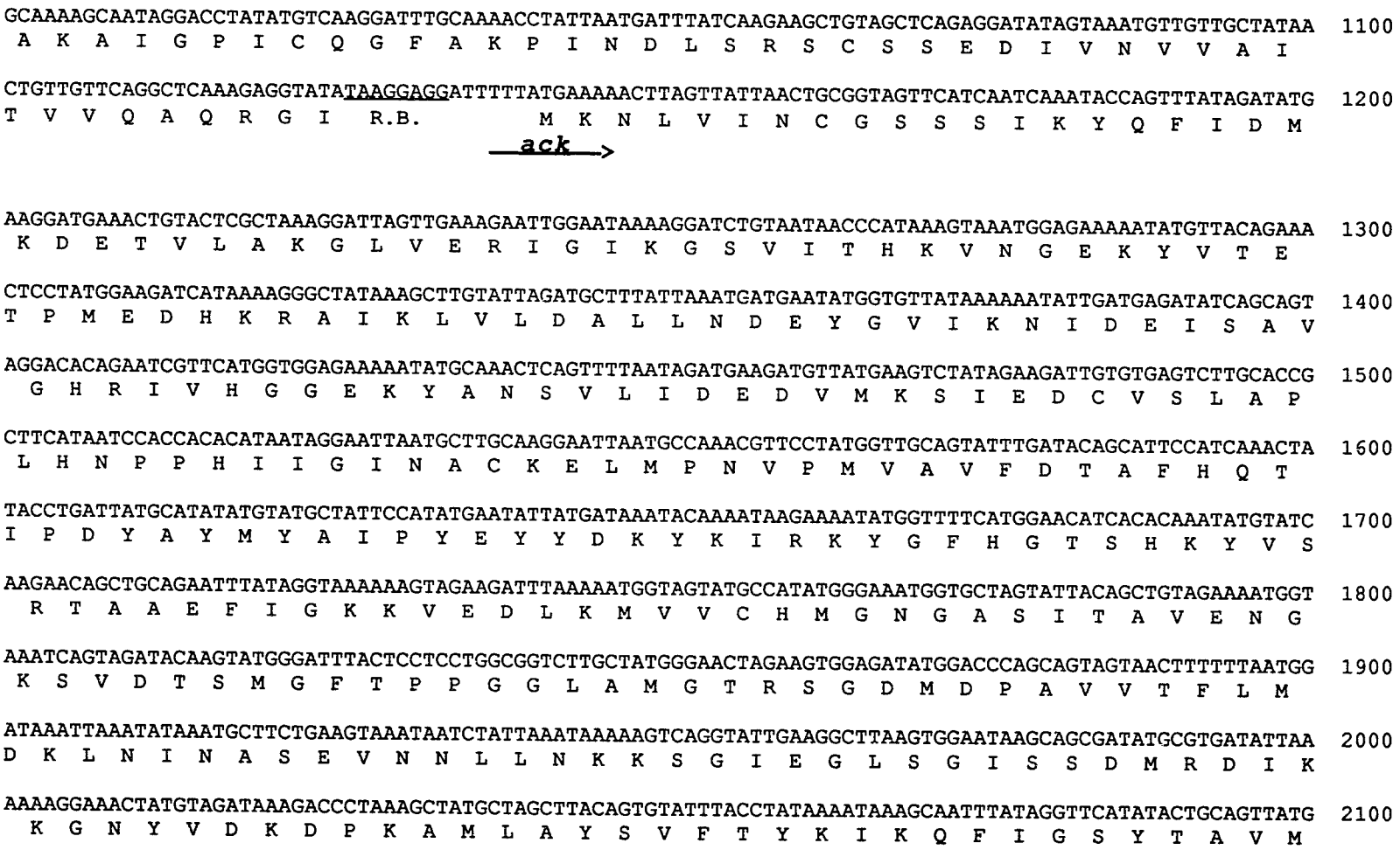

Fig. 4.5. Continued.

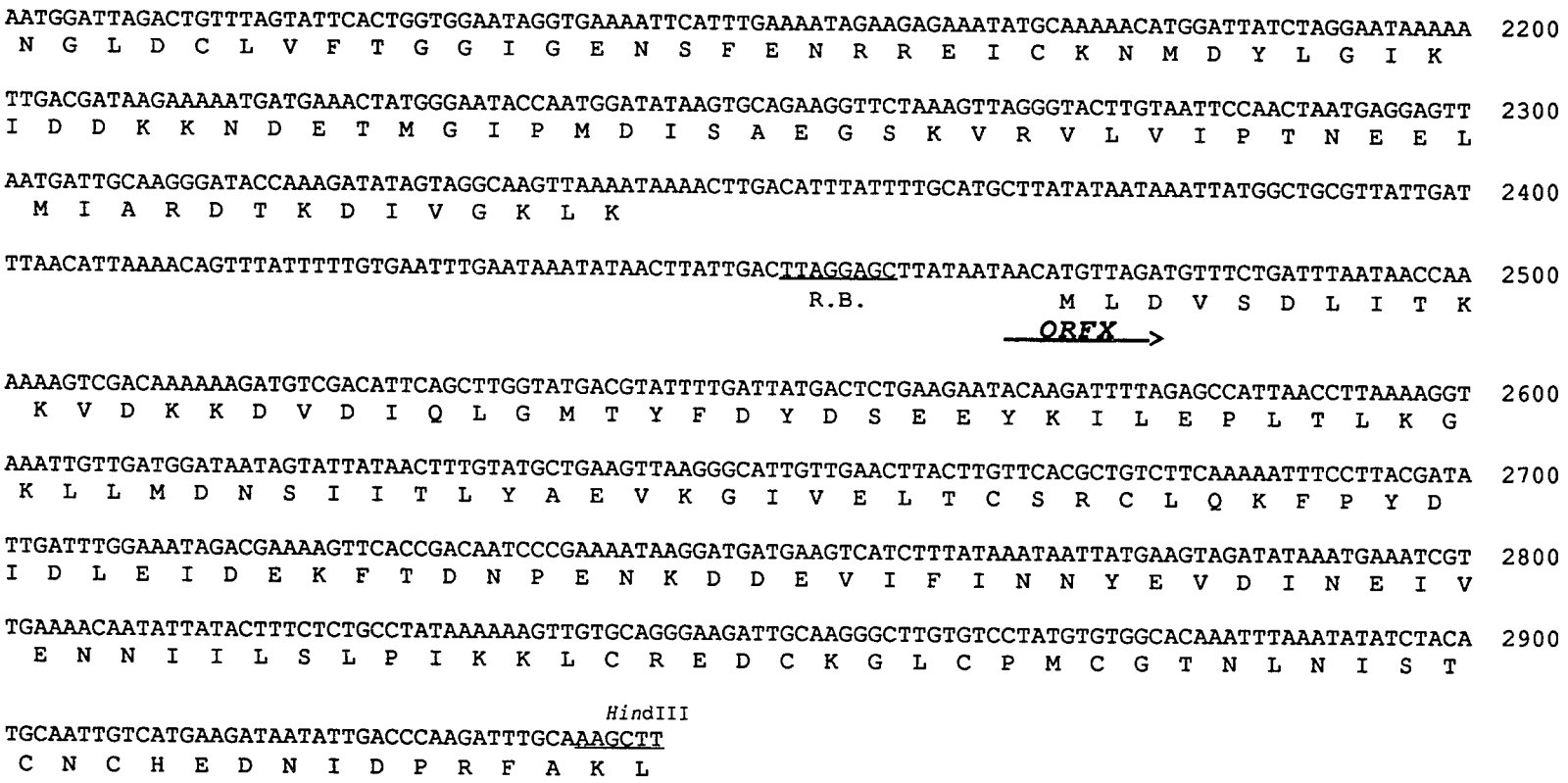

Fig. 4.5. Continued.

did not reveal any high similarity between the deduced peptide sequence of *orfX* and other known genes.

In order to sequence the entire AK-encoding gene, a longer 3.7 kb *Sal*I/*Eco*RI fragment was subcloned into the pUC19 vector, and the resulting plasmid was designated as pUC-PTAK. Various restriction enzymes were used for mapping, and the aligned maps of the *C. acetobutylicum* chromosome and subcloned segments in plasmids pUC-PTAK and pUC-AKX are shown in Fig. 4.4. The 1.6 kb *Hind*III-insert of pUC-AKX overlaps with the 3.7 kb *Sal*I/*Eco*RI-insert of the pUC-PTAK plasmid. A *Sal*I site was located 20 bp downstream of the *Sal*I site of the pUC-PTAK insert. No restriction sites were found for *Kpn*I, *Cla*I, *Sma*I and *Nco*I.

Sequencing data revealed a complete ORF was located at the 3' end of the insert of pUC-PTAK. The high homology level between the deduced peptide sequence of this ORF and the known *ackA* genes indicated that this ORF was a putative *ack* gene, encoding AK of 401 amino acids with a calculated Mr of 44.3 kDa from *C. acetobutylicum*. The *ack* gene was preceded by a putative ribosome-binding site with the sequence TAAGGAGG located 6 bp upstream of the ATG start codon (Fig. 4.5).

Continued sequencing upstream of the *ack* gene revealed another ORF, separated by only a 14-bp spacing. The deduced peptide sequences showed a high similarity and identity level to those of cloned *pta* genes. This ORF was therefore designated as a putative *pta* gene, encoding a PTA of 333 residues with a calculated Mr of 36.2 kDa from *C. acetobutylicm*. It is also

preceded by a putative S.D. sequence (GAAGGGAG) located 9 bp upstream of the methionine start codon (see Fig. 4.5).

Further sequencing up to a point 400 bp upstream of *pta* revealed no other ORFs which would encode metabolically related enzymes. No obivious transcriptional termination sequences were found in the intergenic regions between the tandem gene pair and *orfX* in this study (Fig. 4.5).

4.2.4. Primer extension. Primers homologous to the N-terminal nucleotide sequences of the *pta* (nucleotides 149 to 169, Fig. 4.5) and *ack* (nucleotides 1159 to 1175, Fig. 4.5) genes, as well as *orfX* (nucleotide 2520 to 2540, Fig. 4.5), were used to identify the transcriptional start site for these tandem genes. Only one single transcriptional start site (see Fig. 4.6) was determined and located 70 bp upstream of the *pta* start codon. The corresponding -10 (TATA) and -35 regions (TTGCAA) for this site closely matched the consensus promoter sequences. No transcriptional start sites were found within 150 bp of the start codon of *ack* and *orfX*, suggesting that the *ack* and *pta* genes were co-transcribed as a single unit. The complete nucleotide and amino acid sequences of this structure are summarized in Fig. 4.5.

4.2.5. Protein sequence alignment. The alignment of the deduced polypeptide sequences of *pta* and *ack* from *C. acetobutylicum* with those from their functionally related proteins are shown in Figs. 4.7. and 4.8., respectively. A summary of the peptide similarity and identity of the PTA and AK with those from other sources is shown in Table 4.1.

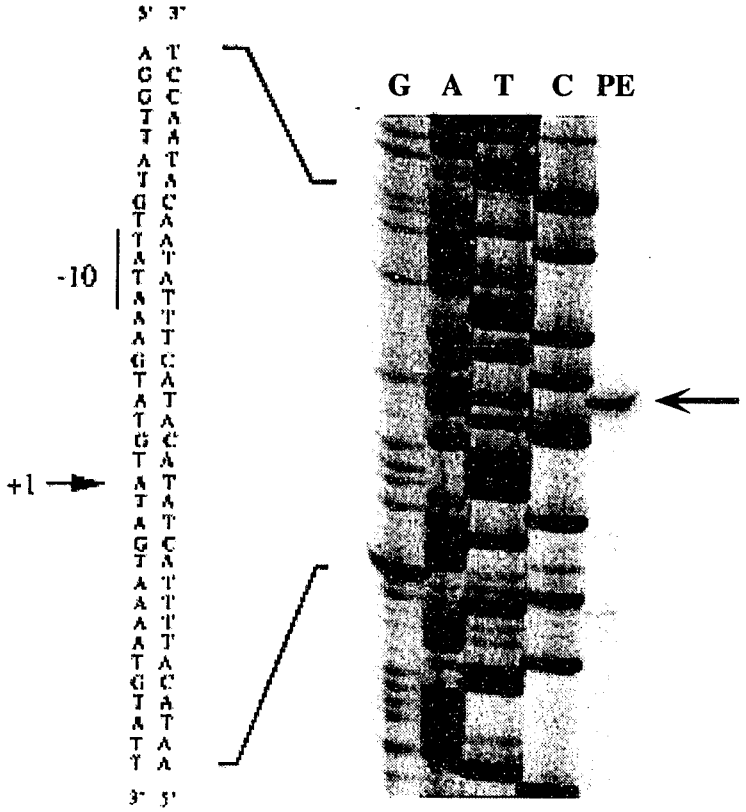

Fig. 4.6. Primer extension analysis. An oligonucleotide complementary to the *pta* sequence was hybridized to RNA isolated from the exponential phase culture of *C. acetobutylicum* and extended by reverse transcriptase. Lane PE represents the primer extension product. Lanes G, A, T and C represent the sequencing reaction products using the same oligonucleotide as primer and the recombinat plasmid pUC-PTAK as template.

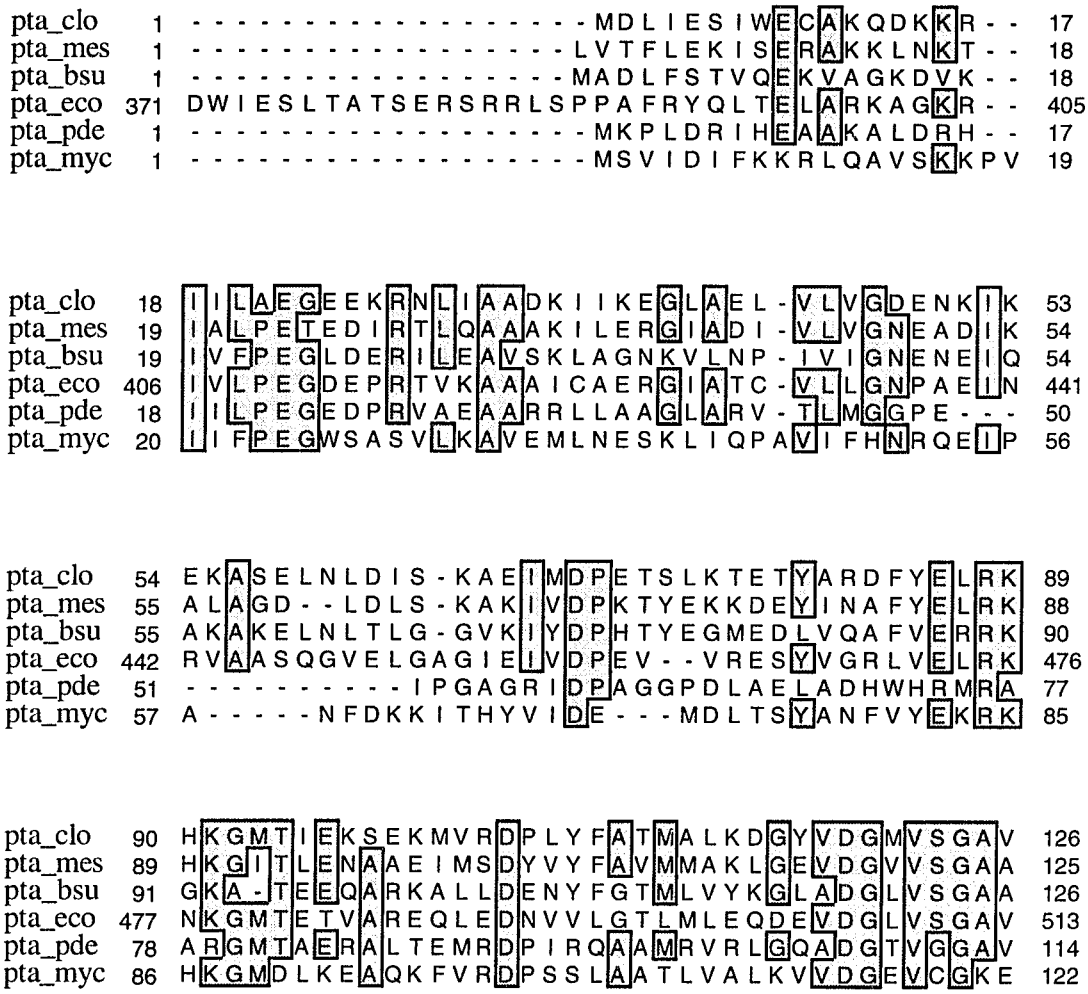

Fig. 4.7. Alignment of the deduced amino acid sequences of PTA. Those sequences from *C. acetobutylicum* (pta_clo), *M. thermophila* (pta_mes, GenBank/EMBL accession no [GBAN] L23147), *B. subtilis* (pta_bsu, GBAN X73124), *E. coli* (pta_eco, GBAN D21123), *P. denitrificans* (pta_pde, GBAN U08864), and *M. genitalium* (pta_myc, Genome Sequence DataBase [GSDB] accession number L43967) are shown. The amino acid sequence numbers of each protein are shown on the right of the plot. For PTA from *E. coli*, only the C-terminal amino acid sequences were shown to conserve space.

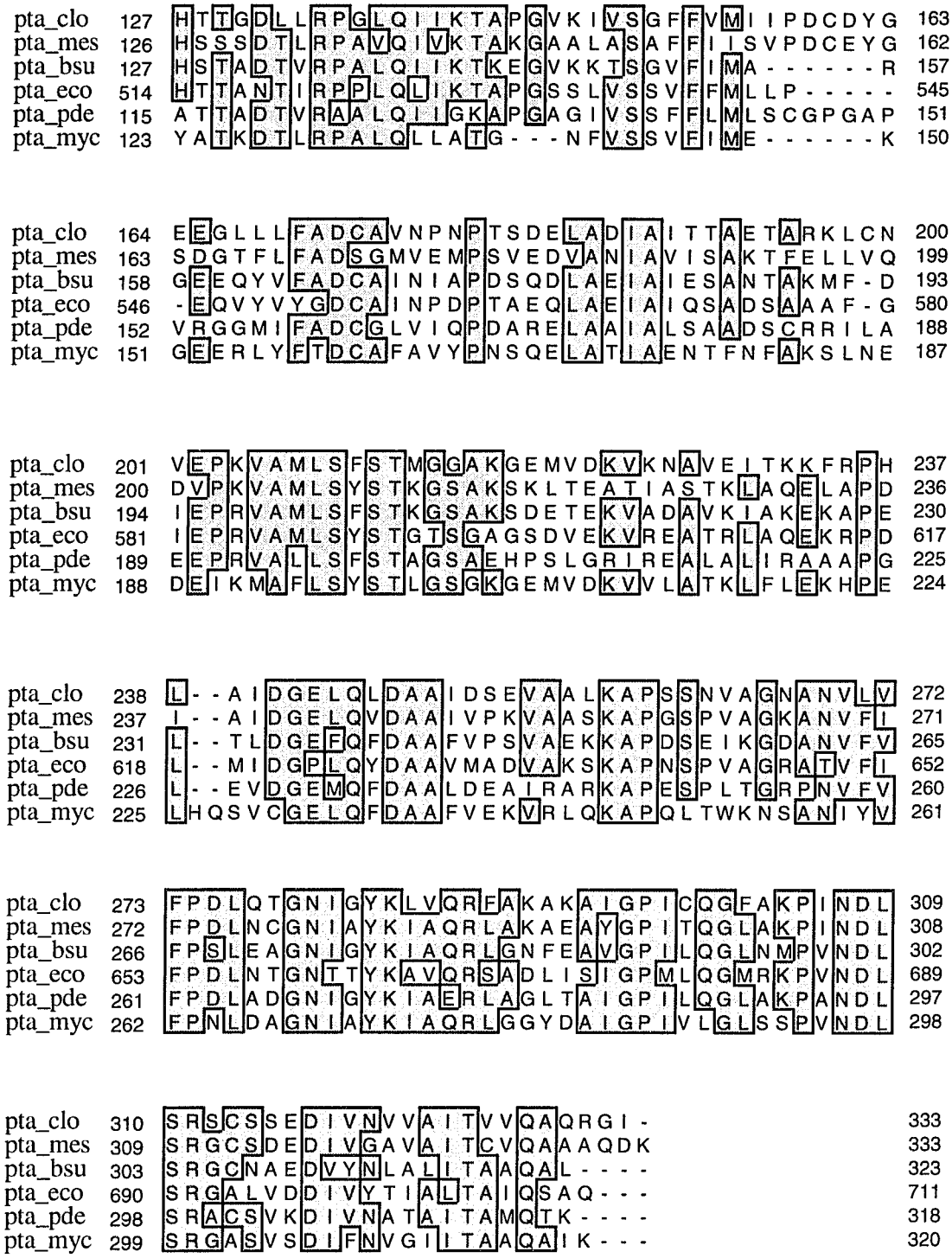

Fig. 4.7. Continued.

Fig. 4.8. Alignment of the deduced amino acid sequences of AK. Those sequences from *H. influenzae* (acka_hae, GBAN L45839), *E. coli* (acka_eco, GBAN M22956), *C. acetobutylicum* (ack_clo, GBAN U38234), *M. thermophila* (ack_mes, GBAN L23147), *B. subtilis* (acka_bsu, GBAN L17320), and *M. genitalium* (acka_myc, GSDB L43967) are shown. The amino acid sequence numbers for each enzyme are shown on the right of the plot. The arginine and glutamic acid residues that are suggested to be in or close to the active sites are marked with asterisk (*).

```
acka_hae  185 FVSREVAKYVGKPADQVNAIIICHLGNGGSVSVVRNGQC 222
acka_eco  188 YVTQEAAKMLNKPVEELNIITCHLGNGGSVSAIRNGKC 225
ack_clo   185 YVSRTAAEFIGKKVEDLKMVVCHMGNGASITAVENGKS 222
ack_mes   186 YVAERAALMLGKPAEETKIITCHLGNGSSITAVEGGKS 223
acka_bsu  184 YVTERAAELLGRPLKDLRLISCHLGNGASIAAVEGGKS 221
acka_myc  184 YINEFLEKKFNK--KPLNLIVCHLGNGASVCAIKQGKS 219

                              *
acka_hae  223 IDTSMGLTPLEGLVMGTRCGDIDPAIVFYLYKTLGMSM 260
acka_eco  226 VDTSMGLTPLEGLVMGTRSGDIDPAIIFHLHDTLGMSV 263
ack_clo   223 VDTSMGFTPPGGLAMGTRSGDMDPAVVTFLMDKLNINA 260
ack_mes   224 VETSMGFTPLEGLAMGTRCGSIDPAIVPFLMEKEGLTT 261
acka_bsu  222 IDTSMGFTPLAGVAMGTRSGNIDPALIPYIMEKTGQTA 259
acka_myc  220 LNTSMGFTPLEGLIMGTRSGDIDPAIVSYIAEQQKLSC 257

                                      *
acka_hae  261 DQIEETLVKKSGLLGLTEVTSDCRYAEDNYDDESKPET 298
acka_eco  264 DAINKLLTKESGLLGLTEVTSDCRYVEDNY--ATKEDA 299
ack_clo   261 SEVNNLLNKKSGIEGLSGISSDMRDIKKGNYVDKDPKA 298
ack_mes   262 REIDTLMNKKSGVLGVSGLSNDFRDLDEAA-SKGNRKA 298
acka_bsu  260 DEVLNTLNKKSGLLGISGFSSDLRDIVEAT-KEGNERA 296
acka_myc  258 NDVVNELNKKSGMFAITG-SSDMRDIFD-----KPEIN 289

                                                  *
acka_hae  299 RRALNVYSYRLAKYIGAYMAVLGDDHLDAIAFTGGIGE 336
acka_eco  300 KRAMDVYCHRLAKYIGAYTALM-DGRLDAVVFTGGIGE 336
ack_clo   299 MLAYSVFTYKIKQFIGSYTAVMNG--LDCLVFTGGIGE 334
ack_mes   299 ELALEIFAYKVKKFIGEYSAVLNG--ADAVVFTAGIGE 334
acka_bsu  297 ETALEVFASRIHKYIGSYAARMSG--VDAIIFTAGIGE 332
acka_myc  290 DIAIKMYVNRVADYIAKYLNQLSGE-IDSLVFTGGVGE 326

acka_hae  337 NSAHVREELALNHLKLFGIKIDNERNLATRFGKDGVITT 374
acka_eco  337 NAAMVRELSLGKLGVLGFEVDHERNLAARFGKSGFINK 374
ack_clo   335 NSFENRREICKNMDYLGIKIDDKKNDETM-GIPMDISA 371
ack_mes   335 NSASIRKRILTGLDGIGIKIDDEKN-KIR-GQEIDIST 370
acka_bsu  333 NSVEVRERVLRGLEFMGVYWDPALN-NVR-GEEAFISY 368
acka_myc  327 NASYCVQLIIEKVASLGFKTNS--NLFGNYQDSSLIST 362

                              **
acka_hae  375 DDSAFKAIVLPTNEELVIAQDTAKLCF---------- 401
acka_eco  375 EGTR-PAVVIPTNEELVIAQDASRLTA---------- 400
ack_clo   372 EGSKVRVLVIPTNEELMIARDTKDIVG---KLK----- 401
ack_mes   371 PDAKVRVFVIPTNEELAIARETKEIVETEVKLRSSIPV 408
acka_bsu  369 PHSPVKVMIIPTDEEVMIARDVVRLAK---------- 395
acka_myc  363 NESKYQIFRVRTNEELMIVEDALRVSTNIKK------- 393
```

Fig. 4.8. Continued.

Table 4.1. Sequence comparison of PTA and AK from *C. acetobutylicum* and other organisms.

Strain and enzymes	Length (aa[a])	Mr (kDa)	Similarity	Identity	References
PTA					
C. acetobutylicum	333	36.2	100	100	This work
M. thermophila	333	35.2	70	58	Latimer and Ferry 1993
B. subtilis	323	34.8	66	47	Glaser et al., 1993
E. coli	713	77.0	67	46	Matsuyama et al., 1994
M. Genitalium	320	35.5	59	40	Fraser et al., 1995
P. denitrificans	318	33.2	65	44	Van Spanning et al., 1994
AK					
C. acetobutylicum	401	44.1	100	100	This work
M. thermophila	408	44.5	75	59	Latimer and Ferry 1993
B. subtilis	395	42.2	75	54	Grundy et al., 1993
E. coli	400	43.3	65	44	Matsuyama, et al., 1994
H. influenza	401	43.8	65	43	Fleischmann et al., 1995
M. Genitalium	393	44.3	64	42	Fraser et al., 1995

a. Length of the amino acids.

4.2.6. Enzyme activities and expression. For the study of *pta* and *ack* expression, the 3.7 kb-insert of pUC-PTAK was subcloned into the shuttle vector pIA, which contained both *E. coli* and clostridial origins of replication (Wong, 1995). The resulting plasmid was designated as pIA-PTAK (Fig. 4.4). Both pIA and pIA-PTAK were either directly transformed to *E. coli* XL1-Blue cells or first methylated and then electroporated into *C. acetobutylicum* (described in Materials and Methods). Crude cell extracts from cultures harboring either pIA (controls) or pIA-PTAK were assayed for PTA and AK activities, and the results are shown in Table 4.2. During the exponential growth phase, the PTA and AK activity levels were elevated from 3-to-5 fold in *C. acetobutylicum* when harboring the pIA-PTAK plasmid. Additionally, *E. coli* cells harboring pUC-PTAK exhibited a 4-fold increase in the PTA activity level and a 15-fold increase for AK when compared to controls.

4.2.7. Gene inactivation. To better evaluate the functions of AK and PTA and to direct the carbon flow for greater solvent production, the gene encoding PTA was inactivated in the chromosome. Since the integrative vector, pJC4, contains only the *E. coli* origin of replication (ColE1), it cannot be replicated in *C. acetobutylicum*. This vector was therefore used for the purpose of inactivation. An internal *Bam*HI/*Hin*dIII fragment of *pta* was ligated to pJC4, yielding pJC4-PTAK (see Fig. 4.9). This plasmid and pJC4 (control) were methylated by transforming each to ER2275, which coharbored the methylating plasmid pAN1. Significant amounts of the methylated plasmids were then electroporated into *C. acetobutylicum* and plated. Of the seven erythromycin-resistant colonies, corresponding to putative integrants that contain the erythromycin

Table 4.2. Enzyme activities of recombinant plasmids in *E. coli* and *C. acetobutylicum*.

Plasmid	Specific Activities (Mean Value[a]) (U[b]/mg)			
	PTA	AK	PTB	BK
***E. coli* culture**[c]				
pIA	2.1	1.7		
pIA-PTAK	8.3	25.3		
***C. acetobutylicum* culture**				
pIA	1.8	3.0	4.4	2.7
pIA-PTAK	8.5	9.2	4.7	2.6

a. Data shown are based on two different measurements and are reproducible within 7% of the value given.

b. One unit was defined as the amount of the enzyme that converts one micromole substrate to product per minute.

c. Assay was conducted in XL1-Blue strain.

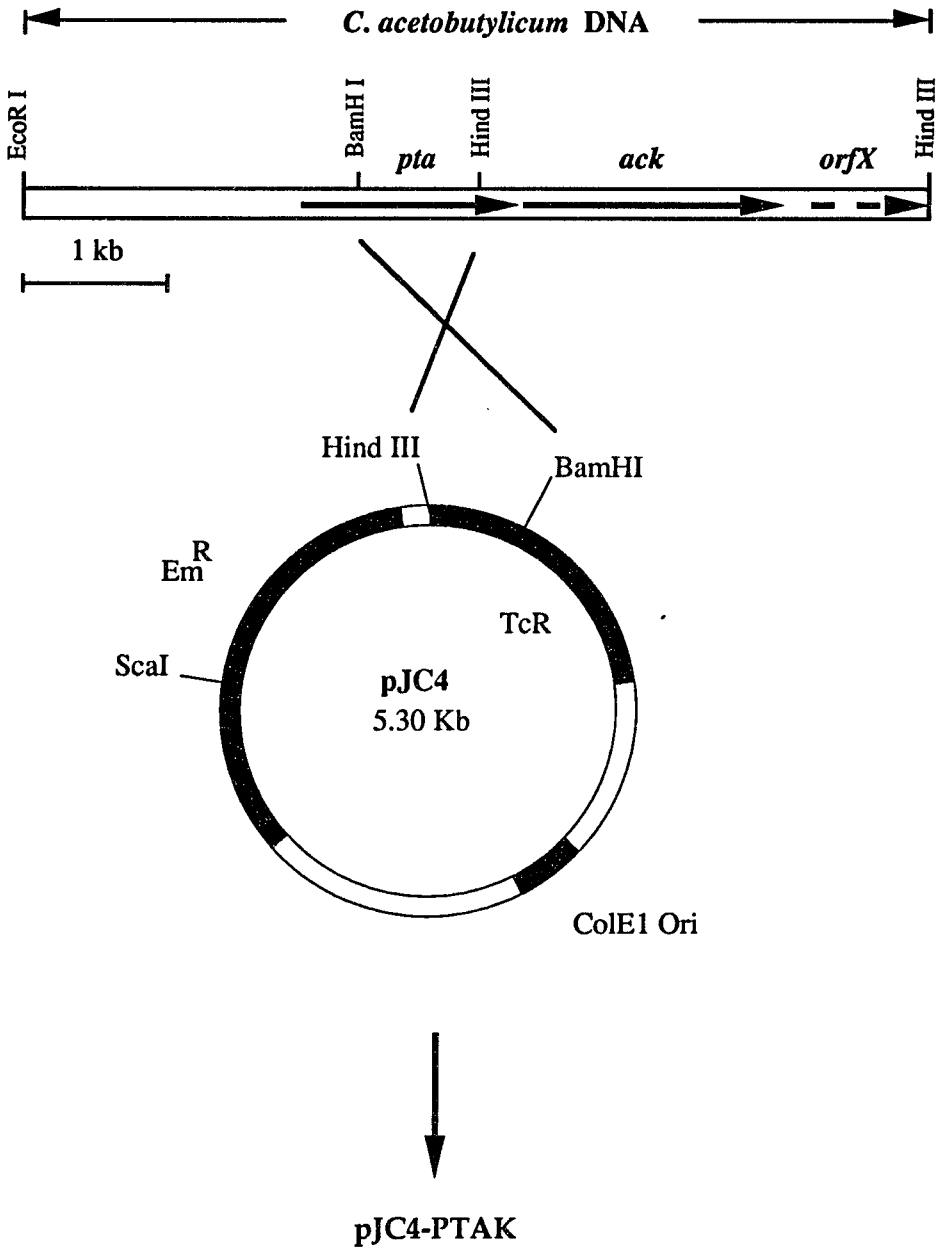

Fig. 4.9. The generation of integrational plasmid pJC4-PTAK

resistant gene combined into the genome (see Fig. 4.10), one was picked for further analysis.

To determine if integration did occur, PTA and AK enzyme activities were assayed, and a Southern hybridization was performed using genomic DNA prepared from the selected colony. The mutant, designated as 824::ptak$^-$, showed much lower PTA and AK activities than the wild type (Table 4.3).

Chromosomal DNA from wild-type and mutant strains were digested using *Sca*I. This enzyme was chosen because it would only digest pJC4-PTAK once, and the restriction site would be located only at the erythromycin-resistant gene. It was reasoned that if a single copy of pJC4-PTAK integrated into the wild-type chromosome, digestion with *Sca*I would generate two restriction fragments. The combined size of these two fragments ought to then be the same as that of the combined sizes of the pJC4-PTAK and *Sca*I digested fragments of the wild-type chromosome (see Fig. 4.10 for mechanism). The integration process was performed, and the Southern hybridization results are shown in Fig. 4.11. It can be seen in the figure that the size of the pJC4-PTAK plasmid is ~5.5 kb, and the *Sca*I-digested wild-type genomic DNA showed a signal at 6.5 kb. The combined 12 kb size is equal to that of the *Sca*I-digested mutant genomic DNA, which exhibited two signals at approxiamately 3.6 kb and 8.4 kb. It therefore appears that the pJC4-PTAK plasmid integrated successfully, by single crossover into the *pta* gene of the wild-type clostridial chromosome.

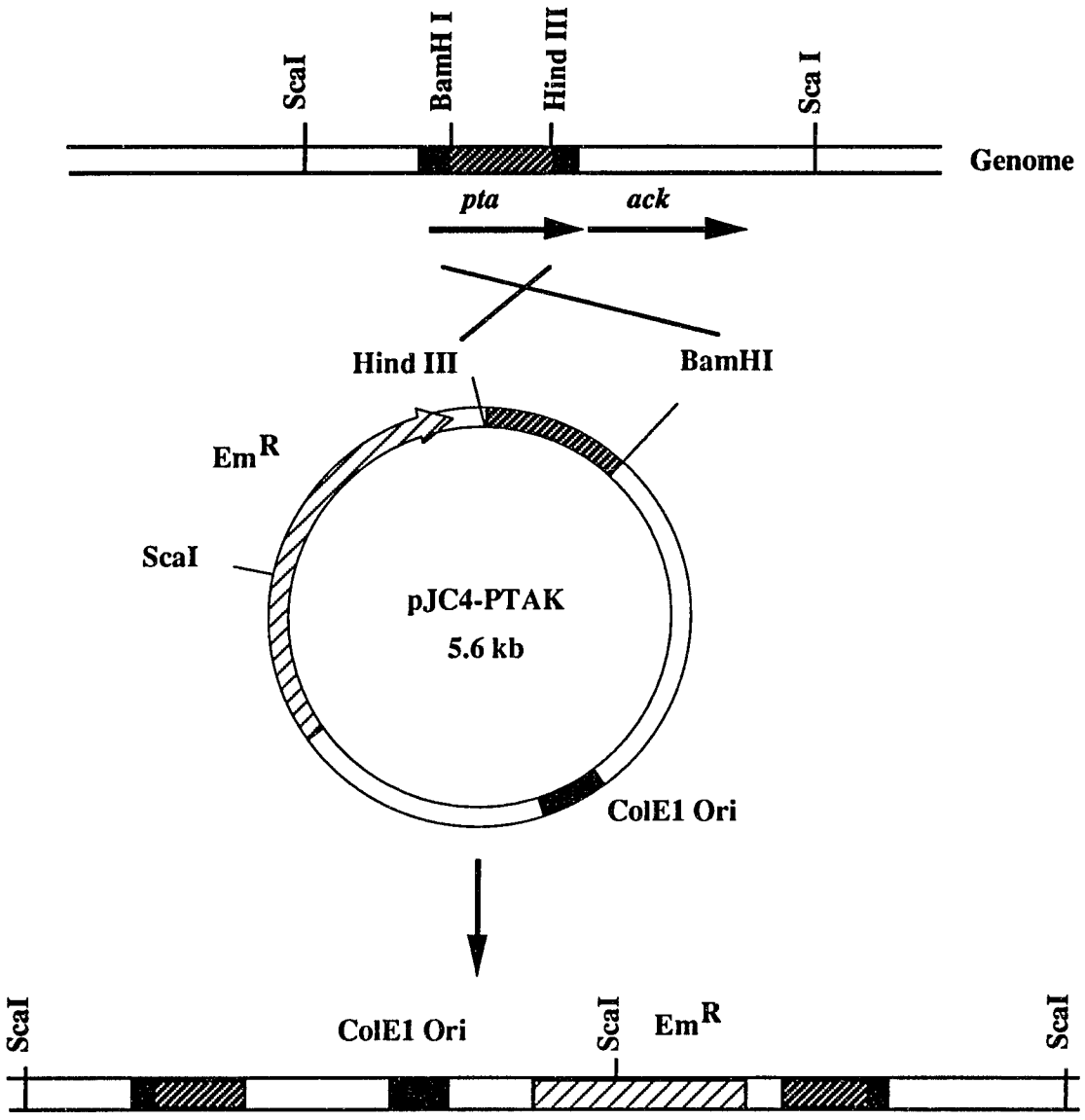

Fig. 4.10. Genetic recombination using integrative plasmid pJC4-PTAK.

Table 4.3. Enzyme activities of *C. acetobutylicum* wild-type and *pta*-knockout mutant strains.

Strains	Specific Activities (Mean Value[a]) (U^b/mg)			
	PTA	AK	PTB	BK
ATCC 824	1.35	1.27	2.36	2.69
824::ptak$^-$	0.17	0.30	5.70	3.07

a. Data shown are based on two different measurements and are reproducible within 14% of the value given.

b. One unit was defined as the amount of the enzyme that converts one micromole substrate to product per minute.

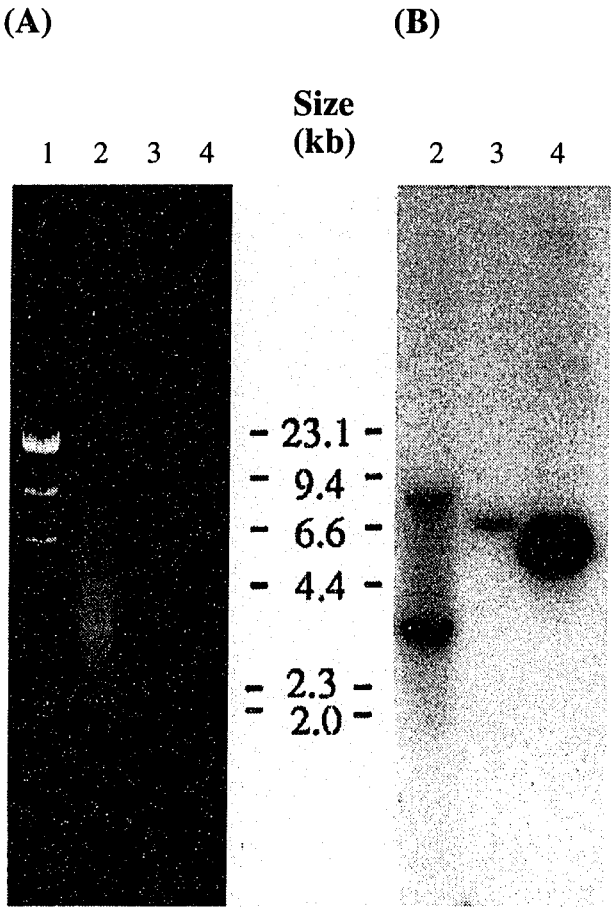

Fig. 4.11. Southern blot analysis of *Sca*I-digested genomic DNA from wild-type and mutant strains.

(A) Samples were electrophoresed on an 0.8% agarose gel and stained with ethidium bromide. lanes:

1. Lambda phage DNA digested with *Hin*dIII as size standard.

2-3. *Sca*I-digested genomic DNAs from mutant 824::ptak$^-$ and wild-type ATCC 824, respectively.

4. *Sca*I digested pJC4-PTAK plasmid.

(B) Autoradiogram of lanes 2-4 after Southern hybridization using the ^{32}P-labeled internal-*pta*-fragment as a probe.

4.2.8. Analysis of the product yield. Gas chromatography was used to measure the fermentation product yield. All fermentations using recombinant 824 strains were carried out in the presence of 100 ug/ml of erythromycin to increase the plasmid stability. It was noted that introducing plasmids into *C. acetobutylicum* can increase the solvent yield by about 15% (Mermelstein et al., 1994, Walter et al., 1994). The clostridial cell culture harboring the pIA vector was therefore used as a control for the overexpressed strain, and the results are shown in Table 4.4. Overexpression of *pta* and *ack* in *C. acetobutylicum* resulted in moderately higher acetate (+25%) and lower acetone (-33%) and butanol (-20%) yields. The butyrate level was approximately the same (+9%). The pIA-PTAK bearing strain also produced a higher acetate concentration at an earlier stage than for the control.

The product concentrations of wild-type and the *pta*-integrant grown in pH-uncontrolled tube cultures are shown in Table 4.5. It can be seen that the acetate concentration level in the mutant decreased significantly from that of the wild-type culture. The product concentrations of mutant 824::ptak$^-$ was further characterized by Dr. Edward Green using a pH-controlled fermentor (Green et al., 1996), and the results are shown in Tables 4.6. Following inoculation, the mutant grew exponentially. However, little acetate was produced at this stage whereas butyrate was overproduced and reach a maximal level of 109 mM after 16 hours (Table 4.6). During the stationary phase, where acetate and butyrate production in wild-type culture are commonly slowed down, the mutant 824::ptak$^-$ started to overproduce acetate and the concentration reached a maximal level of 63 mM after 24 hours. At the end of the fermentation process,

Table 4.4. Effect of *pta* and *ack* overexpression on product concentrations in tube cultures.

		Final Concentrations (Mean value[a]) (mM)				
Strain	A600[b]	acetate	butyrate	ethanol	acetone	butanol
ATCC 824 (pIA)	3.4	25.6	27.3	6.9	17.4	39.6
ATCC 824 (pIA-PTAK)	3.5	31.9	29.8	5.7	11.7	31.5

a. Data were collected from three GC measurements and are reproducible within 10% of the value given.

b. Maximal O.D. of the cultures.

Table 4.5. Product concentrations of wild-type and *pta*-integrant in tube cultures.

			Concentrations (mean value[a]) (mM)				
Strain	Time (hr)	A600	acetate	butyrate	ethanol	acetone	butanol
ATCC 824	20	1.3	12.0	11.2	0	0	0
	21	1.7	13.7	14.0	3.9	1.6	5.2
	24	2.3	20.9	18.6	3.3	1.8	9.3
	48	3.3	28.2	42.2	6.0	4.7	22.4
	54	3.8	24.9	33.2	7.0	10.2	28.4
	72	3.5	27.0	35.0	7.7	11.4	32.8
824::ptak-[b]	18	1.0	0	9.8	0	0	0
	20	2.0	6.3	32.7	0	0	0
	48	2.4	9.6	52.4	0	4.8	10.6
	54	2.9	10.4	46.1	4.0	7.0	15.9

a. Data were collected from three GC measurements and are reproducible within 15% of the value given.

b. Cells were grown in 10 ml CGM supplemented with 100 ug/ml of erythromycin as required.

Table 4.6. Product concentrations of *pta*-integrant in batch culture controlled at pH 5.5[a].

			Concentrations (mean value[b]) (mM)				
Strain	Time (hr)	A600	acetate	butyrate	acetone	ethanol	butanol
824::ptak⁻	2.5	0.1	0.9	1.2	0	0	0
	4.5	0.2	1.6	3.2	0	0	0
	6.5	0.5	2.0	7.6	0	0	0
	8.5	1.7	3.7	20.2	0	0	0
	10.5	3.6	5.9	37.8	0.8	0.1	0
	12.5	6.6	10.2	78.9	3.1	1.1	0
	14.5	7.0	15.8	83.2	14.9	0	6.0
	16.5	7.5	31.2	109.4	34.7	4.5	22.2
	18.5	7.6	44.3	109.9	51.0	5.4	42.8
	23.5	6.8	63.2	93.5	86.4	8.0	93.9
	36.2	3.4	58.2	73.4	108.4	11.8	127.0
	40.0	3.2	60.9	78.0	109.5	10.1	131.4

a. Experiment was conducted by Dr. Edward Green.

b. Data were collected from three GC measurements and are reproducible within 10% of the value given.

approximately 30% of the butyrate and an unknown amount of the acetate were reassimilated. A comparison of the final and maximal product concentration levels of wild-type and mutant cultures grown in pH-controlled fermentor is shown in Table 4.7.

Table 4.7. Comparison of product concentrations of wild-type and *pta*-integrant in batch cultures controlled at pH 5.5.

Strain	Doubling Time (hr)	A600	Concentrations (mean value[a]) (mM) acetate	butyrate	ethanol	acetone	butanol
			Maximum levels				
ATCC 824[b]	1.0	7.7	115.0	77.5	13.0	76.6	129.0
824::ptak-[c]	1.5	8.3	60.9	109.9	11.8	109.5	131.4
			Final levels				
ATCC 824[b]	1.5	4.0	115.0	77.5	13.0	76.6	129.0
824::ptak-[c]	1.0	3.2	60.9	78.0	10.0	109.5	131.4

a. Data were collected from three GC measurements and are reproducible within 10% of the value given.

b. From Mermelstein et al., 1994.

c. Data were collected by Dr. Edward Green.

4.3. Discussion

The ability to express genes in *C. acetobutylicum* as a way of altering cell metabolism is critical to the generation of highly efficient strains for industrial application. The attempt to redirect the flux of carbon away from the acetate pool toward more solvent production, by inactivating the genes involved in acid production, requires a thorough understanding of the genetic structures of the AK- and PTA-encoding genes.

Bacterial genes are often organized in operons, which correspond to regulatory units of associated functions. Previous research had shown that the AK and PTA enzymes in *C. acetobutylicum* are expressed in a similarly parallel pattern (Andersch et al., 1983). These two acetate-formation enzymes reached their highest activity levels at the end of the acidogenic phase and declined from 50 to 90 percent during the solventogenic phase. It was therefore not surprising that genes encoding these two enzymes are adjacent in the clostridial chromosome, indicating an operon arrangement (Fig. 4.4). This result was further confirmed through primer extension experiments (Fig. 4.6). One single transcriptional start site was identified upstream of the *pta* gene but not of *ack*.

The comparison of the deduced amino acid sequences for the cloned *ack* and *pta* genes respectively, showed relatively high degrees of similarity and identity (50-80%) to those of the corresponding genes from other microorganisms, especially *M. thermophila* (Table 4.1). The *pta* gene from *M. thermophila* encodes a 333-residue protein with an Mr of 35.2 kDa (Latimer and Ferry, 1993), very close to that for *C.*

acetobutylicum. The clostridial PTA is also a 333-residue protein with a calculated Mr of 36.2 kDa. The AK-encoding gene from *M. thermophila* encodes a peptide of 408 residues with an Mr of 44.5 kDa (Latimer and Ferry, 1993), which is close in value to the AK from *C. acetobutylicum* (a 401 residue protein with a calculated Mr of 44.3 kDa). A plot of the predicted Kyte-Doolittle hydrophilicity values from *C. acetobutylicum* indicates that both PTA and AK have approximately equal amounts of hydrophobic and hydrophilic residues with no potential trans-membrane domains (data not shown).

The AK enzyme from *E. coli* has been studied extensively. Previous research has shown that a γ-phosphorylated glutamyl residue was formed during the phosphorylation of the enzyme, suggesting glutamic acid is in or close to the active site (Todhunter and Purich, 1974). Wong and Wong (1980) suggested that acetate and acetyl-phosphate have a common binding site which is different from that of the adenosine binding domain. In addition, using an arginine inactivating reagent, these researchers (1981) have shown that the AK activity loss also resulted in a loss of an arginine residue. The inactivation could be prevented by adenine nucleotide and acetyl-phosphate but not acetate, suggesting that arginine was acting as a binding site for the phosphate group of the substrate. The alignment of AK-encoding genes identified four of each of the conserved glutamic acid and arginine residues (marked by asterisks in Fig. 4.8), all of which have been suggested to be in or close to the active site for the *E. coli* acetate kinase (Todhunter and Purich, 1974, Wong and Wong, 1980, 1981).

Two types of nucleotide-binding domains were suggested for the bacterial ATP-binding proteins (Albano et al., 1989, Walker et al., 1982). Type A is characterized by a G-N4-G-K-T nucleotide-binding loop structure and is important in binding the α-phosphate group of ATP. Type B is characterized by a series of hydrophobic amino acids which are then followed by negatively charged residues (Walker et al., 1982). Type B is the domain that is important in interacting with the substrate ATP through Mg^{2+}. The peptide sequence comparison of AK (Fig. 4.8) did not reveal any conserved sequence that conforms to the consensus Walker-type nucleotide-binding domains, even though there are multiple conserved glycine regions throughout the entire sequence. The reason for the absence of a binding domain is not clear but probably is related to the fact that the type A loop structure is important in the binding of the α-phosphate in other ATP-requiring enzymes whereas the activating mechnism for AK is probably related to the binding of the γ-phosphate from ATP (Todhunter and Purich, 1974). Nevertheless, a fully meaningful explanation would require a three-dimensional structural analysis for AK and the results of site-directed mutagenesis.

In the clostridial metabolic pathway, two similarily acting enzymes, butyrate kinase (BK) and phosphotransbutyrylase (PTB), are involved in butyrate formation. Previous research has shown that, even though PTB and PTA catalyze similar reactions, they are functionally distinct enzymes (Gavard et al., 1957). PTB (Wiesenborn et al., 1989) and BK (Hartmanis, 1987) have been purified from *C. acetobutylicum* ATCC 824 and their encoding genes have been cloned (Cary et al., 1988) and sequenced (Walter et al., 1994b). In addition, PTB and BK encoding genes have also been

cloned from *C. acetobutylicum* NCIMB 8052 (Oultram et al., 1993). PTB is an octamer with a subunit Mr of 31 kDa, and BK is a dimer with an identical subunit Mr of 39 kDa. The PTB enzyme showed only a 2% activity toward acetyl-CoA, and BK only displayed a 6% activity toward acetate, despite broad substrate specificities from both enzymes (Hartmanis, 1987, Wiesenborn et al., 1989).

The deduced peptide sequences for *ack* and *pta* were compared to those for *buk* and *ptb*, encoding BK and PTB from *C. acetobutylicum* ATCC 824 respectively (Walter et al., 1994b). The peptide sequence for *ack* showed a 49% similarity and a 27% identity with that for *buk* . For *pta*, a similarity of 47% and an identity of 27% were found when compared to *ptb*. The alignment of the AK and BK peptide sequences did not reveal any obvious type of nucleotide-triphosphate-binding site.

The gene arrangement of *pta* and *ack* from *C. acetobutylicum* is in the same relative order as those from *M. thermophila*, with *pta* next to and upstream of *ack* (Latimer and Ferry, 1993, Singh-Wissmann and Ferry, 1995). This arrangement is also the same as for the corresponding genes involved in the butyrate formation pathway, with the *ptb* gene upstream of *buk* (Cary et al., 1990, Walter et al., 1994b). However, this arrangement is opposite to that of the *ackA-pta* order for *E. coli* (Kakuda et al., 1994). In *M. genitalium*, the *pta* and *ackA* genes are separated by 57 ORFs in the chromosome (Fraser et al., 1995). In *B. subtilis*, the *ackA* and *pta* genes are not adjacent, and are probably far apart as in *M. genitalium* (Glaser et al., 1993, Grundy et al., 1993). In fact, a

transcriptional start site for *B. subtilis ackA* was located 90 bp upstream from the start site of the *ackA* coding region (Grundy et al., 1993).

In *C. acetobutylicum, pta* and *ack* are separated by only 14 bp and no consensus promoter region is found in the intergenic region (Fig. 4.5). *M. thermophila* has the same *pta-ack* operon arrangement as *C. acetobutylicum*. However, two putative promoters were detected in *M. thermophila,* one which transcribes the entire operon and the other which only transcribes the downstream *ack* gene (Singh-Wissmann and Ferry, 1995). In *E. coli,* the *ackA-pta* genes form an operon, and two putative promoters were detected. One transcribes the entire operon and the other only transcribes the downstream *pta* gene (Kakuda et al., 1994).

Downstream of the *ack* gene is an incompletely cloned *orfX*, which separated from *ack* by a 124-bp spacing (Fig. 4.5). No significant homology was found using a Blast search at either the DNA or peptide levels. However, the deduced amino acid sequence for *orfX* showed a 42% similarity and a 24% identity in a 146-aa overlap with ORF1, an incompletely characterized ORF downstream of the *buk* gene derived from *C. acetobutylicum* ATCC 824 (Walter et al., 1994b). In addition, the deduced peptide sequence of *orfX* also shared a 49% similarity and a 21% identity with that for ORF 4, an ORF (157 aa) located downstream of the *buk* gene from *C. acetobutylicum* NCIMB 8052 (Oultram et al., 1993). Unlike *orfX* and ORF 4, which is encoded by the same DNA strand as the acetate- and butyrate-forming genes, ORF1 is in the strand opposite to *pta* and *buk*. A structure similar to that of putative Rho-factor independent trabscription termination sequences was identified upstream of ORF 4 and

downstream of *buk* from *C. acetobutylicum* NCIMB 8052. However, no such structure was identified in the intergenic region of *ack* and *orfX*.

The introduction of subclone pIA-PTAK into *E. coli* and *C. acetobutylicum* resulted in expression of the *pta* and *ack* genes to relatively high activity levels (Table 4.2). In *C. acetobutylicum*, the AK and PTA activity levels were elevated from three-to-five fold when compared to the control strain. In addition, the activities of the PTB and BK enzymes in the butyrate-formation pathway are maintained at approximately the same level (Table 4.2). In *E. coli*, the AK activity is expressed at a greater level than that for PTA. The reason for this higher expression level might be due to the supportive interaction between a bacterial ribosome and its initiation sequence. From Fig. 4.5, it can be seen that the putative ribosome binding site for the *pta* gene is GAAGGGAG, whereas the putative binding site for *ack* is TAAGGAGG. The latter sequence matches the classic S.D. designation for *E. coli* exactly (Shine and Dalgarno, 1974) and therefore might provide a stronger guidance for the ribosome toward the initiation site.

The effect of *pta* and *ack* overexpression on the metabolic product pattern in clostridia was measured in small batch cultures. The overexpression of *pta* and *ack* from *C. acetobutylicum* produced about 25% higher acetate and 20% lower butanol and 33% lower acetone levels than their respective controls (Table 4.3). These data are similar to those from the overexpression of *ptb* and *buk*, where an increased dosage of the butyrate-formation genes in *C. acetobutylicum* results in an increase of PTB and BK activity levels but only minor changes in the amounts of

acids and solvents produced (Walter et al., 1994a). The reason for the limited effect of overexpression might be that a surplus of acid-formation-pathway enzymes exists within the cells. Therefore, increasing the gene dosages will only have a slight effect on the product concentrations.

However, the overexpression of *pta* and *ack* did result in higher final concentration-ratios of acetate to other major products. The corresponding ratio values of acetate to butyrate, ethanol, acetone, and butanol levels from the overexpressed strain are 1.1, 5.6, 2.7 and 1.0, respectively, versus 0.9, 3.7, 1.5 and 0.6 for the controls. In addition, the overexpression of *pta* and *ack* resulted in a greater proportion of two-carbon-derived products (acetate and ethanol) over four-carbon-derived products (acetone, butyrate and butanol). The ratio of two-carbon- over four-carbon-derived products for the overexpressed culture is 0.52, versus 0.39 for the control. These data are consistent with the expectation that a higher PTA activity will compete for the available acetyl-CoA pool with ethanol-forming dehydrogenase and thiolase.

In order to enhance the production of clostridial solvents, particularly acetone and butanol, redirecting the carbon flow from the acid-producing toward the solvent-producing pathway seems to be a logical strategy. Since the *ack* and *pta* genes cotranscribed as a single unit with *pta* upstream, the inactivation of *pta* will subsequently abolish the expression of *ack*. The gene encoding PTA is therefore chosen to be inactivated in the clostridial chromosome. Southern hybridization (Fig. 4.11) indicates that the chromosomal copy of the *pta* gene was integrated into the

chromosome of an engineered mutant strain, 824::ptak$^-$. In addition, the integration of *pta* resulted in the essentially abolished expression of *ack*, as was shown in four separate enzyme activity assays (Table 4.3), where both the PTA and the AK activities decreased significantly in the crude extract of 824::ptak$^-$ compared to those found in 824.

The *pta*-integrant still exhibited some residual PTA and AK activity. After carefully examing all the possibilities, the most plausible explanation for this remaining activity could have come from PTB and BK, the two enzymes involved in the butyrate-producing pathway. Previous research on PTB and BK purification has shown that PTB exhibited a 2 percent activity toward acetyl-CoA and AK a 6 percent activity toward acetyl-phosphate (Wiesenborn et al., 1989, Hartmanis, 1987). It was observed that in complex primary metabolism, production pathways can exhibit control architectures that resist flux alterations at branch points. Deregulation of the acetate-formation pathway during acidogenesis could likely result in elevation of the acetyl-CoA concentration level, which would subsequently trigger the clostridial cells to adjust their metabolic rate. PTB would be overproduced and would partially perform the PTA function. In fact, the enzyme activity assay (Table 4.3) shows that the specific activity of PTB from the *pta*-knockout strain was more than two-fold higher than the wild type. The enzyme activity level of BK also increased slightly, in contrast to the significantly decreased levels of PTA and AK.

The inactivation of acetate production could have a significant effect on cell growth, since the acetate and butyrate production pathways in

clostridia are important in generating ATP. It is seen that the mutant strain 824::ptak$^-$ grew more slowly than the wild-type and therefore was represented by a longer doubling time (1.5 vs 1.0 hr for the wild-type in Table 4.7). However, the mutant strain achieved a higher biomass concentration. It seems that the mutant culture thus compensated for the lack of an energy source from the acetate-production pathway by increasing the production of the butyrate pathway without significant change in cell growth.

The product pattern was carefully examined using cultures from either small-scale test-tube growth or large-scale fermentors (by Dr. Edward Green) with pH control and continuous mixing. The results are shown in Tables 4.5 and 4.6, respectively. It is seen from the controlled-pH batch fermentation that, during exponential growth, the acetate-butyrate ratio was approximately 1:6 for mutant strain, versus 1:1 for wild-type (Mermelstein et al., 1994). Butyrate was overproduced (which is consistent with the higher PTB and BK activities), reaching a maximal level of 109.9 mM. Approximately 30% of the overproduced butyrate was reassimilated, resulting in a higher acetone level than for the wild-type. The butanol level was approxiamately the same as that from the wild-type. The maximal amount of acetate produced by the *pta*-integrant was approximately half of that produced by the wild-type.

It should also be noted that acetate production remained at low levels until after the onset of solventogenesis (Table 4.6). Thereafter, cell metabolism was adjusted and acetate was more readily produced. However, final acetate production levels were still only half of that using

the wild-type strain (Mermelstein et al., 1994). The delayed and reduced formation of acetate from 824::ptak$^-$ was most probably catalyzed by the corresponding enzymes for butyrate production. Other possibilities, however, cannot be neglected, such as the existence of AK and PTA isozymes. Even though the biochemical pathways of *C. acetobutylicum* are reasonably well understood, some specific areas might still require definition. An alternative pathway leading to acetate production might still exist in the primary metabolic path. The purification and characterization of PTA and AK from *C. acetobutylicum* could then provide insights into these possibilities. In addition, it would be interesting to study further the intracellular levels of acetyl-CoA and butyryl-CoA of this mutant.

In summary, the genes encoding PTA and AK from *C. acetobutylicum* were cloned, sequenced and overexpressed. The chromosomal copy of the *pta* gene was inactivated, and the engineered mutant produced less acetate and more acetone. This work represents a clear example of specific gene isolation and use of the DNA material for gene inactivation, pathway enzyme analysis and specific metabolic studies. It is believed that additional work of this type will yield important new information about biochemical responses related to solvent and acid production and could thus advance recombinant technology for specific commercial applications using controlled clostridial fermentation.

Chapter 5. Intracellular Concentrations of CoA and Its Derivatives

This chapter introduces the physiological factors suggested to be involved in the solventogenic shift of *C. acetobutylicum*, and a specific example of CoA and its derivatives is discussed. It continues with a detailed description of the method used in extracting the CoA and its derivatives and the reliability and reproducibility of this method. The results of samples from wild-type and mutant clostridial strains are then described throughout the entire fermentation process. The data are compared with the known physiological and kinetic data of the specific enzymes involved, and the roles of the CoA and its derivatives in regulating specific enzyme reactions are evaluated.

5.1. Introduction

Although many investigators have studied the biochemistry of acetone-butanol fermentation, the detailed mechanisms which control the shift from acid to the solvent formation are still not well understood (Davis, 1942, Papoutsakis, 1984, Rosenfeld and Simon, 1950, Wood et al., 1945). The physiological conditions that are suggested for initiating the switch include the butyrate concentration, a low pH, a growth-limiting factor such as phosphate depletion, and excess glucose and nitrogen. Significant progress has been reported on the analysis of the enzyme activities (Colby and Chen, 1992, Hartmanis and Gatenbeck, 1984, Husemann et al., 1989, Jungermann et al., 1971, 1973) and internal pH involved in the clostridial pathway (Gottwald and Gottschalk, 1985, Grupe and Gottschalk, 1992, Hartmanis et al., 1984, Husemann et al., 1988).

However, only recently have the *in vivo* levels of intermediate metabolites and cofactors, which may play an important role in enzyme regulation, been studied (Grupe and Gottschalk, 1992).

From the metabolic pathways related to the solvent-producing clostridia (Fig. 1.1), it is clear that different CoA derivatives in the central fermentation pathway, acetyl-CoA, acetoacetyl-CoA, β-hydroxyl-butyryl-CoA, crotonyl-CoA and butyryl-CoA are key intermediates in the metabolism of this organism. The metabolic fate of these compounds may have some role in regulating specific enzymes involved and subsequently affect the product pattern of the fermentation (Colby and Chen, 1992, Jones and Woods, 1986).

The structure of CoA and the metabolic conversion of butyryl-CoA from acetyl-CoA is shown in Fig. 5.1. Free CoA and its derivatives participate in amino acid, carbohydrate and lipid metabolism. However, they are very unstable and are sensitive to changes of pH, temperature and light. In addition, the intracellular levels of CoA compounds are usually at low levels. All these characteristics make it difficult to measure the intracellular levels of CoA and its derivatives. In the past, such measurements could be made only by indirect methods (Ingebresten and Farstad, 1980). Recently, however, several reports have described the separation and measurement of CoA and acyl-CoA esters from mammalian cells by reverse-phase high-performance liquid chromatography (HPLC). The purpose of this project is therefore to modify this latest method and apply it to clostridial study.

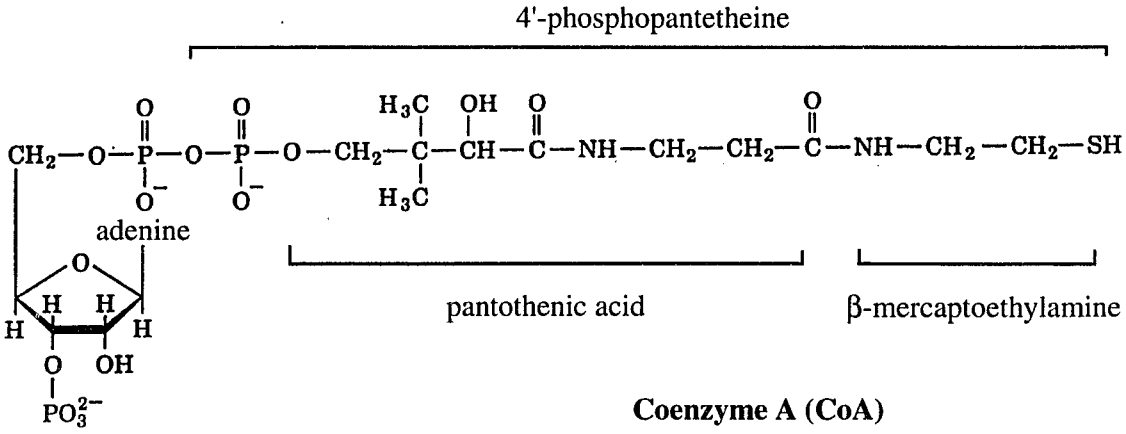

Coenzyme A (CoA)

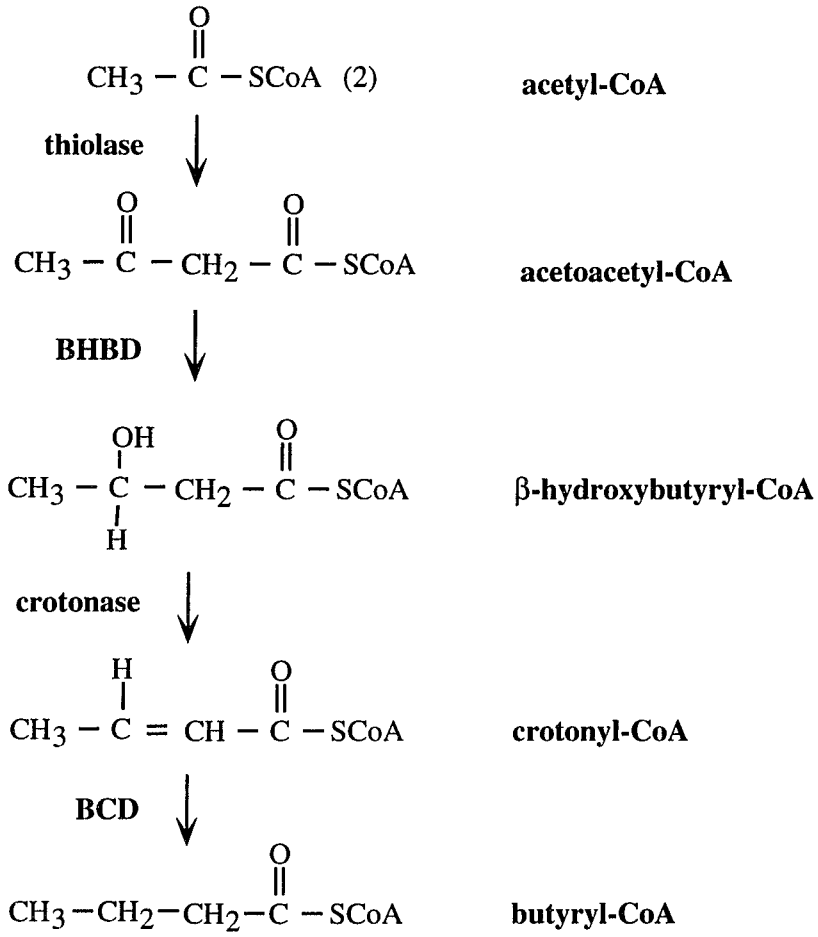

acetyl-CoA

acetoacetyl-CoA

β-hydroxybutyryl-CoA

crotonyl-CoA

butyryl-CoA

Fig. 5.1. The metabolic conversion of butyryl-CoA from acetyl-CoA and the structure of CoA.

Reported here are the intracellular concentrations of free CoA and various CoA derivatives during the entire fermentation process, as measured using a reverse-phase chromatographic system. Assays were also carried out on several non-solvent-producing mutant cultures for comparison. Furthermore, it was of interest to study the correlations of CoA-compound concentrations with the specific enzyme-activity levels before and during the onset of solventogenesis. The possible roles of the CoA derivatives in regulating specific enzymatic reactions are evaluated.

5.2. Materials and Methods

5.2.1. Reagents. HPLC-grade acetonitrile was purchased from EM Science (Gibbstown, NJ.) and sodium phosphate from Mallinckrodt, Inc. (Paris, Ky.). Deionized water was further purified by passing it through a Milli-Q water purification system (Millipore Corporation, Bedford, Mass.). CoA and its derivatives were obtained from Sigma Chemical Company (St. Louis, Mo.). The dye-binding protein assay kit was obtained from Bio-Rad Laboratories (Richmond, Calif.)

5.2.2. HPLC apparatus. Separations of CoA compounds were performed with a LDC/Milton Roy GM 4000 HPLC system (Riviera Beach, Fla.). Two Model-III pumps were used to deliver eluants through a 5 micron, ODS column (4.6 X 250 mm) from Custom LC, Inc. (Houston, Tex.). A model 1203 UV-III detector was employed to monitor column effluent at 254 nm. The signal from the UV monitor was delivered to a CI-10B integrator for quantification.

5.2.3. Chromatography. The two mobile-phase solvents used were: buffer A (0.2 M sodium phosphate, pH 5.0) and buffer B (800 mL of 0.25 M sodium phosphate, pH 5.0, mixed with 200 mL acetonitrile) (King and Reiss, 1985). These buffers were passed through glass microfibre GF/F filters (Whatman Int'l Ltd., Maidstone, England) prior to use. The chromatographic separations were performed at room temperature and at a flow rate of 1 ml/min. The mobile phase composition profile, after a 2.5-minute constant-B-buffer level of 3-percent (i.e. 97% buffer A), was divided into several linear-gradient segments, with sequential segment end points of 7.5 minutes (where 18% of buffer B was reached), 10 minutes (28% B), 15 minutes (30%), 25 minutes (40%), 26 minutes (42%) and 35 minutes (90%). At the 90% B level, the percentage of buffer B was reduced, over one minute, to the original 3% level and then maintained to the end of the HPLC cycle (45 minutes). Data collection was stopped at 40 min., and column reequilibration was complete after 47 min. The injection volume of 10 ul was maintained constant for all HPLC runs.

CoA and the various acyl-CoA derivatives were made up as 5 mM stock solutions in a 100 mM sodium phosphate buffer (pH 3.0), and were stored at -80^{o}C. Stock solutions prepared in this way were stable for at least a month.

5.2.4. Strains and culture conditions. The wild-type strain was *C. acetobutylicum* ATCC 824. Mutants 2BBD, M5 and 2BBR were isolated and previously described by Clark et al (1989). Mutants 34, 4145, 1013 and 6a5 were Tn-916 mutants prepared by Sass and Bennett as described (1993). Maintenance of these organisms, including preparation of the medium,

inoculation, heat-shocking and anaerobic growth have been described previously (Clark et al., 1989, Sass and Bennett, 1993).

5.2.5. Culture preparation. Strains were grown anaerobically in 600 mL of RSM soluble medium (Clark et al., 1989) at 37°C. The pH was not controlled. Samples were taken at 2- to 4-hr intervals in order to obtain data corresponding to the maximal solvent-producing stage. The appropriate harvest time was determined initially by measuring pH and absorbance at 600 nm. Samples were centrifuged at 19,000 g for 20 min at 4°C, the supernatants were analyzed for solvent production by the nitroblue tetrazolium method (Clark et al., 1989), and the pellets were resuspended in the cold soluble medium and centrifuged at 34,000 g for another 20 min at 4°C. No significant loss of metabolite levels was observed with this second step which allowed better chromatographic separations. The pellets were immediately powdered in a porcelain mortar-and-pestle cooled to -80°C with liquid nitrogen. The frozen powder was stored at -80°C until required.

5.2.6. Enzyme assays. Cell extracts were prepared as previously described (Clark et al., 1989) except that the protein concentration was measured by the method of Bradford (1976), with bovine serum albumin (BSA) as the standard. Measurement of each enzyme activity was performed as described previously (Clark et al., 1989).

5.2.7. CoA-compound extraction and recovery. Frozen powder (0.4 g) was weighed out into a polystyrene centrifuge tube precooled with liquid nitrogen, and 0.8 ml of cold 6% perchloric acid (PCA) containing 2 mM

DTT was added. The mixture was sonicated at 90% power for 9 min for acidogenic cells and 15-18 min for solventogenic cells. The denatured protein was removed by centrifugation and 0.8 mL of the PCA extract was transferred to a precooled Eppendorf centrifuge tube and adjusted to a pH of 3.0 by dropwise addition of 3 M K_2CO_3, with vortexing during the addition. The neutralized sample was centrifuged at 4°C, and the supernatant was filtered through a 10,000 NMWL ultrafree-MC filter (Millipore Products Division, Bedford, Mass.) The resulting aliquot was stored at -20°C when not immediately analyzed using the HPLC. Solutions stored in this manner were stable for a week or more.

Recovery of added standard CoA compounds was accomplished as follows. Either a 100 ul standard CoA mixture or the 100 mM NaH_2PO_4, pH 3.0 solution was added to a centrifuge tube and cooled to liquid nitrogen temperature. A 0.4g amount of frozen powder was then added to the tube and extracted with 0.8 mL of ice-cold 6% PCA, as described above. The resulting aliquot was analyzed in the HPLC. Each sample was run at least twice in the HPLC.

5.2.8. Determination of biomass concentration. Biomass concentration of the culture broth was measured by reading the absorbance at 600 nm (OD_{600}) and converting the readings to concentrations in g/liter (wet weight) using a mass extinction coefficient of 0.89 ± 0.03 L $g^{-1}cm^{-1}$. The mass extinction coefficient was determined by measuring the actual biomass concentration and the corresponding OD_{600} under various conditions.

5.2.9. Intracellular and extracellular aqueous space measurement. In order to measure the intracellular volume at various times during the batch fermentation, a 5ml cell suspension was incubated anaerobically in a 15ml disposable tube at 37° in the incubator, with 1 μCi of [^{14}C-carboxyl]-dextran (American Radiolabeled Chemicals Inc., St. Louis, MO) and 10 μCi of $^{3}H_2O$ (New England Nuclear, Boston, MA) added to the assay. Dextran was used for the measurement of the extracellular water volume of the pellets and had a final concentration of 0.142 g/l and a radioactivity 1.4 mCi/g. Tritium water ($^{3}H_2O$) was used for measuring the total aqueous space in the pellet and had a final concentration of 110.7 mM with 18.0 mCi/mol. The intracellular aqueous volume for the growing cells in their growth medium was determined by subtracting the extracellular space occupied by dextran from the total aqueous space (Husemann, 1989, Husemann and Papoutsakis, 1988). Based on twelve independent measurements each, the intracellular aqueous volumes of the acid-phase, solvent-phase and late-solvent-phase cells are 0.21±0.01, 0.36±0.02 and 0.45±0.02 ml per gram wet cell, respectively.

5.2.10. Calculations. Radioisotopes were used to measure the total (Vt), intracellular (Vi) and extracellular (Vo) aqueous volumes of the cell pellets. All units are ml/g (wet weight).

Perchloric acid in the amount of 0.8 ml was added to 0.4 g of frozen cell powder (weight/volume ratio of 1:2). After extraction, total aqueous volume for the CoA-compound solutions dissolved was 0.4Vt+0.8, expressed in ml.

After centrifugation, neutralization and filtration to separate out unwanted cell debris, the aliquot was HPLC analyzed maintaining 10 ul of injection volume. The total amount of a measured CoA compound was determined from the expression Cn(0.8+0.4Vt)/0.4 g, or Cn(2+Vt), expressed in nmol/g (wet cell), where Cn is the concentration of a specific CoA compound, which was derived from the HPLC analysis. The intracellular concentration is therefore Cn(2+Vt)/Vi, expressed in μM.

5.3. Results

5.3.1. Recovery. Four different samples from wild-type *Clostridium* cultures were extracted and the recoveries calculated, and the results were shown in Table 5.1. The percent recovery for free CoA was found to be a mean of 95% with a ±3% standard deviation, 97±18% for acetyl-CoA, 81±6% for acetoacetyl-CoA, 93±2% for β-OH-butyryl-CoA, 82±3% for crotonyl-CoA and 89±13% for butyryl-CoA. Values for percent recovery were used to correct measured CoA compound concentrations.

5.3.2. Chromatography. A standard solution of all the CoA compounds involved in the clostridial pathway is separated to a useful degree in 40 min by reverse-phase chromatography (see Fig. 5.2). CoA and its derivatives were distinctively separated while maintaining the baseline approximately level, thereby allowing for more accurate quantification of CoA compounds.

Table 5.1. Recovery of CoA compounds from *C. acetobutylicum* cultures extracted with perchloric acid.

Sample	CoA	Acetyl-CoA	Acetoacetyl-CoA	β-OH-Butyryl-CoA	Crotonyl-CoA	Butyryl-CoA
WT acid cells OD600 2.7 pH 4.22	93.0%	98.0%	72.6%	93.3%	84.6%	87.2%
WT solvent cells OD600 6.86 pH 4.06	98.6%	90.9%	78.6%	90.2%	79.7%	90.6%
WT early solvent cells OD600 5.0 pH 3.82	92.6%	120.8%	86.5%	95.1%	84.8%	105.2%
WT late- solvent Cells OD600 9.4 pH 4.06	97.8%	77.4%	84.6%	93.3%	79.3%	74.5%
Mean±SE	95±2%	97±9%	81±6%	93±1%	82±2%	89±6%
Mean±SD	95±3%	97±18%	81±12%	93±2%	82±3%	89±13%

Note. Each sample was run at least twice and the percentage of recovery was the mean of different runs.

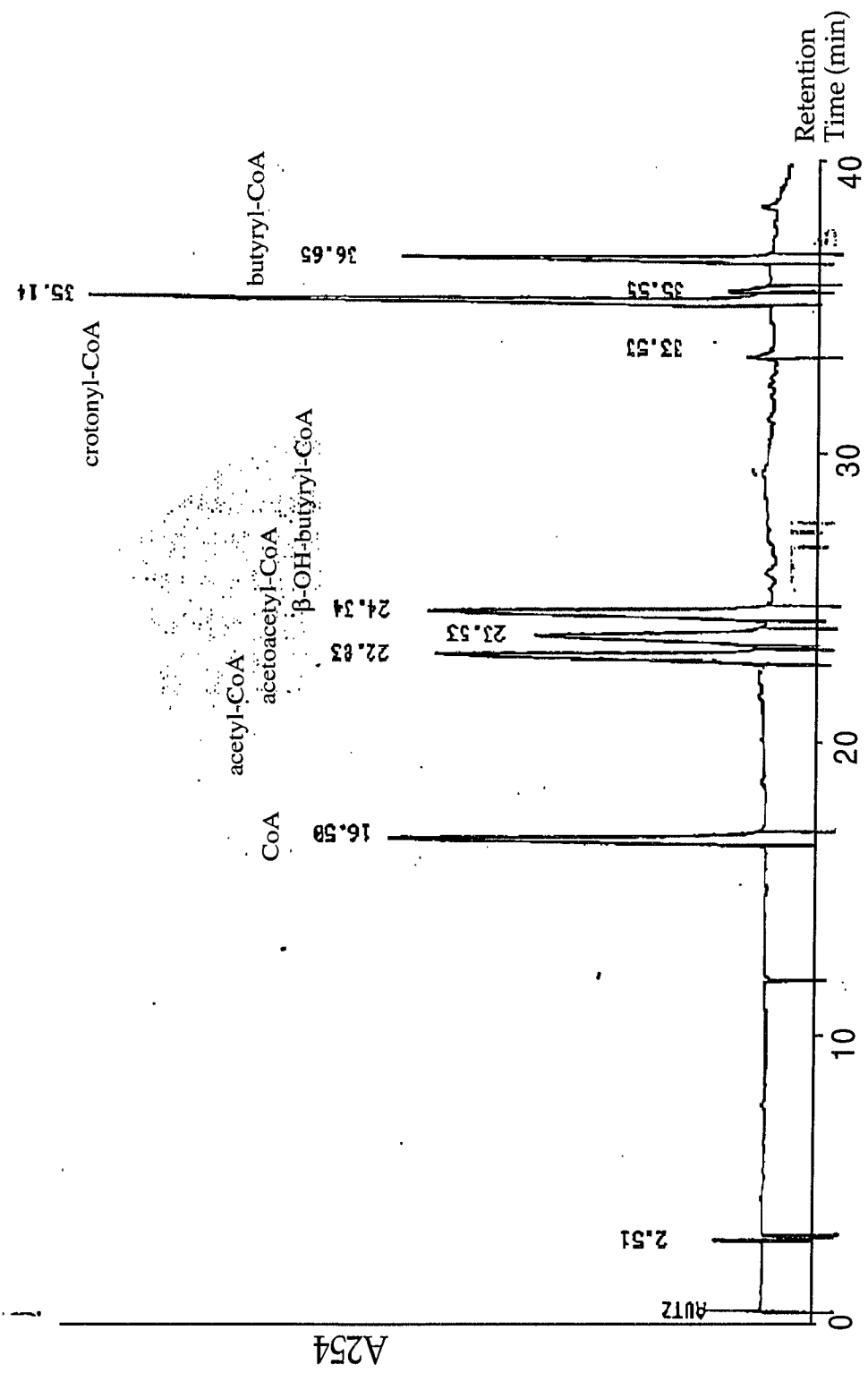

Fig. 5.2. Elution profile of a mixture containing 1 nmol of CoA and noted acyl-CoA intermediate standards. Absorbance recorded at 254 nm. Flow rate, 1 ml/min. Total run time, 40 mins. Detector sensitivity, 0.128 AUFS.

The typical chromatograms of PCA extract from *C. acetobutylicum* a wild-type solventogenic culture and a mutant culture were shown in Figs. 5.3 and 5.4, respectively. Peaks were identified through their retention times and through spiking by adding corresponding standards. Peak areas were plotted against concentration for each CoA compound for quantification. CoA, acetyl-CoA and butyryl-CoA were well separated and found in measurable quantities. Acetoacetyl-CoA, β-OH-butyryl-CoA and crotonyl-CoA were separated in standard solutions but have not been found in measurable amounts in the cell extract.

5.3.3. Linearity, Detection Limits and Recovery. Linear relationships were observed between the ratios of the peak areas of CoA compounds to the amounts added in the range of from 25 to 4000 pmol, using full-scale absorbance (AUFS) from 0.016 to 0.128. The respective lower limits of detection for CoA, acetyl-CoA, acetoacetyl-CoA, β-OH-butyryl-CoA, crotonyl-CoA and butyryl-CoA were 15, 15, 25, 15, 12.5, and 15 pmol (with corresponding intracellular concentrations of 11, 11, 21, 11, 10 and 12 uM for solvent phase cells) at a maximum observed signal-to-noise ratio of 3.5.

5.3.4. Levels of intracellular CoA compounds from wild-type cultures. The intracellular CoA compound levels were measured from wild-type pH-uncontrolled batch culture, with results shown in Table 5.2. The cultures were harvested more frequently during the onset of the solventogenic phase so that the rapidly changing metabolic levels could be more clearly delineated.

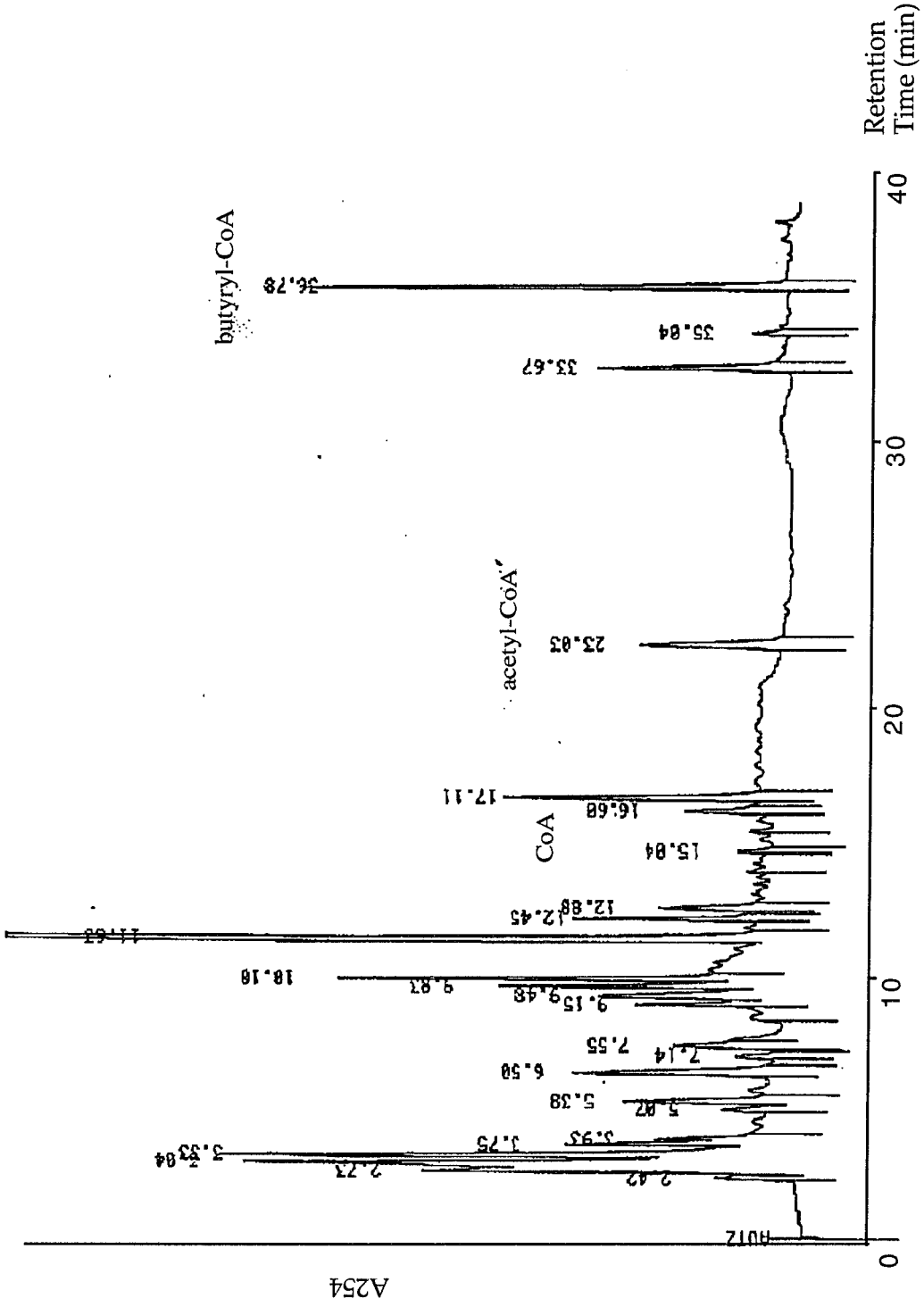

Fig. 5.3. Elution profile of a 10-µl PCA extract from *clostridium* wild-type solventogenic cells.

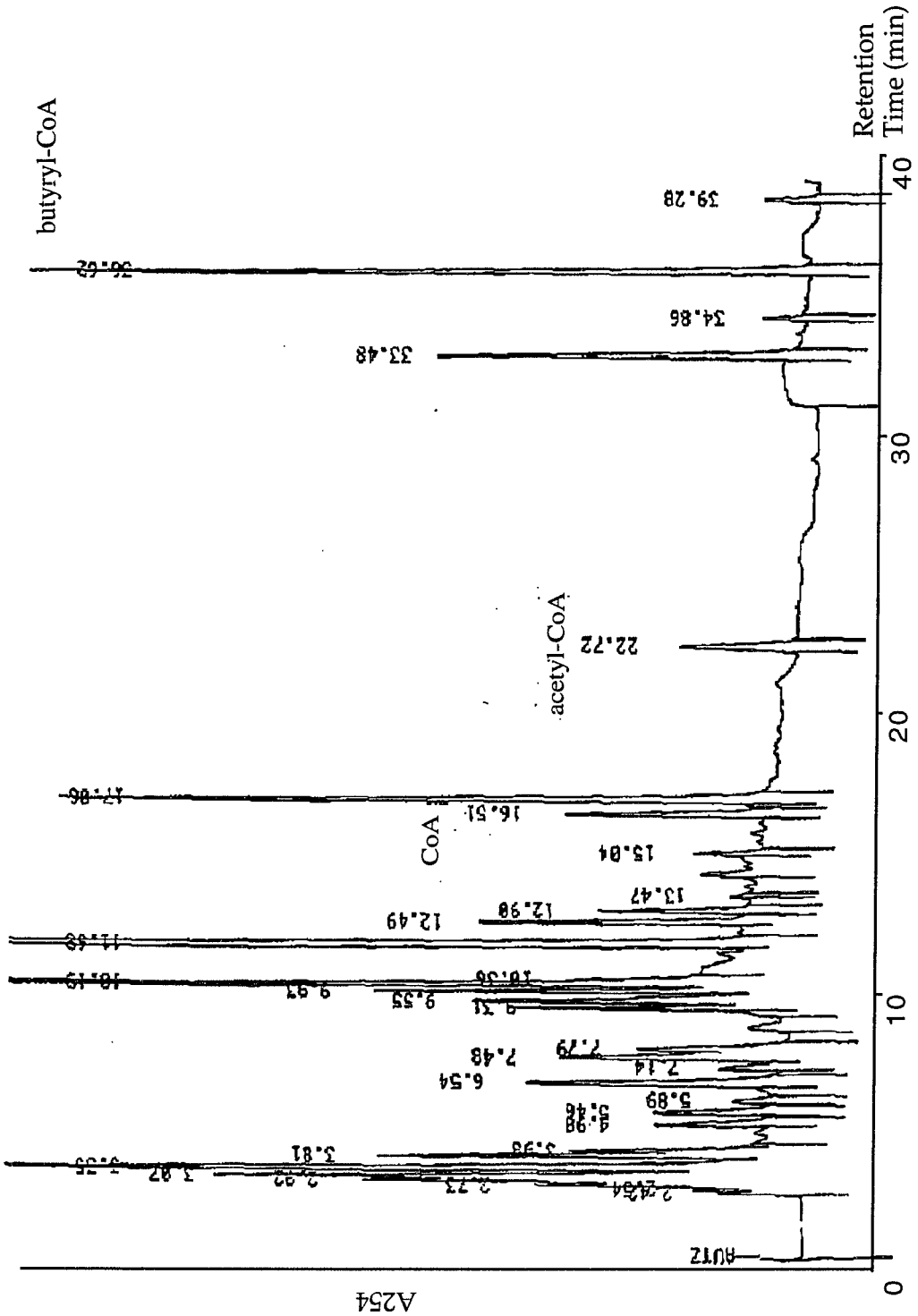

Fig. 5.4. Elution profile of a 10-µl PCA extract from *clostridium* mutant culture M5.

Table 5.2. Intracellular CoA-compound concentrations and the solvent-pathway enzyme activities in a pH-uncontrolled batch culture of wild type *C. acetobutylicum*. Enzyme activity (U/mg protein)[a]

Sample	OD600	pH	Time (hr)	butanol conc. (mM)	CoA (uM)	Acetyl -CoA (uM)	Butyryl -CoA (uM)	PTB	BK	NADH -BDH	NADPH -BDH	NAD -BAD	NADP -BAD	CoA Transferase
acid cells	2.40	4.27	11	0	185±16	436±22	574±39							
late acid cells	4.47	3.89	15	4.0	161±14	456±14	512±18	20,100	900	5.7	22.5	14.6	12.6	17.9
early solvent cells	5.12	3.82	16.5	21	124±7	316±9	810±24	16,500	840	16.6	50.0	30.4	47.0	316
	5.14	3.82	18	>40	102±3	327±11	857±23	12,400	680	4.8	47.7	22.3	22.3	613
solvent cells	5.86	3.79	20		145±6	396±19	882±30	13,200	600	7.8	85.7	51.6	34.4	1,200
	6.13	3.80	22		122±10	327±5	1002±19							
	6.26	3.93	23		154±12	383±21	690±25							
	7.82	3.92	27		140±1	368±11	645±21							

a. Units for each enzyme are defined as nanomoles of product formed per mg of protein.

It is known that the enzyme profiles of acid-phase and solvent-phase cells are different. The enzymes needed for acid production, detected from their catalytic activity in cell-free extracts, decrease in solvent-phase cells. Solvent-producing enzyme activity, in contrast, is present only in cells harvested during the solvent phase (Andersch et al., 1983, Hartmanis and Gatenbeck, 1984). To further characterize the correlation of enzyme induction with intracellular concentrations of key intermediates, the enzyme activity and the corresponding CoA-compound concentrations around the onset of solventogenesis were measured. These results are also shown in Table 5.2.

5.3.5. Intracellular levels of CoA compounds from mutant cultures. To form a better understanding of the relationship between the CoA-compound concentrations and solventogenesis, various non-solvent-producing mutants isolated before in this laboratory (Clark et al., 1989, Sass and Bennett, 1994) were analyzed. Either these mutants, such as 6a5, 1013, M5 and 4145, did not produce any solvents, or, for mutants 2BBD and 34, produced amounts lower than for wild-type strains. Except for mutant 34, all mutants are non-spore-forming strains. These mutants either lack or only have low levels of the enzymes involved in the solvent production. The CoA-compound concentrations for these mutants and the corresponding solvent-pathway enzyme activities are listed in Table 5.3. Cultures were judiciously harvested during the early-stationary phase. Cultures harvested past this point were difficult to sonicate and therefore could lose their enzyme activity quickly, the CoA-compound levels would also decrease rapidly.

Table 5.3. Intracellular CoA-compound concentrations and the solvent-pathway enzyme activities from various *Clostridium* mutants at the onset of the stationary phase. Enzyme activities (U/mg of protein)[a]

Strain	OD_{600}	pH	solvent conc. (mM)	CoA (uM)	Acetyl-CoA (uM)	Butyryl-CoA (uM)	PTB	BK	NADH BDH	NADPH BDH	NAD BAD	NADP BAD	CoA Transferase
wild type	5.12	3.82	21	124±7	316±9	810±24	16,500	840	16.6	50.0	30.4	47.0	316
1013	5.28	3.88	0	136±2	319±20	1,180±61	10,900	1,480	1.1	17.2	0	0	0
6a5	5.34	3.95	0	76.4±14.2	193±18	1,101±42	22,600	813	0	20.8	0	0	0
M5	6.00	3.92	0	284±12	222±8	1,169±34	9,600	1,190	1.6	83.1	0	0	0
2BBD	6.26	3.76	NT[b]	162±2	398±1	679±3	9,300	1,020	0	26.0	NT	NT	NT
34	4.52	3.93	7.0	88.0±6.9	302±3	761±51	12,900	1,380	4.4	35.7	1.5	1.5	79.2
4145	5.27	3.72	0	159±4	225±7	1,326±16	14,900	1,170	21.2	27.0	28.4	34.0	39.0

a. Units for each enzyme are defined as nanomoles of product formed per mg of protein.

b. NT: not tested.

5.4. Discussion

The production of solvents using clostridia is well-known, but the initiation mechanisms for the switch to solvent production are still being widely studied. Current hypotheses proposed for the triggering mechanism that cause the shift from the acid- to the solvent-production phase involve the regulation of catalytic pathways in response to the cellular concentrations of intermediates (Datta and Zeikus, 1985, Gottwald and Gottschalk, 1985). Gottwald and Gottschalk (1985) point out that, at the end of the acidogenic phase, where the reactions which lead from butyryl-CoA via butyryl-phosphate to butyrate are reversible, an elevated concentration of butyrate will result in higher levels of butyryl-phosphate and butyryl-CoA accumulating in the cell. This will result in significant decreases in both the CoA and the phosphate pools, triggering activation or synthesis of the enzymes for solventogenesis. Results herein show that, during the switch to solvent production, the butyryl-CoA concentration exhibited a marked increase from 512 to 810 uM. Correspondingly the CoA concentration decreased from 161 to 124 uM and acetyl-CoA from 456 to 316 uM. In other stages of the fermentation, this concentration remains relatively constant (Table 5.2).

Recent data from Grupe and Gottschalk (1992), who used a continuous culture of *C. acetobutylicum* DSM 1731 show that, during the shift, contrary to the expected positive pattern (first-increase-then-decrease) for acetyl-CoA and butyryl-CoA, a negative (first-decrease-then-increase) pattern for CoA, acetyl-CoA and butyryl-CoA was observed. Results herein showed a similar negative pattern of CoA and acetyl-CoA

compared to their results. However, during the shift, a consistent increase in butyryl-CoA concentration was detected, until the highest level of 1000 uM was observed (Table 5.2). This discrepancy may result from the differences in the mode of the culture growth (continuous vs. batch) and the culture operation. The batch cultures are in less steady state conditions than continuous cultures therefore some transient effect may not be observed.

To further characterize the correlation of solvent-pathway enzyme induction and intracellular concentration of key intermediates, representative enzyme activities and CoA-compound concentrations were also measured relative to the shift to the solventogenic phase (Table 5.2). These data clearly show that, along with the rapid increase of Bu-CoA concentration, the activity level of solvent-pathway enzymes, namely CoA transferase (CoA Tr), butyraldehyde dehydrogenase (BAD), and butanol-dehydrogenase (BDH), also increase rapidly. Conversely, the activity of the acid-producing enzymes, PTB and BK decreased.

As a control, the results from a wild-type culture were compared with various mutant cultures at the onset of the stationary phase. These mutants are either non-solvent-producing strains (1013, 6a5, 4145 and M5) or are reduced-solvent-producing strains (2BBD and 34), because they lack the solvent-producing enzymes mentioned above. From these results (Tables 5.3), it is seen that the mutants, generally exhibit reduced BDH levels and no CoA-Tr or BAD activity. However, these mutants can produce Bu-CoA concentrations comparable to, or even higher than those

for wild-type cultures, possibly because the higher levels of butyrate cannot be reassimilated.

The main advantage of knowing the concentrations of metabolic intermediates is that, after comparing the kinetic and physiological propertities of the enzymes involved, the influence of the metabolite in regulating a specific reaction can be evaluated. Those enzymes which react with the CoA derivatives are marked in Fig. 5.5, along with the Km's for the purified enzymes. Except for BHBD, which was purified from *C. butylicum* NRRL B593 (Colby and Chen, 1992), all other noted enzymes are derived from *C. acetobutylicum* (usually ATCC 824) (Palosaari and Rogers, 1988, Waterson et al., 1972, Wiesenborn et al., 1988, 1989a and 1989b). However, it should be noted that different strains of *C. acetobutylicum* are phylogenetically quite distinct (Woods, 1995). The kinetic data derived from strains different from *C. acetobutylicum* ATCC 824 might not apply to this study exactly.

The measured intracellular concentrations of CoA, acetyl-CoA and butyryl-CoA (Table 5.2) were generally above 100, 316 and 512 uM, respectively. These values are sufficient to allow maximal flux through the BAD and AAD (acetaldehyde dehydrogenase) reactions for which the Km values of 55 uM for butyryl-CoA and 45 uM for acetyl-CoA were determined (Palosaari and Rogers, 1988). These values should also be able to nearly saturate the PTB reaction, for which a Km value of 110 uM for butyryl-CoA in the forward direction was reported (Wiesenborn et al., 1989a). In fact, a change in internal pH may be an important factor in the regulation of PTB reaction (Wiesenborn et al., 1989a). Within the

Fig. 5.5. Metabolic pathway of *C. acetobutylicum* and the kinetic properties of the enzymes. The Km values are given in parentheses. The intracellular CoA, acetyl-CoA and butyryl-CoA concentrations are given in brackets.

Note. a. The Km values derived from *C. acetobutylicum* (1) ATCC 824 (2) B643.

b. The Km values derived from *C. butylicum* NRRL B593.

c. NK: not known.

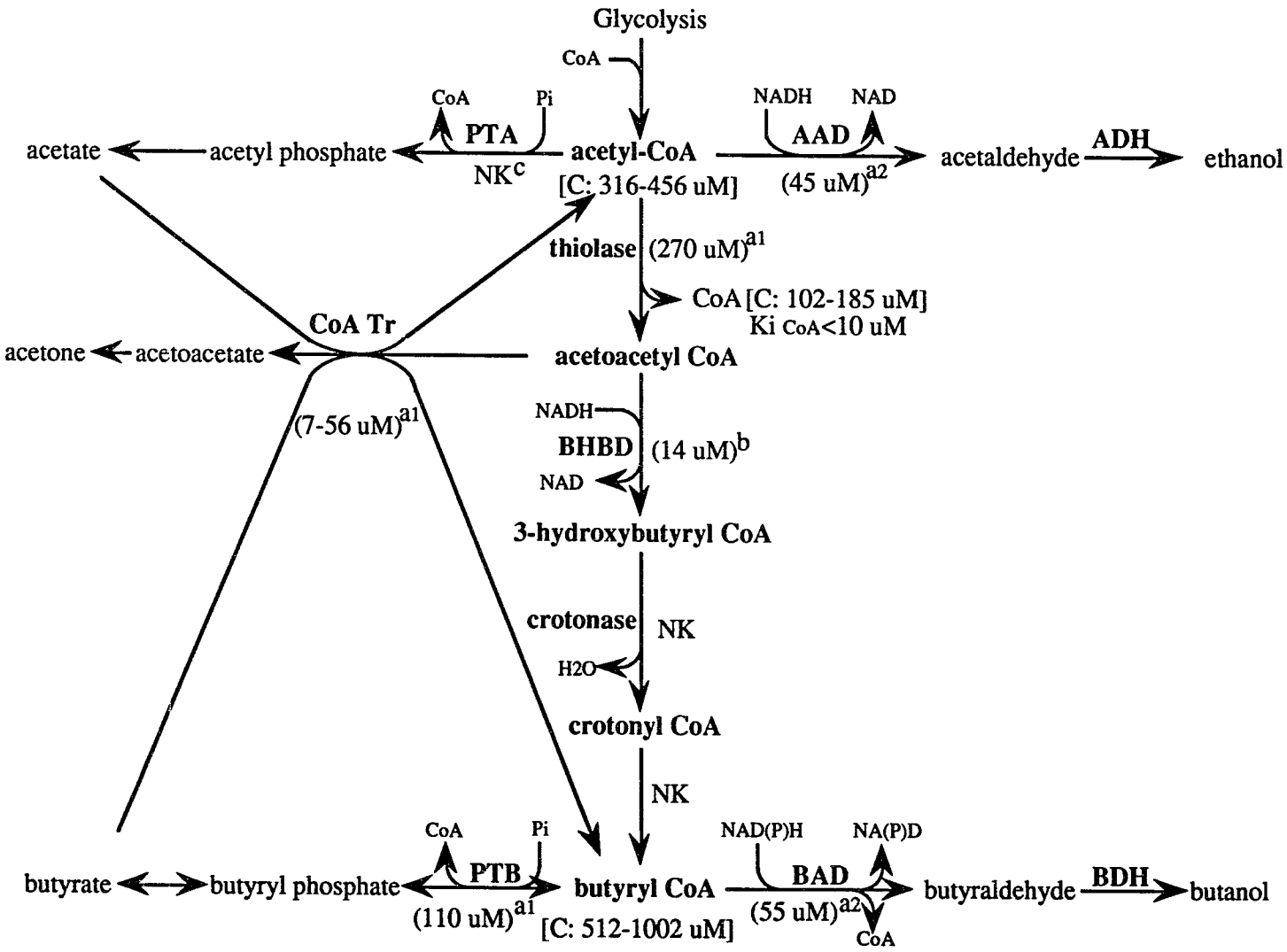
Glycolysis
CoA
CoA
Pi
PTA
NK^c
acetate
acetyl phosphate
acetyl-CoA
[C: 316-456 uM]
NADH
NAD
AAD
(45 uM)^a2
acetaldehyde
ADH
ethanol
thiolase
(270 uM)^a1
CoA [C: 102-185 uM]
Ki CoA<10 uM
CoA Tr
acetone
acetoacetate
acetoacetyl CoA
(7-56 uM)^a1
NADH
BHBD
(14 uM)^b
NAD
3-hydroxybutyryl CoA
crotonase
NK
H2O
crotonyl CoA
NK
CoA
Pi
NAD(P)H
NA(P)D
butyrate
butyryl phosphate
PTB
(110 uM)^a1
butyryl CoA
[C: 512-1002 uM]
BAD
(55 uM)^a2
butyraldehyde
BDH
butanol
CoA

physiological pH change of from 5.5 to 7, the internal pH range for typical fermentations (Huang et al., 1985), the PTB activity decreases significantly in the forward direction as pH decreases, and shows virtually no activity below a pH of 6. Therefore, the level of butyryl-CoA is not seen as an important regulating factor for PTB activity, as suggested previously (Wiesenborn et al., 1989a).

In the condensation reaction with thiolase, the Km value for acetyl-CoA had been determined to be 270 uM, and the thiolase activity was found to be inhibited by even micromolar levels of free CoA (Wiesenborn et al., 1988). Under these conditions, the intracellular CoA levels should be very inhibitory to this reaction, and the acetyl-CoA would still be below a saturating level. The intracellular concentrations of CoA and acetyl-CoA are likely important factors in regulating the net condensation of acetyl-CoA to acetoacetyl-CoA, and in regulating the pattern of product formation.

Three of the CoA derivatives involved in the metabolic pathways, namely acetoacetyl-CoA, β-OH-butyryl-CoA and crotonyl-CoA were not detected. It was known that these compounds are unstable, thus several extractions were carried out with externally added CoA compounds to check the reproducibility and recoverability of the extraction and assay procedures. From four different samples, the recoveries of acetoacetyl-CoA, β-OH-butyryl-CoA and crotonyl-CoA were 81%, 93% and 82%, respectively. Based on these recoveries, the corresponding intracellular concentrations of acetoacetyl-CoA, β-OH-butyryl-CoA and crotonyl-CoA should be less than 21, 11 and 10 uM. The enzymes which react with these

CoA derivatives, except BCD, have been purified from either *C. acetobutylicum* (CoA Tr, crotonase, (Wiesenborn et al., 1989b, Waterson et al., 1972)) or *C. butylicum* (BHBD, (Colby and Chen, 1992)) and the Km values are shown in Fig. 5.5. In the crotonase reaction, the Km value for the product crotonyl-CoA was 30 μM, and the enzyme was reported to be sensitive to levels of crotonyl-CoA above those observed here. However, the Km value for β-OH-butyryl-CoA was not determined (Waterson et al., 1972). For the BHBD from *C. butylicum*, a Km value for acetoacetyl-CoA of 14 uM was determined (Colby and Chen, 1992). This reference also reported that inhibition of BHBD activity by acetoacetyl-CoA was observed at concentrations at or above its Km when the NADH concentration was near its Km, suggesting that acetoacetyl-CoA plays an important role in the *in-vivo* regulation of BHBD.

None of the three CoA intermediates could be detected when the mutant cultures were used (Tables 5.2 and 5.3). Even in the absence of solvent-pathway enzymes, these compounds do not accumulate, thus suggesting a tight regulation of their synthesis. Further investigation of the role of these three CoA derivatives in enzyme regulation awaits the isolation of mutants having specific enzymes (BHBD, crotonase or BCD) removed.

Chapter 6. Summary and Conclusions

In this study, five genes encoding enzymes involved in the production of butyryl-CoA from acetoacetyl-CoA were cloned, sequenced and expressed. The intracellular levels of metabolites for these enzymes were measured, and their roles in regulating the specific enzymes involved were evaluated. Two genes encoding enzymes catalyzing the conversion of acetyl-CoA to acetate were also cloned, sequenced and expressed. In addition, the gene encoding PTA was also inactivated in the clostridial genome, and the interesting results, reported herein, derived from this parallel mutant study were evaluated carefully.

Three of the CoA derivatives involved in the metabolic pathways, namely acetoacetyl-CoA, β-OH-butyryl-CoA and crotonyl-CoA were not detected. The cloning of genes encoding BHBD, crotonase and BCD provided DNA materials for generation of mutants which will facilitate the further study of the putative roles of these undetectable CoA derivatives in regulating these three enzymes. It is seen from the DNA study that the *pta* gene was inactivated in the clostridial genome. However, the mutant still exhibited residual amounts of PTA and AK activity and produced a reduced amount of acetate. A mechanism was proposed whereby the inactivation of the acetate-production pathway resulted in the elevation of intracellular acetyl-CoA levels, which subsequently trigger the overproduction of butyrate-formation enzymes. It would be useful in future studies to examine intracellular acetyl-CoA and butyryl-CoA levels of this mutant and compare the data with those

from wild-type strain. The precise regulatory mechanisms could therefore be confirmed.

It would also be useful to study the cellular basis for the delayed and reduced production of acetate using the engineered mutant. However, since the study of CoA and its derivatives was the initial project in this study, the *pta*-knockout mutant (in the last project conducted) was not available at that time. Nevertheless, the present work generates many useful and interesting ideas and results which will inspire incoming graduate students to further study. As was mentioned earlier, BHBD, BCD and its related ETF, as well as PTA and AK, have never before been purified nor characterized from *C. acetobutylicum* ATCC 824. The cloning of their encoding genes provided an excellent beginning for total enzyme purification and for later, more detailed, metabolic studies. Overall, this work represents a clear example of beneficial gene regulation in commercial viable metabolic studies. Continued work of this type will most assuredly generate improved mutant strains resulting in more desirable product and will eventually advance metabolic engineering techniques using clostridial metabolism to practical applications.

References

Aceti, D.J., and J.G. Ferry. 1988. Purification and characterization of acetate kinase from acetate-grown *Methanosarcina thermophila.* J. Biol. Chem. **263:**15444-15448.

Albano, M., R. Breitling, and D.A. Dubnau. 1989. Nucleotide sequence and Genetic organization of the *Bacillus subtilis* comG operon. J. Bacteriol. **171:**5386-5404.

Andersch, W., H. Bahl, and G. Gottschalk. 1983. Levels of enzymes involved in acetate, butyrate, acetone and butanol formation by *Clostridium acetobutylicum.* Eur. J. Appl. Microbiol. Biotechnol. **18:**327-332.

Arigoni, F., P.A. Kaminski, H. Hennecke, and C. Elmerich. 1991. Nucleotide sequence of the *fixABC* region of *Azorhizobium caulinodans* ORS571: similarity of the *fixB* product with eukaryotic flavoproteins, characterization of *fixX* and identification of *nifW.* Mol. Gen. Genet. **225:**514-520.

Becker, D.F., J.A. Fuchs, D.K. Banfield, W.D. Funk, R.T.A. MacGillivray, and M.T. Stankovich. 1993. Characterization of wild-type and an active-site mutant in *Escherchia coli* of short-chain acyl-CoA dehydrogenase from *Megasphaera elsdenii.* Biochemistry **32:**10736-10742.

Bedzyk, L.A., K.W. Escudero, R.E. Gill, K.J. Griffin, and F.E. Frerman. 1993. Cloning, sequencing, and expression of the genes encoding subunits of *Paracoccus denitrificans* electron transfer flavoprotein. J. Biol. Chem. **268:**20211-20217.

Beinert, H. 1963. Acyl coenzyme A dehydrogenases. *In* P.D. Boyer, H. Lardy, and K. Myrback (ed.), The Enzymes, 2nd ed., **7:**447-466. Academic Press, New York.

Benton, W.D., and R.W. Davis. 1977. Screening λ*gt* recombinant clones by hybridization to single plaques *in situ*. Science **196**:180-182.

Birktoft, J.J., H.M. Holden, R. Hamlin, N.H. Xuong, and L.J. Banaszak. 1987. Structure of L-3-hydroxyacyl-coenzyme A dehydrogenase: prelimanary chain tracing at 2.8-Å resolution. Proc. Natl. Acad. Sci. **84**:8262-8266.

Bitar, K.G., A. Pepez-Aranda, R.A. Bradshaw. 1980. Amino acid sequence of L-3-hydroxyacyl-CoA dehydrogenase from pig heart muscle. FEBS Lett. **116**:196-198.

Bradford, M.M. 1976. A rapid and sensitive method for the quantitation of microgram quantities of protein utilizing the principle of protein-dye binding. Anal. Biochem. **72**:248-254.

Brock, T.D. 1979. Biology of microorganisms, 3rd edition. Prentice-Hall. Englewood Cliffs, New Jersey.

Bross, P., S. Engst, A.W. Strauss, D.P. Kelly, I. Rasched, and S. Ghisla. 1990. Characterization of wild-type and an active mutant of human medium chain acyl-CoA dehydrogenase after expression in *Escherichia coli*. J. Biol. Chem. **265**:7116-7119.

Brown, T.D.K., M.C. Jones-Mortimer, and H.L. Kornberg. 1977. The enzymatic interconversion of acetate and acetyl-coenzyme A in *Escherichia coli*. J. Gen. Microbiol. **102**:327-336.

Bullock, W.O., J.M. Fernandez, and J.M. Short. 1987. XL1-Blue: a high efficiency plasmid transforming recA *Escherichia coli* strain with beta-galactosidase selection. Biotechniques **5**:376-379.

Cary, J.W., D.J. Petersen, E.T. Papoutsakis, and G.N. Bennett. 1988.

Cloning and expression of *Clostridium acetobutylicum* phosphotransbutyrylase and butyrate kinase genes in *Escherichia coli*. J. Bacteriol. **170**:4613-4618.

Cary, J.W., D.J. Petersen, E.T. Papoutsakis, and G.N. Bennett. 1990. Cloning and expression of *Clostridium acetobutylicum* ATCC 824 acetoacetyl-coenzyme A:acetate/butyrate:coenzyme A-transferase in *Escherichia coli*. Appl. Environ. Microbiol. **56**:1576-1583.

Chung, C.T., and R.H. Miller. 1988. A rapid and convenient method for the preparation and storage of competent bacterial cells. Nucleic Acids Res. **16**:3580.

Chen, J.-S. 1993. Properties of acid- and solvent-forming enzymes of clostridia, p.54-60. *In* D.R. Woods, (ed.), The Clostridia and Biotechnology. Butterworth-Heinemann, Stoneham, MA.

Chow, L-P., H. Iwadate, K. Yano, M. Kamo, A. Tsugita, L. Gardet-Salvi, A-L. Stritt-Etter, and P. Schürmann. 1995. Amino acid sequence of spinach ferredoxin:thioredoxin reductase catalytic subunit and identification of thil groups constituting a redox-active disulfide and a [4Fe-4S] cluster. Eur. J. Biochem. **231**:149-156.

Clark., S.W., G.N. Bennett, and F.B. Rudolph. 1989. Isolation and characterization of mutants of *Clostridium acetobutylicum* ATCC 824 deficient in Acetoacetyl-Coenzyme A: Acetate/Butyrate: coenzyme A-Transferase (EC 2.8.3.9) and in other solvent pathway enzymes. Appl. Environ. Microbiol. **55**:970-976.

Colby, G.D., and J.S. Chen. 1992. Purification and Properties of 3-hydroxybutyryl-coenzyme A dehydrogenase from *Clostridium beijerinckii* (syn. *C. butylicum*) strain NRRL B593. Appl. Environ. Microbiol. **58**:3297-3302.

Datta, R., and J.G. Zeikus. 1985. Modulation of acetone-butanol-ethanol fermentation by carbon monooxide and organic acids. Appl. Environ. Microbiol. **49:**522-529.

Davies, R., and M. Stephenson. 1941. Studies on the acetone-butyl alcohol fermentation. 1. Nutritional and other factors involved in the preparation of active suspensions of *C. acetobutylicum* (Weizmann). Biochem. J. **35:**1320-1331.

Davies, R. 1942. Studies on the acetone-butyl alcohol fermentation. 2. Intermediates in the fermentation of glucose by *Cl. acetobutylicum*. 3. Potassium as an essential factor in the fermentation of maize meal by *Cl. acetobutylicum* (BY). Biochem. J. **36:**582-599.

Dietrichs, D., M. Meyer, B. Schmidt, and J.R. Andreesen. 1990. Purification of NADPH-dependent electron-transferring flavoproteins and N-terminal protein sequence data of dihydrolipoamide dehydrogenases from anaerobic, glycine-utilizing bacteria. J. Bacteriol. **172:**2088-2095.

Djordjevic, S., C.P. Pace, M.T. Stankovich, and J.-J. P. Kim. 1995. Three-dimensional structure of butyryl-CoA dehydrogenase from *Megasphaera elsdenii*. Biochemistry **34:**2163-2171.

Doelle, H.W. 1975. Bacterial Metabolism, 2nd edition. Academic Press. New York.

Drake, H.L., S.-I. Hu, and H.G. Wood. 1981. Purification of five components from *Clostridium thermoaceticum* which catalyze synthesis of acetate from pyruvate and methyltetrahydrofolate. J. Biol. Chem. **256:**11137-11144.

Earl, C.D., C.W. Ronson, and F.M. Ausubel. 1987. Genetic and structural analysis of the *Rhizobium meliltoti fixA, fixB, fixC* and *fixX* genes. J. Bacteriol. **169:**1127-1136.

Engel, P.C. 1981. Butyryl-CoA dehydrogenase from *Megasphaera elsdenii*. Methods in Enzymol. **71**:359-366.

Engel, P.C., and V. Massey. 1971a. The purification and properties of butyryl-coenzyme A dehydrogenase from *Peptostreptococcus elsdenii*. Biochem. J. **125**:879-887.

Engel, P.C., and V. Massey. 1971b. Green butyryl-coenzyme A dehydrogenase, an enzyme-acyl-coenzyme A complex. Biochem. J. **125**:889-902.

Fendrich, G., and R.H. Abeles. 1982. Mechanism of action of butyryl-CoA dehydrogenase: reactions with acetylenic, olefinic, and fluorinated substrate analogues. Biochemistry **21**:6685-6695.

Fink, C.W., S. Soltysik, and M.T. Stankovich. 1986. Oxidation-reduction potentials of butyryl-CoA dehydrogenase. Biochemistry **25**:6637-6643.

Finocchiaro, G., M. Ito, Y. Iketa, and K. Tanaka. 1988. Molecular cloning and nucletide sequence of cDNAs encoding the α-subunit of human electron transfer flavoprotein. J. Biol. Chem. **263**:15773-15780.

Finocchiaro, G., I. Colombo, B. Garavaglia, C. Gellera, G. Valdameri, N. Garbuglio, and S. Didonato. 1993. cDNA cloning and mitochondrial import of the β-subunit of the human electron-transfer flavoprotein. Eur. J. Biochem. **213**:1003-1008.

Fischer, R.J., J. Helms, and P. Dürre. 1993. Cloning, sequencing, and molecular analysis of the *sol* operon of *Clostridium acetobutylicum*, a chromosomal locus involved in solventogenesis. J. Bacteriol. **175**:6959-6969.

Fleischmann, R.D., M.D. Adams, O. White, R.A. Claton, E.F. Kirkness, A.R. Kerlavage, C.J. Bult, J.-F. Tomb, B.A. Dougherty, J.M.

Merrick, K. McKenney, G. Sutton, W. FitzHugh, C. Fields, J.D. Gocayne, J. Scott, R. Shirley, L-I. Liu, A. Glodek, J.M. Kelley, J.F. Weidman, C.A. Phillips, T. Spriggs, E. Hedblom, M.D. Cotton, T.R. Utterback, M.C. Hanna, D.T. Nguyen, D.M. Saudek, R.C. Brandon, L.D. Fine, J.L. Fritchman, J.L. Fuhrmann, N.S.M. Geoghagen, C.L. Gnehm, L.A. McDonald, K.V. Small, C.M. Fraser, H.O. Smith, and J.C. Venter. 1995. Whole-genome random sequencing and assembly of *Haemophilus influenzae* Rd. Science **269**:496-512.

Fox, D.K., and S. Roseman. 1986. Isolation and characterization of homogeneous acetate kinase from *Salmonella typhimurium* and *Escherichia coli*. J. Biol. Chem. **261**:13487-13497.

Fraser, C.M., J.D. Gocayne, O. White, M.D. Adams, R.A. Clayton, R.D. Fleischmann, C.J. Bult, A.R. Kerlavage, G. Sutton, J.M. Kelley, J.L. Fritchman, J.F. Weidman, K.V. Small, M. Sandusky, J. Fuhrmann, D. Nguyen, T.R. Utterback, D.M. Saudek, C.A. Phillips, J.M. Merrick, J.-F. Tomb, B.A. Dougherty, K.F. Bott, P.-C. Hu, T.S. Lucier, S.N. Peterson, H.O. Smith, C.A. Hutchison III, and J.C. Venter. 1995. The minimal gene complement of *Mycoplasma genitalium*. Science **270**:397-403.

Frischauf, A.-M., H. Lehroch, A. Poustka, and N. Murray. 1983. Lambda replacement vectors carrying polylinker sequences. J. Mol. Biol. **170**:827-842.

Frisell, W.R., J.R. Cronin, and C.G. Mackenzie. 1966. *in* Flavins and Flavoproteins (Slater, E.C., ed) pp. 367-386, Elsevier, Amsterdam.

Gavard, R., B. Hautecoeur, and H. Descourtieux. 1957. Phosphotransacetylase de *Clostridium acetobutylicum*. C.R. Acad. Sci. Ser. D **244**:2323-2326.

George, H.A., and J.S. Chen. 1983. Acidic conditions are not obligatory for onset of butanol formation by *Clostridium beijernckii*. Appl. Environ. Microbiol. **46**:321-327.

Glaser, P., F. Kunst, M. Arnaud, M.-P. Coudart, W. Gonzales, M.-F. Hullo, M. Ionescu, B. Lubochinsky, L. Marcelino, I. Moszer, E. Presecan, M. Santana, E. Schneider, J. Schweizer, A. Vertes, G. Rapoport, and A. Danchin. 1993. *Bacillus subtilis* genome project: cloning and sequencing of the 97 kb region from 325° to 333°. Mol. Microbiol. **10**:371-384.

Gerischer, U., and P. Dürre. 1990. Cloning, sequencing, and molecular analysis of the acetoacetate decarboxylase gene region from *Clostridium acetobutylicum*. J. Bacteriol. **172**:6907-6918.

Gerischer, U., and P. Dürre. 1992. mRNA analysis of the *adc* gene region of *Clostridium acetobutylicum* during the shift to solventogenesis. J. Bacteriol. **174**:426-433.

Gottschalk, G. 1979. Bacterial Metabolism. Springer-Verlag. New York.

Gottwald, M., and G. Gottschalk. 1985. The internal pH of *Clostridium acetobutylicum* and its effect on the shift from acid to solvent formation. Arch. Microbiol. **143**:42-46.

Green, E.M., and G.N. Bennett. 1996. Inactivation of an aldehyde/alcohol dehydrogenase gene from *Clostridium acetobutylicum* ATCC 824. Appl. Biochem. Biotech. In press.

Green, E., Z.L. Boynton, L. Harris, F.B. Rudolph, E.T. Papoutsakis, and G.N. Bennett. 1996. Genetic manipulation of acid formation pathways by gene inactivation in *Clostridium acetobutylicum* ATCC 824. Microbiology In press.

Green, D.E., S. Mii, R. Mahler, and R.M. Rock. 1954. Studies on the

fatty acid oxidation system of animal tissues. III. Butyryl-CoA dehydrogenase. J. Biol. Chem. **206**:1.

Grundy, F.G., D.A. Waters, S.H.G. Allen, and T.M. Henkin. 1993. Regulation of the *Bacillus subtilis* acetate kinase gene by CcpA. J. Bacteriol. **175**:7348-7355.

Grupe, H., and G. Gottschalk. 1992. Physiological events in *Clostridium acetobutylicum* durin g the shift from acidogenesis to solventogenesis in continuous culture and presentation of a model for shift induction. Appl. Environ. Microbiol. **58**:3896-3902.

Gustafson, W.G., B.A. Feinberg, and J.T. McFarland. 1986. Energetics of β-oxidation: reduction potentials of general fatty acyl-CoA dehydrogenase, electron transfer flavoprotein, and fatty acyl-CoA substrates. J. Biol. Chem. **261**:7733-7741.

Hartmanis, M.G.N. 1987. Butyrate kinase from *Clostridium acetobutylicum.* J. Biol. Chem. **262**:617-621.

Hartmanis, M.G.N., and S. Gatenbeck. 1984. Intermediary Metabolism in *Clostridium acetobutylicum*: levels of enzymes involved in the formation of acetate and butyrate. Appl. Environ. Microbiol. **47**:1277-1283.

Hartmanis, M.G.N., T. Klason, and S. Gatenbeck. 1984. Uptake and activation of acetate and butyrate in *Clostridium acetobutylicum.* Appl. Microbiol. Biotechnol. **20**:66-71.

Huang, L., L.N. Gibbins, and C.W. Forsberg. 1985. Transmembrane pH gradient and membrane potential in *Clostridium acetobutylicum* during growth under acetogenic and solventogenic conditions Appl. Environ. Microbiol. **50**:1043-1047.

Husain, M., M.T. Stankovich, and B.G. Fox. 1984. Measurement of the oxidation-reduction potentials for one-electron and two-electron

reduction of electron-transfer flavoprotein from pig liver. Biochem. J. **219**:1043-1047.

Husain, M. and D.J. Steenkamp. 1983. Electron transfer flavoprotein from pig liver mitochondria: a simple purification and re-evaluation of some of the molecular propertities. Biochem. J. **209**:541-545.

Husain, M. and D.J. Steenkamp. 1985. Partial purification and characterization of glutaryl-coenzyme A dehydrogenase, electron transfer flavoprotein, and electron transfer flavoprotein-Q oxidoreductase from *Paracoccus denitrificans*. J. Bacteriol. **163**:709-715.

Husemann, M H. W. 1989. Ph.D. thesis. Dept. of Chemical Engineering, Rice University (available from Rice Fondren library).

Husemann, M.H.W., and E.T. Papoutosakis. 1988. Solventogenesis in *Clostridium acetobutylicum* fermentations related to carboxylic acid and proton concentrations. Biotechnol. Bioeng. **32**:843-852.

Husemann, M.H.W., and E.T. Papoutosakis. 1989. Enzymes limiting butanol and acetone formation in continuous and batch cultures of *Clostridium acetobutylicum*. Appl. Microbiol. Biotechnol. **31**:435-444

Ikeda, Y., S.M. Geese, and K. Tanaka. 1986. Biosynthesis of electron transfer flavoprotein in a cell-free system and in cultured human fibroblasts. Defect in the alpha subunit synthesis is a primary lesion in glutaric aciduric type II. J. Clin. Invest. **78**:997-1002.

Jones, D.T., and D.R. Woods. 1986. Acetone-butanol fermentation revisited. Microbiol. Rev. 50:484-524.

Jungermann, K., E. Rupprecht, C. Ohrloff, R. Thauer, and K. Decker. 1971. Regulation of the reduced nicotinamide adenine dinucleotide-ferredoxin reductase system in *Clostridium kluyveri*. J. Biol. Chem.

246:960-963.

Jungermann, K., R.K. Thauer, G. Leimenstoll, and K. Decker. 1973. Function of reduced pyridine nucleotide-ferredoxin oxidoreductases in saccharolytic clostridia. Biochim. Biophys. Acta. **305**:268-280.

Kakuda, H., K. Hosono, K. Shiroshi, and S. Ichihara. 1994. Identification and characterization of the *ackA* (Acetate Kinase A)-*pta* (phosphotransacetylase) operon and complementation analysis of acetate utilization by an *ackA-pta* deletion mutant of *Escherichia coli*. J. Biochem. **116**:916-922.

Kelly, D.P., J.J. Kim, J.J. Billadello, B.E. Hainline, T.W. Chu, and A.W. Strauss. 1987. Nucleotide sequence of medium-chain acyl-CoA dehydrogenase mRNA and its expression in enzyme-deficient human tissue. Proc. Natl. Acad. Sci. **84**:4068-4072.

Kim, J.-J.P., M. Wang, S. Djordjevic, R. Paschke, D.W. Bennett. 1994. Three dimensional structures of acyl-CoA dehydrogenases: structure basis of substrate specificity, p. 273-282. *In* K.Yagi (ed.), Flavins and Flavoproteins 1993, Walter de Gruyter, Berlin·New York.

Kim, J.-J.P., M. Wang, and R. Paschke. 1993. Crystal structures of medium-chain acyl-CoA dehydrogenase from pig liver mitochondria with and without substrate. Proc. Natl. Acad. Sci. **90**:7523-7527.

Kim, J.-J.P., and J. Wu. 1988. Structure of the medium-chain acyl-CoA dehydrogenase from pig liver mitochondria at 3-Å resolution. Proc. Natl. Acad. Sci. **85**:6677-6681.

King, M.T., and P.D. Reiss. 1985. Separation and measurement of short-chain coenzyme-A compounds in rat liver by reverse-phase high-performance liquid chromatography. Anal. Biochem. **146**:173-179.

Komuniecki, R., J. McCrury, J. Thissen, and N. Rubin. 1989. Electron-

transfer flavoprotein from anaerobic *Ascaris suum* mitochondria and its role in NADH-dependent 2-methyl branched-chain enoyl-CoA reduction. Biochim. Biophys. Acta. **975**:127-131.

Latimer, M.T., and J.G. Ferry. 1993. Cloning, sequence analysis, and hyperexpression of the genes encoding phosphotransacetylase and acetate kinase from *Methanosarcina thermophila.* J. Bacteriol. **175**:6822-6829.

Lee, S.Y., G.N. Bennett, and E.T. Papoutsakis. 1992a. Construction of *Escherichia coli-Clostridium acetobutylicum* shuttle vectors and transformation of *Clostridium acetobutylicum* strains. Biotechnol. Lett. **14**:427-432.

Lee, S.Y., L.D.Mermelstein, G.N. Bennett, and E.T. Papoutsakis. 1992b. Vector construction, transformation, and gene amplification in *Clostridium acetobutylium* ATCC 824. Ann. N.Y. Acad. Sci. **665**:39-51.

Lee, S.Y., L.D. Mermelstein, G.N. Bennett, and E.T. Papoutsakis. 1993. Determination of plasmid copy number and stability in *Clostridium acetobutylicum* ATCC 824. FEMS Microbiol. Lett. **108**:319-323.

Lehman, T.C., D.E. Hale, A. Bhala, and C. Thorpe. 1990. An acyl-coenzyme A dehydrogenase assay utilizing the ferricenium ion. Anal. Biochem. **186**:280-284.

Lenn, N.D., M.T. Stankovich, and H.-W. Liu. 1990. Regulation of the redox potential of general acyl-CoA dehydrogenase by substrate binding. Biochemistry **29**:3709-3715.

Lundberg, N.N., and C. Thorpe. 1993. Inactivation of short-chain acyl-coenzyme A dehydrogenase from pig liver by 2-pentynoyl-coenzyme A. Arch. Biochem. Biophy. **305**:454-459.

Lundie, L. L. Jr, and J.G. Ferry. 1989. Activation of acetate by *Methanosarcina thermophila*-purification and characterization of phosphotransacetylase. J. Biol. Chem. **264:**18392-18396.

Madan, V.K., P. Hillmer, and G. Gottschalk. 1973. Purification and properties of NADP-dependent L(+)-3-hydroxybutyryl-CoA dehydrogenase from *Clostridium kluyveri.* Eur. J. Biochem. **32:**51-56.

Maniatis, T., E.F. Fritsch, and J. Sambrook. 1982. Molecular cloning: a laboratory manual. Cold Spring Harbor Laboratory, Cold Spring Harbor, N.Y.

Matsubara, Y., J. Kraus, H. Ozasa, R. Glassberg, G. Finocchiaro, Y. Ikeda, J. Mole, L.E. Rosenberg, and K. Tanaka. 1987. Molecular cloning and nucleotide sequence of cDNAs encoding the entire precursors of rat liver medium chain acyl coenzyme A dehydrogenase. J. Biol. Chem. **262:**10104-10108.

Matsubara, Y., Y. Indo, E. Naito, H. Ozasa, R. Glassberg, J. Vockley, Y. Ikeda, J. Kraus, and K. Tanaka. 1989. Molecular cloning and nucleotide sequence of cDNAs encoding the precursors of rat long chain acyl-coenzyme A, short chain acyl-coenzyme A, and isovaleryl-coenzyme A dehydrogenases. J. Biol. Chem. **264:**16321-16331.

Matsuyama, A., H. Yamamoto-Otake, and E. Nakano. 1989. Cloning, expression and nucleotide sequence of the *Escherichia coli* K-12 *ackA* gene. J. Bacteriol. **171:**577-580.

Matsuyama, A., H. Yamamoto-Otake, J. Hewitt, R.T.A. MacGillivray, and E. Nakano. 1994. Nucleotide sequence of the phosphotransacetylase gene of *Escherichia coli* strain K-12. Biochim. Biophys. Acta. **1219:**559-562.

McLaughlin, J.K., C.L. Meyer, and E.T. Papoutsakis. 1985. Gas chromatography and gateway sensors for on-line state estimation of complex fermentations (butanol-acetone fermentation). Biotechnol. Bioeng. **27**:1246-1257.

Mermelstein, L.D., and E.T. Papoutsakis. 1993a. In vivo methylation in *Escherichia coli* by the *Bacillus subtilis* phage Ø3T I methyltransferase to protect plasmids from restriction upon transformation of *Clostridium acetobutylicum* ATCC 824. Appl. Environ. Microbiol. **59**:1077-1081.

Mermelstein, L.D., and E.T. Papoutsakis. 1993b. Evaluation of macrolide and lincosamide antibiotics for plasmid maintenance in low pH *Clostridium acetobutylicum* ATCC 824 fermentations. FEMS Microbiol. Lett. **113**:71-76.

Mermelstein, L.D., N.E. Welker, G.N. Bennett, and E.T. Papoutsakis. 1992. Expression of cloned homologous fermentative genes in *Clostridium acetobutylicum* ATCC 824. Bio/Technology **10**:190-195.

Mermelstein, L.D., N.E. Welker, D.J. Peterson, G.N. Bennett, and E.T. Papoutsakis. 1994. Genetic and metabolic engineering of *Clostridium acetobutylicum* ATCC 824. Ann. N.Y. Acad. Sci. **721**:54-67.

Minami-Ishii, N., S. taketani, T. Osumi, and T. Hashimoto. 1989. Molecular cloning and sequence analysis of the cDNA for rat mitochondrial enoyl-CoA hydratase. Eur. J. Biochem. **185**:73-78.

Mullany, P., C.L. Clayton, M.J. Pallen, R. Slone, A. Al-Saleh, and S. Tabaqchali. 1994. Genes encoding homologues of three consecutive enzymes in the butyrate/butanol-producing pathway of *Clostridium acetobutylicum* are clustered on the *Clostridium difficile* chromosome. FEMS Microbiol. Lett. **124**:61-68.

Murray, M.G., and W.F. Thompson. 1980. Rapid isolation of high molecular weight plant DNA. Nucl. Acids Res. **8**:4321-4326

Nagao, M., and K. Tanaka. 1992. FAD-dependent regulation of transcription, translation, posttranslational processing, and post-processing stability of various mitochondrial acyl-CoA dehydrogenases and of electron transfer flavoprotein and the site of holoenzyme formation. J. Biol. Chem. **267**:17925-17932.

Nair, R.V., G. N. Bennett and E.T. Papoutsakis. 1994. Molecular Characterization of an aldehyde/alcohol dehydrogenase gene from *Clostridium acetobutylicum* ATCC 824. J. Bacteriol. **176**:871-885

Nair, R.V., and E.T. Papoutsakis. 1994. Expression of plasmid-encoded *aad* in *Clostridium acetobutylicum* M5 restores vigorous butanol production. J. Bacteriol. **176**:5843-5846.

Naito, E., H. Ozasa, Y. Ikeda, and K. Tanaka. 1989. Molecular cloning and nucleotide sequence of complementary DNAs encoding human short chain acyl-coenzyme A dehydrogenase and the study of the molecular basis of human short chain acyl-coenzyme A dehydrogenase deficiency. J. Clin. Invest. **83**:1605-1613.

Onualláin, E.M., and S.G. Mayhew. 1986. Properties of the complexes formed between 8-halogenated flavins and apo-electron-transferring flavoprotein from *Megasphaera elsdenii.* Biochem. Soc. Trans. **14**:440-441.

Osumi, T., N. Ishii, M. Hijikata, K. Kamijo, H. Ozasa, S. Furuta, S. Miyazawa, K. Kondo, K. Inoue, H. Kagamiyama, and T. Hashimoto. 1985. Molecular cloning and nucleotide sequence of the cDNA for rat peroxisomal enoyl-CoA: hydratase-3-hydroxyacyl-CoA dehydrogenase bifunctional enzyme. J. Biol. Chem. **260**:8905-8910.

Oultram, J.D., I.D. Burr, M.J. Elmore and N.P. Minton. 1993. Cloning and sequence analysis of the genes encoding phosphotransbutyrylase and butyrate kinase from *Clostridium acetobutylicum* NCIMB 8052. Gene **131**:107-112.

Pace, C.P., and M.T. Stankovich. 1987. Redox properties of electron-transferring flavoprotein from *Megasphaera elsdenii.* Biochim. Biophys. Acta. **911**:267-276.

Palosaari, N.R., and P. Rogers. 1988. Purification and properties of the inducible coenzyme-A-linked butyraldehyde dehydrogenase from *Clostridium acetobutylicum.* J. Bacteriol. **170**:2971-2976.

Papoutsakis, E.T. 1984. Equations and calculations for fermentation of butyric acid bacteria. Biotechnol. Bioeng. **26**:174-187.

Peterson, D.J. 1991. Characterization of the acetone production pathway genes from *Clostridium acetobutylicum* ATCC 824. Ph.D. thesis, Rice University, Houston, Texas.

Peterson, D.J., J.W. Cary, J. Vanderleyden, and G.N. Bennett. 1993. Sequence and arrangement of genes encoding enzymes of the acetone-production pathway of *Clostridium acetobutylicum* ATCC 824. Gene **123**:93-97.

Peterson, D.J., R.W. Welch, F.B. Rudolph, and G.N. Bennett. 1991. Molecular cloning of an alcohol (butanol) dehydrogenase gene cluster from *Clostridium acetobutylicum* ATCC 824. J. Bacteriol. **173**:1831-1834.

Phillips, M.K., L. Hederstedt, S. Hasnain, L. Rutberg, and J.R. Guest. 1987. Nucleotide sequence encoding the flavoprotein and iron-sulfur protein subunits of the *Bacillus subtilis* PY79 succinate dehydrogenase complex. J. Bacteriol. **169**:864-873.

Powell, P.J., and C. Thorpe. 1988. 2-Octonoyl coenzyme A is a mechanism-based inhibitor of pig kidney medium-chain coenzyme A dehydrogenase: isolation of the target peptide. Biochemistry **27**:8022-8028.

Pramanik, A., S. Pawar, E. Antonian, anf H. Schultz. 1979. Five different enzymatic activities are associated with the multienzyme complex of fatty acid oxidation from *Escherichia coli.* J. Bacteriol. **137**:469-473.

Raleigh, L.A. 1984. RbCl transformation procedure for improved efficiency. NEB Transcript **6**:7.

Robinson, J.R., and R.D. Sagers. 1972. Phosphotransacetylase from *Clostridium acidiurici.* J. Bacteriol. **112**:465-473.

Roos, J.W., K. McLaughlin, and E.T. Papoutsakis. 1985. The effect of pH on nitrogen supply, cell lysis and solvent production in fermentations of *Clostridium acetobutylicum.* Biotechnol. Bioeng. **27**:681-694.

Rose, I.A. 1955. Acetate kinase of bacteria. Methods Enzymol. **1**:591-595.

Rosemann, M.G., A. Liljas, C.I. Branden, and L.J. Banaszak. 1975. Evolutionary and structural relationship among dehydrogenases, p.61-102. *In* P.D. Boyer (ed) The enzymes, volume 2. Academic Press, Inc., New York.

Rosenfeld, B., and E. Simon. 1950. The mechanism of the butanol-acetone fermentation. 1. The role of pyruvate as an intermediate. 2. Phosphoenolpyruvate as a new intermediate. J. Biol. Chem. **186**:395-410.

Ruzicka, F.J., and H. Beinert. 1977. A new iron-sulfur flavoprotein of the respiratory chain: a component of the fatty acid β oxidation pathway. J. Biol. Chem. **252**:8440-8445.

Sancar, A., R.P. Wharton, S. Seltzer, B.M. Kacinski, N.D. Clark, and W.D. Rupp. 1981. Identification of the *uvr* gene product. J. Mol. Biol. **148**:45-62.

Sanger, F., S. Nicklen, and A.R. Coulson. 1977. DNA sequencing with chain-terminating inhibitors. Proc. Natl. Acad. Sci. USA **74**:5463-5467.

Sass, C., J. Walter, and G.N. Bennett. 1993. Isolation of mutants of *Clostridium acetobutylicum* ATCC 824 deficient in protease activity. Current Microbiology. **26**:151-154.

Sauer, U., and Dürre, P. 1995. Differential induction of genes related to solvent formation during the shift from acidogenesis to solventogenesis in coutinuous culture of *Clostridium acetobutylicum.* FEMS Microbiol. Lett. **125**:115-120.

Schaupp, A., and L.G. Ljungdahl. 1974. Purification and properties of acetate kinase from *Clostridium thermoaceticum.* Arch. Microbiol. **100**:121-129.

Schiffer, S.P., M. Prochazka, P.F. Jezyk, T.H. Roderick, M. Yudkoff, and D.F. Patterson. 1989. Organic aciduria and butyryl-CoA dehydrogenase deficiency in BALB/cByJ mice. Biochem. Genet. **27**:47-58.

Schimizu, M., T. Suzuki, K.-Y. Kameda, and Y. Abiko. 1968. Phosphotransacetylase of *Escherichia coli* B, purification and properties. Biochim. Biophys. Acta. **191**:550-558.

Shine, J., and L. Dalgarno. 1974. The 3'-terminal sequence of *Escherichia coli* 16S ribosomal RNA: complementary to nonsense triplets and ribosome binding sites. Proc. Natl. Acad. Sci. **71**:1342-1346.

Shinzawa, K., T. Inagaki, N. Ohishi, C. Ichihara, N. Tsukagoshi, S. Udaka, and K. Yagi. 1988. Molecular cloning of a cDNA for α-subunit of rat liver electron transfer flavoprotein. Biochem. Biophys. Res. Commun. **155**:300-304.

Singh-Wissmann, K., and J.G. Ferry. 1995. Transcriptional regulation of the phosphotransacetylase-encoding and acetate kinase-encoding genes (*pta* and *ack*) from *Methanosarcina thermophila*. J. Bacteriol. **177**:1699-1702.

Southern, E.M. 1975. Detection of specific sequences among DNA fragments separated by gel electrophoresis. J. Mol. Biol. **98**:503-517.

Spivey, M.J. 1978. The acetone-butanol-ethanol fermentation process. Process. Biochem. **13**:2-5.

Spratt, S.K., P.N. Black, M.M Ragozzino, and W.D. Nunn. 1984. Cloning, mapping and expression of genes involved in the fatty acid degradative multienzyme complex of *Escherichia coli*. J. Bacteriol. **158**:535-542.

Stadtman, E.R. 1955. Phosphotransacetylase from *Clostridium kluyveri*. Methods Enzymol. **1**:596-599.

Stanton, T.B. 1989. Glucose metabolism and NADH recycling by *Treponema hyodysenteriae*, the agent of swine dysentery. Appl. Environ. Microbiol. **55**:2365-2371.

Stankovich, M.T., and S. Soltysik. 1987. Regulation of the butyryl-CoA dehydrogenase by substrate and product binding. Biochemistry **26**:2627-2632.

Stouthamer, A.H. 1980. Bioenergetic studies on *Paracoccus denitrificans*. Trends Biochem. Sci. **5**:164-166.

Terracciano, J.S. and E.R. Kashket. 1986. Intracellular conditions required for initiation of solvent production of *Clostridium acetobutylicum*. Appl. Environ. Microbiol. **52**: 86-91.

Thompson, D.K., and J.S. Chen. 1990. Purification and properties of an acetoacetyl coenzyme A-reacting phosphotransbutyrylase from

Clostridium beijerincki (*"clostridium butylicum"*) NRRL B593. Appl. Environ. Microbiol. **56**:607-613.

Thompson, S., F. Mayerl, O.P. Peoples, S. Masamune, A.J. Sinskey, and C.T. Walsh. 1989. Mechanistic studies on β-ketoacyl thiolase from *Zoogloea ramigera*: identification of the active-site nucleophile as Cys_{89}, its mutation to Ser_{89}, and kinetic and thermodynamic characterization of wild-type and mutant enzymes. Biochemistry **28**:5735-5742.

Todhunter, J.A., and D.L. Purich. 1974. Evidence for the formation of a γ-phosphorylated glutamyl residues in the *Escherichia coli* acetate kinase reaction. Biochem. Biophys. Res. Commun. **60**:273-280.

Valentine R.C., and R.S. Wolfe. 1960. Purification and role of phosphotransbutyrylase. J. Biol. Chem. **235**:1948-1952.

Van Berkel, W.J.H., W.A.M. Van Den Berg, and F. Muller. 1988. Large-scale preparation and reconstitution of apo-flavoproteins with special reference to butyryl-CoA dehydrogenase from *Megasphaera elsdenii*. Eur. J. Biochem. **178**:197-207.

Van Spanning, R.J.M., A.P.N. De Boer, D.J. Slotboom, W.N.M. Reijnders, and A.H. Stouthamer. 1994. Unpublished data. Sequence from EMBL/Genbank/DDBJ data banks accession # P39197.

Voet, D., and J.G. Voet. 1990. p538-540. Biochemistry. J. Wiley and Sons, New York.

Walker, J.E., M. Saraste, J.J. Runswick, and N.J. Gay. 1982. Distantly related sequences in the α- and β-subunits of ATP synthase, myosin, kinase and other ATP-requiring enzymes and a common nucleotide binding fold. EMBO J. **1**:945-951.

Walter, K.A., G. N. Bennett, and E.T. Papoutsakis. 1992. Molecular characterization of two *Clostridium acetobutylicum* ATCC 824 butanol dehydrogenase isozyme genes. J. Bacteriol. **174**:7149-7158.

Walter, K.A., L.D. Mermelstein, and E.T. Papoutsakis. 1994a. Studies of recombinant *Clostridium acetobutylicum* with increased dosages of butyrate formation genes. Ann. N.Y. Acad. Sci. **721**:69-72.

Walter, K.A., R.V. Nair, J.W. Cary, G.N. Bennett, & E.T. Papoutsakis. 1994b. Sequence and arrangement of two genes of the butyrate-synthesis pathway of *Clostridium acetobutylicum* ATCC 824. Gene **134**:101-111.

Waterson, R.M., F.J. Castelino, G.M. Hass, and R.L. Hill. 1972. Purification and characterization of crotonase from *Clostridium acetobutylicum.* J. Biol. Chem. **247**:5266-5271.

Waterson, R.M., and R.L. Hill. 1972. Enoyl coenzyme A hydratase (Crotonase). Catalytic properties of crotonase and its possible regulatory role in fatty acid oxidation. J. Biol. Chem. **247**:5258-5265.

Watmough, N.J., J. Kiss, and F.E. Frerman. 1992. Structural and redox relationships between *Paracoccus denitrificans*, porcine and human electron-transferring flavoproteins. Eur. J. Biochem. **205**:1089-1097.

Welch, R.W. 1990. Ph.D. thesis. Rice University, Houston, Texas.

Welch, R.W., S. W. Clark, G.N. Bennett and F.B. Rudolph. 1992. Effects of rifampicin and chloramphenicol on product and enzyme levels of the acid- and solvent-producing pathways of *Clostridium acetobutylicum* (ATCC 824). Enzyme Microb. Technol. **14**:277-283.

Welch, R.W., F.B. Rudolph, and E.T. Papoutsakis. 1989. Purification and characterization of the NADH-dependent butanol dehydrogensae from *Clostridium acetobutylicum* (ATCC 824). Arch. Biochem. Biophys. **273**:309-318.

Whitfield, C.D., and S.G. Mayhew. 1974. Purification and properties of electron-transferring flavoprotein from *Peptostreptococcus elsdenii*. J. Biol. Chem. **249**:2801-2810.

Wierenga, R.K., P. Terpstra, and W.G.J. Hol. 1986. Prediction of the occurrence of the ADP-binding βαβ-fold in proteins, using an amino acid sequence fingerprint. J. Mol. Biol. **187**:101-107.

Wiesenborn, D. P. , F. B. Rudolph and E. T. Papoutsakis. 1988. Thiolase from *Clostridium acetobutylicum* ATCC 824 and its role in the synthesis of acids and solvents. Appl. Environ. Microbiol. **54**:2717-2722.

Wiesenborn, D. P. , F. R. Rudolph and E.T. Papoutosakis. 1989. Phosphotransbutyrylase from *Clostridium acetobutylicum* ATCC 824 and its role in acidogenesis. Appl. Environ. Microbiol. **55**:317-322.

Wiesenborn, D. P. , F. R. Rudolph and E.T. Papoutosakis. 1989. Coenzyme A transferase from *Clostridium acetobutylicum* ATCC 824 and its role in the uptake of acids. Appl. Environ. Microbiol. **55**:323-329.

Wilkinson, S.R., and M. Young. 1994. Targeted integration of genes into the *Clostridium acetobutylicum* chromosome. Microbiology **140**:89-95.

Williams, D.R., D.I. Young, and M. Young. 1990. Conjugative plasmid transfer from *Escherichia coli* to *Clostridium acetobutylicum*. J. Gen. Microbiol. **136**:819-826.

Williamson, G., and P.C. Engel. 1984. Butyryl-CoA dehydrogenase from *Megasphaera elsdenii*: specificity of the catalytic reaction. Biochem. J. **218**:521-529.

Wilson R., R. Ainscough, K. Anderson, C. Baynes, M. Berks, J. Bonfield,

J. Burton, M. Connell, T. Copsey, J. Cooper, A. Coulson, M. Craxton, S. Dear, Z. Du, R. Durbin, A. Favello, A. Fraser, L. Fulton, A. Gardner, P. Green, T. Hawkins, L. Hillier, M. Jier, L. Johnston, M. Jones, J. Kershaw, J. Kirstern, N. Laisster, P. Latreille, J. Lightning, C. Lloyd, B. Mortimore, M. O'Callaghan, J. Parsons, C. Percy, L. Rifken, A. Roopra, D. Saunders, R. Shownkeen, M. Sims, N. Smaldon, A. Smith, M. Smith, E. Sonnhammer, R. Staden, J. Sulston, J. Thierry-Mieg, K. Thomas, M. Vaudin, K. Vaughan, R. Waterson, A. Watson, L. Weinstock, J. Wilkinson-Sproat, P. Wohldman. 1994. 2.2 Mb of contiguous nucleotide sequence from chromosome III of *C. elegans.* Nature **368**:32-38.

Wong, J. 1995. Ph.D. thesis. Rice University, Houston, Texas.

Wong, S.S., and L.J. Wong. 1980. Inactivation of *Escherichia coli* acetate kinase by N-ethylmaleimide. Biochim. Biophys. Acta. **615**:121-131.

Wong, S.S., and L.J. Wong. 1981. Evidence for an essential arginine residue at the active site of *Escherichia coli* acetate kinase. Biochim. Biophys. Acta. **660**:142-147.

Wood, H.G., R. W. Brown and C.H. Werkman. 1945. Mechanisms of the butyl alcohol fermentation with heavy carbon acetic and butyric acids and acetone. Arch. Biochem. **6**:243-260.

Woods, D.R. 1995. The genetic engineering of microbial solvent production. Trends Biotechnol. **13**:259-264.

Yamamoto-Otake, H., A. Matsuyama, and E. Nakano. 1990. Cloning of a gene encoding for phosphotransacetylase from *Escherichia coli* . Appl. Microbiol. Biotechnol. **33**:680-682.

Yang, S.Y., and M. Elzinga. 1993. Association of both coenzyme A hydratase and 3-hydroxyacyl coenzyme A epimerase with an active site in the amino-terminal domain of the multifunctional fatty acid oxidation protein from *Escherichia coli.* J. Biol. Chem.

268:6588-6592.

Yang, X.Y.H., H. Schulz, M. Elzinga, and S.-Y. Yang. 1991. Nucleotide sequence of the promoter and *fadB* gene of the *fadBA* operon and primary structure of the multifunctional fatty acid oxidation protein from *Escherichia coli*. Biochemistry **30**:6788-6795.

Yanisch-Perron, C., J. Vieira, and J. Messing. 1985. Improved M13 cloning vectors and host strains: nucleotide sequences of the M13mp18 and pUC19 vectors. Gene **33**:103-119.

Youngleson, J.S., W.A. Jones, D.T. Jones, and D.R. Woods. 1989a. Molecular analysis and nucleotide sequence of the *adh-1* gene encoding an NADPH-dependent butanol dehydrogenase in the gram-positive anaerobe *Clostridium acetobutylicum*. Gene **78**:355-364.

Youngleson, J.S., D.T. Jones, and D.R. Woods. 1989b. Homology between hydroxybutyryl and hydroxyacyl coenzyme A dehydrogenase enzymes from *Clostridium acetobutylicum* fermentation and vertebrate fatty-acid β-oxidation pathways. J. Bacteriol. **171**:6800-6807.

Youngleson, J.S., F.P. Lin, S.J. Reid, and D.R. Woods. 1994. Structure and transcription of genes within the *β-hbd-adh1* region of *Clostridium acetobutylicum* P262. FEMS Microbiol. Lett. 125:185-191.